STUDIES OF INTACT AND MODIFIED ZICONOTIDE BY LIQUID CHROMATOGRAPHY - TANDEM MASS SPECTROMETRY

By

JHOANA AVENDAÑO MENDOZA

A DISSERTATION PRESENTED TO THE GRADUATE SCHOOL
OF THE UNIVERSITY OF FLORIDA IN PARTIAL FULFILLMENT
OF THE REQUIREMENTS FOR THE DEGREE OF
DOCTOR OF PHILOSOPHY

UNIVERSITY OF FLORIDA

2009

To my parents and Dodge

ACKNOWLEDGMENTS

I am grateful to my research advisor, Dr. John R. Eyler, for his support and scientific guidance and belief in my capabilities. I would like to thank Dr. Richard Sams for allowing me to work on the ziconotide project and instilling in me the importance of working systematically. I would also like to extend my gratitude to the rest of my committee members, Dr. Nicole Horenstein, Dr. David Powell and Dr. Richard Yost.

I would like to thank Dr. Laszlo Prokai for paving the way to our collaboration with the College of Veterinary Medicine Racing Laboratory. Special thanks go to Dr. Cynthia Cole for supporting the collaboration and allowing me to work at the Racing Laboratory and for being a former member of my committee. I am also grateful to Dr. Nancy Szabo for her guidance and encouragement. I would like to thank Dr. Nancy Denslow for her generosity in equipment use. I also acknowledge the financial support of the Racing Medication and Testing Consortium.

While at the Racing Laboratory, I was fortunate enough to work with Dr. Keith Zientek who taught me a lot of what I knew about sample preparation and the operation of the LTQ. I would like to thank him and the group of wonderful people who have been my labmates away from Chemistry - Brooks, Vanessa, Christa, Julia and Craig. I would like to thank Patrick Russell especially for his support and willingness to help whenever I need to troubleshoot LC/MS issues and Margaret Wilding for her encouragement and gentle support.

Dr. Cristina Dancel and Dr. Sue Abbatiello have been very great resource persons and good friends too; I have learned a lot of science from them. I am also thankful to the rest of the Eyler-Polfer group for the friendship and helpful discussions during group meetings.

My stay in Florida would not have been as fun and memorable as it is if not for the great company of Filipino friends who have been my family away from home – Jemy, Joy, Mario, Jen, Fair, Emilio, the Pabits, the Javelosas and the rest of Pinoy_UF group; my thanks to you all.

I have been blessed to have a family who's supportive of my dreams. I thank my dear parents, Rodolfo and Evelyn, for their hard work and countless sacrifices to give us a chance at a better life. I thank my sister, Vanessa, for her strength and my brother, BJ, for his joyful ways of encouraging me. I would also like to express my gratitude to the rest of the Avendaño and Mendoza families especially to Auntie Letty, Auntie Josie, Uncle Angel, Uncle Victor, Uncle Alex, Auntie Carmen and Auntie Tessie for their guidance and unwavering support.

Finally, I thank my husband, Dodge, for his support, patience, and sacrifice and for always encouraging and inspiring me to work hard to make it to this point.

TABLE OF CONTENTS

page

LIST OF TABLES

LIST OF FIGURES

Abstract of Dissertation Presented to the Graduate School
of the University of Florida in Partial Fulfillment of the
Requirements for the Degree of Doctor of Philosophy

STUDIES OF INTACT AND MODIFIED ZICONOTIDE BY LIQUID CHROMATOGRAPHY - TANDEM MASS SPECTROMETRY

By

Jhoana Avendaño Mendoza

August 2009

Chair: John R. Eyler
Major: Chemistry

Ziconotide is the synthetic version of ω-conopeptide MVIIA, a 25-amino acid cone snail toxin from *Conus magus*. Its cysteine residues form 3 disulfide bridges, while its arginine, lysine residues and amidated C-terminal make it highly basic. It is a potent analgesic recently approved for the treatment of intense refractory pain in humans. The development of an analytical method for the qualitative and quantitative determination of this peptide in complex matrices is, therefore, of interest to many.

High performance liquid chromatography (HPLC) – tandem mass spectrometric (MS/MS) analyses of intact and modified ziconotide were carried out in this study. The chromatographic performance of various columns for reversed-phase HPLC separation of ziconotide was investigated. The peak shape and retention of ziconotide on the columns used were compared. The effects of solvent composition on the charge state distribution and response of ziconotide were investigated. Optimization of various mass spectrometric parameters such as spray voltage, sheath gas and auxiliary gas flows was also conducted.

Analysis of intact ziconotide showed that the extensive cross-linking from multiple disulfide bridges reduces the structural information that can be derived from the MS/MS

spectrum of ziconotide. Modification of the analyte by reducing the disulfide bonds and alkylating the resulting sulfhydryl groups eliminate cross-linking and increase the probability of fragmentation during collision-induced dissociation (CID). Fragment ions resulting from typical peptide bond cleavage (e.g., b and y ions) were observed after modification of ziconotide and the internal standard, ω-conotoxin GVIA. The limit of quantitation obtained from the modified peptide experiments was 0.500 ng on column.

The HPLC-MS method developed for the analysis of intact ziconotide was successfully validated. The validated method was then used to evaluate the degradation of ziconotide in a test solution similar in composition to the commercially available drug formulation, Prialt® (Elan Pharmaceutical, Inc.) The plot of the natural logarithm of ziconotide concentration versus storage time at 50°C and half-life calculations indicated that the degradation of ziconotide could be a first- or pseudo first-order reaction. Results pertaining to the rate of degradation of a drug substance provide useful information for proper handling and storage of the ziconotide drug solution.

CHAPTER 1
INTRODUCTION

Background of Study

Conotoxins and Ziconotide

Conopeptides or conotoxins are small peptide toxins produced by cone snails for prey capturing and defense.[1, 2] There are about 100 different conotoxins in the venom of each of the 500 living species of *Conus*, with very little sequence similarity between species.[2-5] These unique conopeptides consist of 10 to 30 amino acids and most have multiple disulfide bonds.[2-5] They are broadly categorized into two groups based on the number of disulfide bonds present and then further subdivided based on their pharmacological targets.[4] Conopeptides which act selectively at a number of sites, including sodium and calcium channels and nicotinic acetylcholine receptors, have been reported.[3, 6] The use of these conopeptides as tools in pharmacological research and as potential therapeutic agents in humans is currently being explored.[6-8]

Ziconotide (MW = 2.6 kDa) is the synthetic version of ω-conopeptide MVIIA, a 25-amino acid cone snail toxin from *Conus magus* (Figure 1-1).[9-11] Its cysteine residues form 3 disulfide bridges and are arranged in a 4-loop cysteine scaffold which is a characteristic feature of most ω-conotoxins, while its numerous lysine and arginine residues and amidated C-terminal make it highly basic.[2, 12] It is a potent peptide analgesic recently approved for the treatment of severe chronic pain in humans when administered intrathecally.[10] Toxins belonging to the omega family of conopeptides block cell membrane calcium channels and ziconotide specifically blocks the N-type voltage-sensitive calcium channels.[9, 11, 13]

Analysis of these highly diverse cone snail toxins has been facilitated by reversed- phase high performance liquid chromatography (RP-HPLC) with ultraviolet-visible (UV-vis)

spectrophotometry[2, 14, 15] and mass spectrometry (MS) for detection.[1, 8, 16, 17] The presence of multiple disulfide bonds and post-translational modifications in several of these conopeptides requires derivatization methods and tandem mass spectrometric (MS/MS) analysis for enhanced structural characterization.[1, 18-20] Nuclear magnetic resonance (NMR) spectroscopy has also been employed in the structural determination of conotoxins.[8, 17, 21] However, the detection and quantitation of ziconotide, the conotoxin of interest in this study, in biological samples has only been carried out using a radioimmunoassay method.[13] Radioimmunoassay techniques involve competition between unlabeled antigen in a sample matrix and a known amount of radiolabeled antigen for antibody binding sites.[22] As the concentration of the unlabeled antigen increases, more radiolabeled antigen is displaced and the ratio of antibody-bound radiolabeled antigen to unlabeled antigen decreases. The concentration in an unknown sample is quantified against the inhibition obtained with standard solutions containing known amounts of antigen. A 3-kDa peptide analog, ω-conotoxin GVIA (Figure 1-2), was chosen as the internal standard (IS) in the ziconotide analysis discussed in the succeeding chapters.

High Performance Liquid Chromatography

Reversed-phase high performance liquid chromatography has become an essential tool in the separation and analysis of peptides from complex sample matrices. RP-HPLC separates peptides based on hydrophobicity with the non-polar compounds retained longer in the stationary phase and eluted later than polar compounds.[23] Eluates from the HPLC column can then be directly introduced into a mass spectrometer and analyzed, a technique called on-line LC/MS.[24] There are several advantages to separating a mixture by RP-HPLC prior to mass spectrometric analysis. These include easier data interpretation from generation of mass spectra of single components and improved sensitivity through concentration of a large volume of dilute sample

upon injection onto the column and separation of analytes from salts, buffers and other contaminants.[25] The separation efficiency of RP-HPLC is influenced by the type of resin, size of column and the length and slope of the gradient used.[23] As the need to analyze limited volume of samples emerged, small diameter columns that employ reduced flow rates have become popular for RP-HPLC with current methods using flow rates of 500 nL/min or less and column diameters between 50-100 µm.[26, 27]

Electrospray Ionization

The development of atmospheric pressure ionization techniques such as electrospray ionization (ESI) and chemical ionization (CI) has greatly facilitated LC/MS applications to bioanalytical studies.[28] Electrospray ionization, in particular, involves the generation of charged droplets from a solution sprayed through a high-voltage capillary (Figure 1-3).[29] As the solvent evaporates upon application of drying gas, heat or both and the droplets shrink in size, analyte ions shrink and split through coulombic repulsion until they are transformed into gas phase ions.[28, 29]

The introduction of this technique has allowed for the analysis of most large, non-volatile and thermally labile compounds such as various classes of biomolecules directly from the liquid phase.[30, 31] The generation of multiply-charged ions also enables mass spectrometers with limited mass to charge (*m/z*) ranges, such as ion traps, to analyze high molecular weight molecules.[31] One of this technique's most practical attributes is its ability to couple MS and liquid separation techniques.

Signal enhancement from the use of small diameter capillary columns and low flow rates, coupled with improvements in sensitivity and selectivity provided by MS techniques, have facilitated the detection of peptides present at attomole levels in a complex sample mixture.[32]

Quadrupole Ion Trap Mass Spectrometry

The operation of the linear ion trap is based on the theory of the 3-D quadrupole ion trap.[33] The linear ion trap is composed of 4 parallel hyperbolic shaped rods, divided into 3 sections as opposed to the configuration of the 3D ion trap which consists of a ring and 2 endcap electrodes.[34] For trapping of ions, a radio frequency (RF) electric field is applied radially and a static electric field using DC voltages is applied axially.[34] The application of these voltages creates a homogenous field throughout the trapping region. These modifications have improved the ion storage capacity and trapping efficiency of the linear ion trap when compared to a 3-D trap.[35]

Once ions are trapped, a particular *m/z* can be isolated and fragmented by applying the appropriate supplementary frequency. Like its predecessor, the 3-D ion trap, mass analysis in the linear ion trap involves ejecting the trapped ions in an increasing *m/z* order by linearly ramping the RF amplitude. However, the trapped ions are ejected in the radial direction (instead of axially in the 3D trap) along the x-axis, through the 2 parallel slots in the center of the x-rod pairs.[34] Ejected ions are then detected by a conversion dynode and an electron multiplier placed on each side of the trap. The use of a dual detector system ensures detection of the maximum number of ions, thus improving sensitivity. The enhanced detection efficiency together with the improved storage capacity and trapping efficiency of the linear ion trap offer advantages such as greater sensitivity, increased dynamic range and improved MS^n performance.

Objectives of Research

The development of an HPLC-ESI-MS^n method to detect ziconotide in complex biological matrices is a very promising alternative to radioimmunoassay techniques. The initial goals of this research project were to optimize the HPLC-ESI-MS method and to evaluate its figures of merit for the analysis of intact and modified ziconotide in biological samples. The evaluation of

a stability-indicating assay for ziconotide in commercial-type formulations using the validated HPLC-ESI-MS method for the intact peptide was carried out when method limitations were encountered for the original application.

Analysis of Intact Ziconotide

The optimization of various HPLC and mass spectrometric parameters such as solvent composition, column chemistry, spray voltage, auxiliary and sheath gas flows for the analysis of intact ziconotide is discussed in Chapter 2. The use of small diameter columns and low flow rates to improve the sensitivity of the method is explored. The figures of merit and limitations of the HPLC-ESI-MS method developed are also discussed in this chapter. Analysis of intact ziconotide showed that the extensive cross-linking from its multiple disulfide bridges reduces the structural information that can be derived from its MS/MS spectrum.

Analysis of Modified Ziconotide

Modification of ziconotide by reduction and alkylation of its disulfide bonds eliminates cross-linking and yields fragment ions that are more structurally relevant. Optimization of the parameters affecting reduction and alkylation is presented in Chapter 3 together with the figures of merit and limitations of the HPLC-ESI-MS method for the modified conopeptide. Application of the reduction and alkylation method to ziconotide supplemented in horse plasma was also explored and is discussed in this chapter.

Development of a Stability-Indicating Assay for Ziconotide in Commercial-Type Formulations

The HPLC-ESI-MS method for the analysis of intact ziconotide was validated and evaluated as a stability-indicating assay for ziconotide in test solutions similar in composition to the commercially available drug formulation, Prialt® (Elan Pharmaceutical, Inc.). The results of

the validation study and the determination of a possible rate of reaction for the degradation of ziconotide exposed to harsh oxidative conditions are discussed in Chapter 4.

Figure 1-1. 3-D structure of ziconotide (*left*) and its amino acid sequence (*right*). The N-terminus on the 3-D structure is shown in red, C-terminus in blue, and disulfide bonds in gold.[36] The color scheme used for the amino acids was matched to that of the 3-D structure.

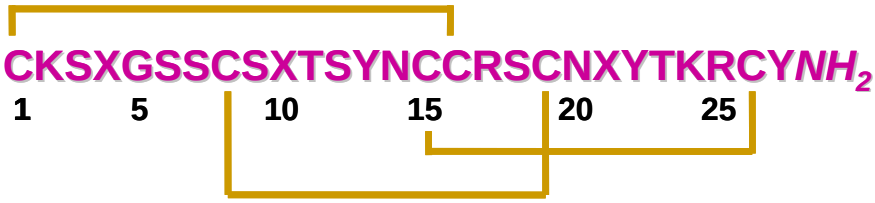

Figure 1-2. Amino acid sequence of ω-conotoxin GVIA. The disulfide bonds are shown in gold and X denotes hydroxyproline residues.

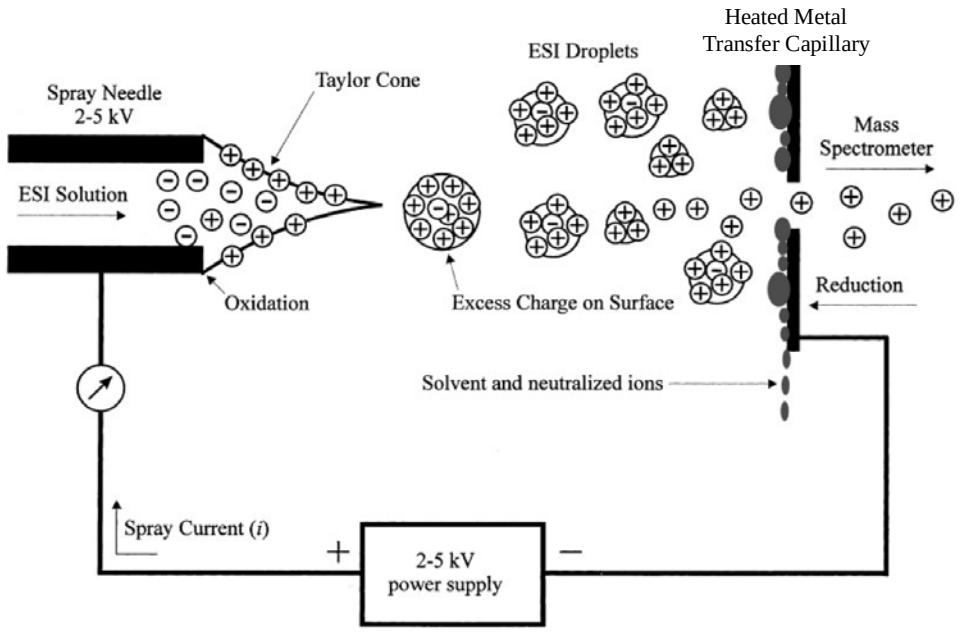

Figure 1-3. Schematic of the electrospray ionization process. This ionization technique produces gaseous analyte ions from a liquid flow introduced into a small capillary that is at a potential difference relative to a counter electrode, from which ions are generated then sampled into the mass analyzer. Adapted from Cech and Enke[29]

CHAPTER 2
HPLC-ESI-MS/MS ANALYSIS OF INTACT ZICONOTIDE

Introduction

Ziconotide, the synthetic version of ω-conotoxin MVIIA, is a potent peptide analgesic that has recently been approved for the treatment of severe chronic pain in humans.[10] The development of an analytical method for determining this peptide in complex matrices, like biological fluids, is of interest to many. At present, the only method available for the detection and quantitation of ziconotide in biological samples is radioimmunoassay which involves the use of a ziconotide-specific antibody and a radioiodinated ziconotide derivative.[13, 37]

Radioimmunoassay is a sensitive and specific technique used mainly for the detection of hormones which are present in micromolar to picomolar range in the blood.[38, 39] However, the cost of generating specific antibodies and radioactive labeled antigens and safety issues involved in handling radioactive substances present some limitations to RIA.

Reversed-phase high performance liquid chromatography (RP-HPLC) coupled to mass spectrometry (MS) has been widely employed for the analysis of peptides and proteins in biological samples.[27, 32] The size of RP-HPLC columns and flow rates have been greatly reduced over the years to allow for the analysis of samples in limited amount. The lower flow rate required for small diameter columns reduces the amount of solvent that reaches the detector, resulting in a higher peptide concentration in the peak and hence, improved sensitivity.[40]

The development of an HPLC-MS method for the qualitative and quantitative determination of ziconotide will be discussed in this chapter. HPLC-tandem mass spectrometry (MS/MS) analysis of ziconotide will be presented. The optimization of various HPLC and mass spectrometric parameters will also be discussed together with the figures of merit of the method developed.

Experimental Section

Chemicals and Reagents

The conopeptides ω-conotoxin MVIIA (0.1 mg, ≥ 95% purity by HPLC) and ω-conotoxin GVIA (0.1 mg, 98.3% purity by HPLC) were purchased from Sigma-Aldrich (St. Louis, MO). Glacial acetic acid (HAc), trifluoroacetic acid (TFA), formic acid (FA) and HPLC-grade acetonitrile (ACN) were obtained from Thermo Fisher (Fair Lawn, NJ). Water used for solution preparation was purified by RiOs™ reverse osmosis and Milli-Q polishing systems (Millipore, Billerica, MA). Water used for peptide solution preparation was also vacuum-degassed to remove dissolved oxygen in order to minimize possible oxidation of ziconotide.

Instrumentation

A Surveyor Autosampler/HPLC system interfaced to a Thermo Finnigan (San Jose, CA) linear ion trap (LTQ) mass spectrometer equipped with an Ion Max electrospray ionization (ESI) source was employed for HPLC-MS/MS analyses. The HPLC system includes a quaternary, low-pressure mixing pump with vacuum degassing, an autosampler with a temperature-controlled tray and a column oven. The ESI needle is oriented at 45^{o} with respect to the axis of the ion transfer capillary. This configuration and the presence of the ion sweep cone prevent large droplets and particulates from entering the ion transfer capillary. A diagram showing the ion source interface, ion guide, mass analyzer and the dual detector system of the LTQ mass spectrometer is shown in Figure 2-1. The mass spectrometer and all peripheral components are controlled through the Xcalibur software (Thermo Scientific, San Jose, CA).

Solvent flow from the HPLC system was split with a stainless steel tee (Upchurch Scientific, Oak Harbor, WA) in order to achieve optimal flow rates (5 to 7 µL/min) for the small diameter column used for low flow ESI-MS analysis of ziconotide. A 0.5 µm pre-column filter (Upchurch Scientific, Oak Harbor, WA) was placed before the split tee to prevent small particles

from clogging the system. The flow coming out of the other end of the tee was connected to the divert valve on the LTQ mass spectrometer while the flow on the other end was sent to waste. The flow rate into the column was adjusted by connecting 15 or 50 cm of a 50 µm inner diameter (i.d.) Peeksil tubing (Upchurch Scientific, Oak Harbor, WA) at the waste end of the split tee. This instrumental set-up is illustrated in Figure 2-2. Black PEEK tubing (1/16" x 0.004") with a smaller i.d. than the red PEEK tubing (1/16" x 0.005") used before the column, was connected post-column to minimize peak broadening. This PEEK tubing was purchased from Thermo Fisher (Fair Lawn, NJ).

Optimization of Mass Spectrometric Parameters

Mass calibration was performed with a calibration solution consisting of caffeine, MRFA (L-Methionyl-arginyl-phenylalanyl-alanine) and Ultramark 1621. The calibration solution was prepared according to the recommended procedure outlined in the Finnigan LTQ Getting Started manual and infused directly into the mass spectrometer at 3 µL/min.[41] Mass spectrometric parameters were optimized using the automatic, semi-automatic and manual tuning features of the LTQ. A 10 ng/µL ziconotide solution in 40:60 ACN: H_2O with 0.1% HAc: 0.01% TFA was used as the tune solution for experiments involving conventional electrospray. Conventional electrospray, in this case, refers to analyte solution flow rates of 75 or 200 µL/min. The ziconotide solution was placed in a 250 µL Hamilton syringe (Reno, NV) and flow from the syringe (10 to 20 µL/min) was teed in with 75 or 200 µL/min of 40:60 ACN: H_2O with 0.1% HAc: 0.02% TFA before introduction into the mass spectrometer. A 1 ng/µL ziconotide solution in 50:50 ACN: H_2O with 0.1% formic acid was used as the tune solution for low flow experiments. The tune solution, in this case, was infused directly into the mass spectrometer at 5 µL/min. Signal intensity from the total ion current (TIC) or specific ions of ziconotide was monitored during tuning. Manual tuning was first performed to determine the optimum ESI

probe position and gas flows. Automatic tuning was then employed to optimize the voltages for the capillary, tube lens and various multipoles and lenses making up the ion optics of the LTQ. Semi- automatic tuning was used to determine if further improvement in signal could be achieved by moderate adjustments in the voltages obtained from automatic tuning.

Optimization of HPLC Parameters

Isocratic elution with solvents containing various concentrations of methanol with 0.5% HAc in water (*i.e.*, 10:90, 20:80, 50:50 and 70:30 MeOH:H_2O mixtures) was employed for the HPLC-low flow ESI-MS analysis of ziconotide. The peak shape and retention time obtained with the various solvents were evaluated. Gradient elution with 0.5% HAc in 10:90, 20:80 and 30:70 MeOH: H_2O mixtures at the start of the gradient was also performed. Chromatographic separation was achieved with a Targa C_{18} column (0.3 x 100 mm, 5 µm particles, 120 Å pore size) from Higgins Analytical (Mountain View, CA). The effects of using acetonitrile with 0.1% FA and other acids such as 0.01% TFA and a combination of HAc and TFA as the organic mobile phase on the peak shape and retention of ziconotide were also explored.

The effects of varying the TFA concentration of the mobile phase on the charge state distribution and response of ziconotide and ω-conotoxin GVIA were systematically investigated using conventional electrospray. A solution containing 1 ng/µL each of ziconotide and the internal standard (IS), ω-conotoxin GVIA, was used for the evaluation. Reversed-phase HPLC was performed with an Atlantis® dC_{18} column (2.1 x 150 mm, 5 µm particles, 300 Å pore size) with a guard column (2.1 x 20 mm, 5 µm particles) from Waters Incorporation (Milford, MA). The following TFA concentrations were used: 0.01, 0.02, 0.025, 0.03, 0.05, 0.075 and 0.1%. The effects of varying the acetic acid composition (0.01, 0.025, 0.05, 0.075 and 0.1%) of the mobile phase while keeping TFA at 0.01% were also investigated.

The peak shape and retention time of ziconotide after elution from the Atlantis® dC_{18} column using 0.1% HAc: 0.02% TFA as the acid component of the mobile phase were compared to those from a Jupiter Proteo C_{12} column (Phenomenex, Torrance, CA). The Jupiter Proteo C_{12} column (2 x 150 mm, 4 µm particles, 90 Å pore size) was used with a Security Guard™ cartridge (4 x 2 mm, C_{12}) to protect the analytical column. The chromatogram of ziconotide eluted with 0.1% formic acid in the mobile phase from a new Jupiter Proteo C_{12} column was also compared to that obtained with 0.1% HAc: 0.02% TFA. A smaller diameter Atlantis® dC_{18} column (1 x 150 mm, 5 µm particles, 300 Å pore size) that required lower flow rates (75 µL/min) of analyte solution was used to determine if improvement in the amount of ziconotide detected could be achieved.

Preparation of Calibration Standards

Serial dilution of a 40 ng/µL aqueous ziconotide solution was carried out to prepare 11 calibration standards with concentrations ranging from 0.05 to 10 ng/µL. A fixed amount of an aqueous internal standard, ω-conotoxin GVIA, was added to each standard to achieve a final concentration of 1 ng/µL in solution. The calibration standards were prepared fresh in 1:99 ACN: H_2O with 0.1 % HAc: 0.01% TFA before each analysis. Six calibration curves from separate sample dilutions were prepared and analyzed. Quality control (QC) samples with ziconotide concentrations at 0.06, 0.6 and 6 ng/µL were prepared in duplicate and analyzed with each calibration curve.

HPLC-ESI-MS/MS Analysis

Manual loop injections of 2 µL of 1 ng/µL ziconotide in 1:99 MeOH:H_2O with 0.5% HAc were carried out with isocratic and gradient elution for analyses involving low flow electrospray Isocratic elution with acidified solvents was performed for 30 min. Pre-mixed solvents were

used for isocratic elution to minimize variability in response caused by inefficient online solvent mixing at low flow rates. Gradient elution with various acidified solvents was also employed for the analysis of ziconotide. The gradient included a 1 min aqueous hold at the start of the run, increase in percentage of the organic solvent from starting conditions to 90% for the next 10 min, and a 4 min organic hold. The column was then allowed to equilibrate to starting conditions for 15 min. The post-column flow rate after splitting was 7 µL/min. The column oven was set to 30 °C while the autosampler tray was maintained at 12 °C.

Gradient elution with 0.1% HAc: 0.02% TFA in water as solvent A and 0.1% HAc: 0.02% TFA in ACN as solvent B, with solvent B raised from 2 to 70% in 9 min was carried out for conventional electrospray experiments. This was followed by a 6.5 min column equilibration to initial solvent composition. A flow rate of 200 µL/min was used. Using the partial loop injection mode, 10 µL of the sample was loaded into the column. External and internal syringe needle washes with 0.1% HAc: 0.01% TFA in 50:50 ACN: water were incorporated in the autosampler method to eliminate carry-over. The column oven and autosampler tray temperatures were the same as those used in the low flow experiments. Similar gradient and instrument conditions were employed in the evaluation of other solvent systems.

Electrospray ionization in the positive mode was employed for both conventional and low flow experiments. Spray voltage for the fused silica capillary used during low flow electrospray analyses was set at 4.25kV while the capillary voltage was at 40 V. The capillary temperature was maintained at 160 °C while a sheath gas flow of 25 arbitrary units was used. A lower spray voltage, 3.75 kV, was used for the metal capillary installed for analyses at higher flow rate to prevent arcing. The capillary voltage was set to 45 V. The capillary temperature was maintained at 300 °C. Sheath gas flow was set to 40 and that of the auxiliary gas to 10 arbitrary units.

Mass spectra for low flow electrospray experiments were acquired for 30 min. The LTQ was programmed for full scan MS then full scan MS/MS (*m/z* 400 – 1400) of *m/z* 661, the quadruply-charged ion of ziconotide. The precursor ion isolation width in full-scan MS/MS mode was set to 3 *m/z* with collision energy (CE) at 30% and activation energy (q) at 0.250. The LTQ mass spectrometer was set to acquire for 10 min for conventional electrospray analyses. Sample from the chromatographic column during the first 2 min and last 0.5 min was diverted to waste. The LTQ was programmed for full-scan MS (*m/z* 500 – 1600) then full-scan MS/MS (*m/z* 500 – 1400) of *m/z* 661 and *m/z* 760, the +4 ions of ziconotide and ω-conotoxin GVIA, respectively. The rest of the parameters used for full-scan MS/MS of the precursor ions were similar to those employed in low flow experiments.

MS Data Analysis

Extracted ion chromatograms (EICs) for the various ions of ziconotide and the IS, ω-conotoxin GVIA, were generated using the Xcalibur software. Chromatograms were processed using a 3-point boxcar smoothing calculation which is available with the software. The peaks for the various charge states of ziconotide and the IS, as well as that of oxidized ziconotide, were manually integrated to determine the area for each. The sum of the contributions of the +3 and +4 ions of oxidized ziconotide was used for its EIC. The ratio of the peak area of the +4 ion of ziconotide to that of the IS was plotted against ziconotide concentration to generate the calibration curve. Weighted least squares linear regression (WLSLR) was used for data fitting, with $1/x^2$ as the weighting scheme of choice.[42, 43] GraphPad Prism® Version 5.01 (San Diego, CA) was used for data processing.

The need to apply weighting was determined by following the statistical evaluation scheme employed by Almeida *et al.*.[43] The evaluation was conducted to establish if a particular data set

exhibited equal variance across the whole range of values being considered, a condition termed as homoscedasticity and to justify the use of weighting if homoscedasticity was not obeyed.[43] An F-test (see Equation 2-1) and a plot of y-residual (difference between experimental and fitted area ratios of the +4 ions of ziconotide to ω-conotoxin GVIA) versus concentration were evaluated to determine if homoscedasticity was obeyed.

$$F_{exp} = s_2^2/s_1^2 \qquad (2\text{-}1)$$

$$F_{tab}\,(f_1, f_2; 0.99)$$

where s_1^2: variance of the lowest calibration standard
s_2^2: variance of the highest calibration standard
F_{tab}: value from F-table at 99%confidence level
f_1, f_2: degrees of freedom, equal to n-1
n: number of replicates

The choice of the appropriate weighting scheme, on the other hand, is based on plots of percent relative error (%RE) versus concentration and the %RE sum.[43] The percent relative error compares the concentration calculated (C_{calc}) from the regression equation obtained for each weighting factor, w_i, with the nominal standard concentration ($C_{nominal}$), see Equation 2-2. The %RE sum is defined as the sum of the absolute values of %RE and is found to be a useful indicator of goodness of fit of the resulting regression line after application of a weighting factor.[43, 44]

$$\%\ RE = [(C_{calc} - C_{nominal})/\ C_{nominal}] \times 100 \qquad (2\text{-}2)$$

Results and Discussion

Optimized Mass Spectrometric Parameters for Ziconotide Analysis

When tuning the LTQ to optimize the signal for ziconotide, manual tuning to determine the best ESI probe position and optimum gas flows was first carried out. The total ion current for ziconotide was monitored while adjusting the ESI probe to a position that yielded the highest

signal for ziconotide. The ESI probe was positioned closer to the ion transfer capillary for optimum response during low flow electrospray analyses. The same procedure of monitoring the TIC for ziconotide was carried out to determine the optimum gas flows. A sheath gas flow of 40 (arbitrary units) and auxiliary gas flow of 20 (arbitrary units) showed the highest signal for ziconotide for experiments conducted at 200 µL/min. The use of auxilliary gas was found to lessen the contribution of TFA adducts, as seen in Figure 2-3. Nitrogen was applied as an inner coaxial gas when sheath gas was used.[41] It facilitated nebulization of the sample solution. Auxiliary gas aided in focusing the spray plume and improved desolvation.[41] In contrast, auxiliary gas was not required for low flow electrospray.

Comparisons of the normalized response of ziconotide (average of 200 scans) at various spray voltages, tube lens offset voltages and capillary temperatures were carried out to determine the optimum setting for these parameters. The effects of the tube lens offset voltage on the response and charge state distribution of ziconotide are illustrated in Figure 2-4. Comparison of these mass spectra and the normalized response of the +3 and +4 ions of ziconotide at *m/z* 661 and *m/z* 881, respectively, established 160 V as the optimum tube lens offset voltage for conventional electrospray. The response of *m/z* 661 was slightly higher at 100 V but contributions from TFA adducts were more significant. Lower normalized responses were obtained for both the +3 and +4 ions of ziconotide at 200 V. The abundance of the higher *m/z* ions (+2 and +3) was observed to be greater than that of the lower *m/z* ions (+4 and +5) at higher tube lens offset voltage. Tuning for the tube lens offset voltage ensures maximum transmission of ions from the electrospray ion source to the mass analyzer.[45] Comparison of the results obtained from various capillary temperatures (*i.e.*, 250, 275 and 300 °C) showed an increase in the abundance of TFA adducts as the temperature was decreased. In order to achieve sufficient

desolvation of the sample and minimize the contribution of TFA adducts, a capillary temperature of 300 °C was used. A lower temperature was required for analyses involving low flow electrospray.

Optimized HPLC Parameters for Ziconotide Analysis

Effect of Various Solvent Systems and Flow Rates on Ziconotide Response

Isocratic elution of 1 ng/µL ziconotide in 1:99 MeOH:H_2O with 0.5% HAc using 70:30 MeOH: H_2O with 0.5% HAc yielded the most satisfactory peak shape for ziconotide compared to acidified 10:90, 20:80 and 50:50 MeOH:H_2O mixtures (Figure 2-5). Peaks eluted with 10:90, 20:80 and 50:50 MeOH:H_2O mixtures were retained in the column extensively. The retention times of ziconotide peaks eluted with 0.5% HAc in 50:50 and 70:30 MeOH:H_2O mixtures follow the expected order of elution based on the organic composition of the solvent. A higher organic composition of the mobile phase facilitates earlier elution of peptide peaks and this was observedwith the ziconotide peaks eluted with 0.5% HAc in 50:50 and 70:30 MeOH:H_2O mixtures. This was not the case, however, with the peaks obtained from 0.5% HAc in 10:90 and 20:80 MeOH:H_2O mixtures. The retention time for ziconotide peak eluted with acidified 10:90 MeOH:H_2O was shorter than that of acidified 20:80 MeOH:H_2O. Inspection of the mass spectra of peaks eluted with 0.5% HAc in 10:90 and 20:80 MeOH:H_2O mixtures (bottom panel in Figure 2-6) showed greater signal of background ions than ziconotide. The increased background signal could have caused the incorrect elution order of ziconotide observed with these solvents.

Gradient elution of ziconotide at low flow rates with solvents containing 0.5% HAc and various methanol concentrations at the start of the gradient was also conducted to evaluate the effect of gradient elution on the peak shape and retention of ziconotide on the Targa column (0.3 x 100 mm, 5 µm particles, 120 Å pore size). Peaks that showed signs of tailing were obtained even with gradient elution (Figure 2-7). The mechanism of peptide and protein retention is based

on their adsorption to hydrophobic surfaces such as the stationary phase in C_{12} or C_{18} columns and desorption from the surface once a specific organic composition is reached.[46] Retention of peptides and proteins on columns changes abruptly when the concentration of organic solvent required to desorb them from the hydrophobic surface is reached and this results to sharper peaks. The absence of narrow peaks from the gradient elution of ziconotide suggests potential silanol interactions with the stationary phase of the column which could be causing the tailing observed. The mass spectra of ziconotide peaks from the gradient elutions showed the +4 ion (*m/z* 661) as the most abundant ion.

Interest in the methanol – acetic acid solvent system was influenced by efforts to repeat the results of HPLC-low flow ESI-MS/MS experiments conducted at the University of North Texas (UNT) Health Science Center as a result of collaboration with the University of Florida Racing Laboratory. Good peak shape (minimal tailing) and retention of ziconotide and one of its MS/MS product ions were obtained with loop injections of 3 µL of 5 ng/µL ziconotide, gradient elution and low flow electrospray analysis using the same Targa column and split flow system (data not shown). Loop injection of a 10 ng/µL ziconotide solution yielded a peak with an area twice as much as that of the peak for 5 ng/µL. These promising preliminary results led us to pursue and repeat the experiments that were conducted at UNT but differences in the HPLC system and instrumental set-up details could have prevented a successful repetition of experimental results.

Isocratic elution using 15:85 ACN:H_2O with 0.1% FA, 0.01% TFA and 0.1% HAc: 0.05% TFA as acid components of the mobile phase was also explored. Improvement in peak shape was observed with the addition of TFA to the mobile phases but its ionization suppression effects were observed with a decrease in peak area of ziconotide (Figure 2-8). The corresponding mass

spectra of ziconotide peaks from the isocratic elution with 15:85 ACN:H_2O containing various acid components exhibited differences in the identity and abundance of ions present (Figure 2-9). The use of 0.1% HAc: 0.05% TFA as acid component of the mobile phase showed the +3 and +4 ions of ziconotide as the abundant ions in the mass spectrum and the signal contribution from TFA adducts to be minimal.

The inability to achieve significant retention of ziconotide on the Targa column and the challenges imposed by modifying a standard HPLC system to carry out gradient elution at low flow rates led us to study and carry out experiments at high flow rates to evaluate how ziconotide behaves at conditions compatible with the HPLC-MS system available. There was a need to achieve significant column retention because polar components of biological samples like salts and other unwanted contaminants elute early during a gradient run. Longer retention time of the analyte of interest is desired to minimize contamination and/or potential signal suppression from these other sample components mentioned. The use of low flow rates is often not compatible with many standard HPLC systems, especially in a gradient mode. The contribution of extracolumn volumes in the injector and connecting tubing to band spreading also becomes more significant at low flow rates.[23] The succeeding sections, therefore, pertain to experiments conducted at high flow rates (*i.e.* 75 and 200 µL/min).

With the tendency of ziconotide to be retained in the column and the ability of TFA to improve peak shape, solvent systems with varying concentrations of TFA and varying concentrations of acetic acid in a solvent mixture with TFA were evaluated for their effects on the charge state distribution and response of ziconotide and ω-conotoxin GVIA. A solution containing 1 ng/µL each of ziconotide and the IS was used for the evaluation. The optimized

MS parameters were used in the analyses. The conopeptide ω-conotoxin GVIA was chosen as the IS because of its similar ESI-MS/MS characteristics to ziconotide.

Results from the various concentrations of TFA (*i.e.*, 0.01, 0.02, 0.025, 0.03, 0.05, 0.075 and 0.1%) used are illustrated in Figure 2-10. The predominant charge state observed for ziconotide with TFA in the mobile phase was the +3 ion (*m/z* 881). The +4 (*m/z* 661) and +5 (*m/z* 529) ions were also present. A TFA adduct at *m/z* 918 was also observed in the mass spectrum of ziconotide. The highest peak area for the +3 ion of ziconotide was observed at 0.025% TFA. There was a good trend in the peak area across the TFA concentrations used, increasing as 0.025% was approached and decreasing towards high concentrations. High concentrations of TFA are known to cause signal suppression when used with an electrospray interface.[47]

The +3 charge state (*m/z* 1014) was also the most predominant ion for ω-conotoxin GVIA (see Figure 2-11). The +4 ion (*m/z* 760) and a TFA adduct (*m/z* 1050) were also observed. The +5 ion (*m/z* 609) was only detected with 0.01% TFA in the mobile phase. The highest signal for the +3 ion of the IS was obtained with 0.025% TFA as well. The use of HAc and TFA mixture as the acid component of mobile phases for HPLC-MS studies of conopeptides has been reported.[48, 49] The effects of varying the HAc composition (0.01, 0.025, 0.05, 0.075 and 0.1%) of the mobile phases while keeping TFA at the lowest concentration, 0.01%, were investigated in this study (see Figure 2-12). The highest response for ziconotide with minimal contribution from TFA adducts were found at 0.1% HAc. The average peak areas for the +3 and +4 ions was comparable at this HAc concentration and the only TFA adduct observed was at *m/z* 918. Significant contribution from other TFA adducts at *m/z* 689 and *m/z* 955 was observed at HAc concentrations lower than 0.1%. Similarly, the highest response for ω-conotoxin GVIA with

minimal contribution from TFA adducts was observed at 0.1% HAc also (see Figure 2-13). The +3 and +4 charge states were the predominant ions in the mass spectra of the peptide at this HAc concentration. The signal for the only TFA adduct observed at *m/z* 1013 decreased as the HAc concentration was increased. Based on the evaluation of the mobile phase acid composition conducted and considerations for minimizing signal suppression and system contamination with TFA, 0.1% HAc with 0.01% TFA proved to be a good choice for the acid component of the mobile phases.

The use of a smaller diameter Atlantis® dC_{18} column (1 x 150 mm, 5 µm particles, 300 Å pore size) was explored to determine if improvements in sensitivity could be achieved. As shown in Figure 2-14, the lowest amount of ziconotide detected on the small diameter column (50 pg), was greater than the lowest amount detected on the larger diameter column (20 pg). There was no enhancement in detection sensitivity observed with the use of small diameter column, in this case. The corresponding mass spectra of the ziconotide peaks detected are presented in Figure 2-15.

Effect of Column Chemistry on Peak Shape and Retention of Ziconotide

The need to use a column with minimal silanol group interaction became evident as ziconotide exhibited a tendency to be retained in the column due to its basicity. Electrostatic interactions of residual silanols with cationic species cause peak tailing which may result in loss of chromatographic resolution.[50] Analysis of ziconotide with a new Jupiter Proteo C_{12} column using 0.1% HAc: 0.01% TFA as the acid component of the mobile phases showed a peak with significant tailing (Figure 2-16). Its peak shape was improved when the TFA concentration was increased to 0.02%. With the reduction of peak tailing observed with 0.02% TFA, 0.1% HAc: 0.02% TFA was used as the acid component of the HPLC solvents for the rest of the experiment conducted. The history of column use seemed to have an effect on the peak shape for ziconotide

analyzed using the Atlantis dC_{18} column. Good peak shape was not obtained with a new Atlantis dC_{18} column as compared to one that had been previously used for analysis of plasma extracts of small drug molecules (data not shown). The peak shape obtained with this particular column even with 0.1% HAc: 0.02% TFA in the solvents was not as good as that from the Jupiter Proteo C_{12} column (Figure 2-16). The use of formic acid was also evaluated on the Jupiter Proteo C_{12} column prior to any column treatment with TFA and results showed extensive retention of ziconotide on the column (Figure 2-16).

The importance of the purity of silica in the choice of column for ziconotide analysis was emphasized by comparing the peak shape obtained with the Jupiter Proteo C_{12} column and Atlantis dC_{18} column using the optimum solvent system. The minimal tailing of the ziconotide peak obtained with the Jupiter Proteo C_{12} column using 0.1% HAc: 0.02% TFA in the HPLC solvents, compared to that from the Atlantis dC_{18} column, indicates that fewer residual silanol groups are present in this particular column. Improvement in peak shape was also observed with a combination of acetic acid and trifluoroacetic acid in the solvents compared to formic acid.

Weighted Least Squares Linear Regression

The use of weighted least squares linear regression counteracts the greater influence of the higher concentrations on the fitted regression line for analyses of drug molecules in biological samples.[42-44] The need to apply weighting, in this case, is supported by the residual versus concentration plot (Figure 2-17) and results from the F-test (Table 2-1). The residual plot showed that the variance was not randomly distributed around the concentration axis. Greater variance was observed for ziconotide standards with higher concentrations compared to those at lower concentrations. Results from the inter-day assay of 6 calibration curves consisting of 11 standards with concentrations ranging from 0.05 to 10 ng/µL were included in the plot. Data for 0.08, 0.3 and 0.8 ng/µL standards were excluded to show the distribution of the low

concentration calibrators more clearly. A data entry for the 3.0 ng/µL standard was excluded due to pipetting error. The experimental F-value (F_{exp} = 1.73 x 10^4) was also significantly higher than the tabulated value (F_{tab} = 10.97). These results suggested that homoscedasticity was not met and supported the need to use WLSLR.

Figure 2-18 shows the percent relative error plots for unweighted (Model 1) and weighted (Models 2-5) regressions of ziconotide standards from the inter-day assay. The %REs for concentrations less than 0.5 ng/µL obtained with Model 1 were much greater than those obtained for the other models. The best accuracy and %RE distribution scatter especially at the low concentration range of the curve was obtained with models that employed $1/x^2$ (Model 2) and $1/y^2$ (Model 3) as the weighting factors.

The regression parameters of the calibration curve generated for each weighting factor (with all the calibration standards included) and the respective sums of the relative errors are summarized in Table 2-2. The most adequate approximation of variance was achieved with the weighting factor $1/x^2$ (Model 2) which provided the least %RE sum for the data. Considering this result and that of the %RE distribution scatter, $1/x^2$ was chosen as the weighting factor.

Generation of the Response Curve for Ziconotide

Eleven ziconotide standards with concentrations ranging from 0.05 to 10 ng/µL, containing 1 ng/µL of the IS, ω-conotoxin GVIA, were analyzed using HPLC-ESI-MS/MS. The area ratio of the quadruply-charged ions of ziconotide at *m/z* 661 to ω-conotoxin GVIA at *m/z* 760 was plotted against ziconotide concentration to generate the calibration or response curve (Figure 2-19). Reagent blanks were not analyzed with the calibration curve standards due to carry-over issues especially after injection of the highest concentration calibrator. Solvent blanks of 50:50 ACN: H_2O with 0.1% HAc: 0.01% TFA were injected instead. Calibration curves from six

independent sample dilutions were prepared and analyzed, one set per day, for six different days. These calibration curves were employed for the determination of the figures of merit of the method and the validation study discussed in detail in Chapter 4. Quality control (QC) samples were analyzed with each calibration curve and the quantitation results for the QCs were used in the validation study.

The regression parameters for the six response curves are shown in Table 2-3. A data entry for the 3.0 ng/µL standard was excluded due to pipetting error. The slope and y-intercept values obtained were reproducible. The range of y-intercepts obtained, however, did not contain zero. Possible suppression of ziconotide's signal due to the IS signal could occur at very low concentrations and account for the negative y-intercepts.[51] Figure 2-20 shows the response of the +4 ion of the IS at *m/z* 760 with increasing ziconotide concentration.

Analysis of back-calculated concentrations of calibration standards yielded percent relative standard deviations (%RSDs) of less than 5.9% and %REs of less than 3.3% (Table 2-4). All the calibration curves satisfied the Food and Drug Administration's (FDA) requirement that at least 67% of the calibrators should have %REs and %RSDs of ≤ 15% except at the lower limit of quantitation (LLOQ) where a value of ≤ 20% is still considered passing.

The limit of detection (LOD) and LLOQ were determined from peak area values for *m/z* 661 recorded from 10 blank analyses. The blank solution, in this case, is the solvent used in preparing the ziconotide standards, 0.1% HAc: 0.01% TFA in water. The average (S_{bl}) and standard deviation (s_{bl}) of the blank measurements were calculated and incorporated into equation 2-3, where S_{LOD} corresponds to the signal required for the LOD.

$$S_{LOD} = S_{bl} + 3(s_{bl}) \qquad (2\text{-}3)$$

The constant 3 in equation 2-3 represents a confidence level of detection of 89% or greater, and is the value recommended in literature.[52-54] The signal at LOD is then incorporated into equation 2-4 to determine the concentration at LOD (C_{LOD}), wherein m is the slope of the calibration plot for the peak area of *m/z* 661 vs. ziconotide concentration (data not shown).

$$C_{LOD} = (S_{LOD} - S_{bl})/m \quad (2\text{-}4)$$

The LOD for intact ziconotide using the HPLC-ESI-MS method developed was found to be 6 pg on column.

The lower limit of quantitation was calculated as 10 times the standard deviation of the blank measurement, s_{bl} (Equation 2-5).

$$C_{LLOQ} = (10 \times s_{bl})/m \quad (2\text{-}5)$$

The LLOQ for intact ziconotide obtained by using the above equation was determined to be 20 pg on column.

Higher values for LOD and LLOQ were obtained when the FDA guidelines were used to evaluate the ziconotide standards analyzed and results from injections of up to 0.001 ng/µL ziconotide solution were considered. The LLOQ according to the FDA is the lowest concentration that can be determined with acceptable accuracy (%RE ≤ 20%) and precision (%RSD ≤ 20%).[55] The lowest calibrator, 0.05 ng/µL, satisfied these criteria and was determined to be the LLOQ. This concentration corresponds to 0.5 ng on column, compared to the 20 pg obtained from blank measurements. A 0.01 ng/µL ziconotide solution was also analyzed with initial calibration curve runs but it did not satisfy the FDA's guidelines for precision and accuracy after performing calculations. The limit of detection was determined from the ziconotide concentration that exhibited a signal to noise ratio (S/N) of at least 3. The LOD using this definition corresponds to 20 pg on column. The presence of other components in the

conopeptide solutions analyzed could have contributed to the differences in LOD and LLOQ values obtained. The response of ziconotide was linear from 0.05 to 10 ng/µL.

Representative extracted ion chromatograms of ziconotide and the internal standard, ω-conotoxin GVIA, are shown in Figure 2-21 with the corresponding mass spectra in Figure 2-22. A peak that eluted earlier than ziconotide was identified as its oxidized form. Its chromatogram and mass spectrum were also included in Figures 2-21 and 2-22, respectively.

One of the identified degradation pathways of ziconotide involves oxidation of its methionine residue.[13, 56] Methionine is first oxidized to its sulfoxide and under strong oxidizing conditions, to a sulfone (Figure 2-23).[57] Reagents like 95% performic acid oxidize methionine to methionine sulfone.[58] The mass of the early eluting peak was found to be 16 Da more than the mass of ziconotide. The addition of 16 Da in mass is commonly associated to oxidation or the incorporation of oxygen to the original structure of a compound. The mass shift observed, in this case, corresponds most likely to the oxidation of the methionine residue of ziconotide to its sulfoxide form. The product ion spectra of the +4 ions of ziconotide and the IS are shown in Figure 2-24. The extensive cross-linking from the multiple disulfide bonds of ziconotide makes it less susceptible to collisional fragmentation. The only product ions identified from its MS/MS spectrum resulted from loss of water molecules. Without the aid of analysis software, identifying the rest of the fragments obtained will be difficult.

Conclusion

A robust and sensitive HPLC-ESI-MS method was developed for the analysis of intact ziconotide. The use of a high purity silica column with low concentration of trifluoroacetic in the HPLC solvents improved the peak shape of ziconotide. The use of acetic and TFA as acid components of the mobile phases enhanced the specificity of detection for ziconotide. Two of

the characteristic ions of ziconotide were present in significant abundance in its mass spectrum when a combination of HAc and TFA was used compared to a single predominant ion when TFA only was added to the mobile phases. Increasing the percentage of HAc improved the response of the ziconotide ions. Optimization of mass spectrometric parameters such as gas flows, tube lens offset voltage and capillary temperature help reduce the signal contribution of TFA adducts which resulted to enhanced signal for ziconotide ions. The limit of quantitation for this method was found to be 0.5 ng of intact ziconotide on column while the limit of detection was 0.02 ng. The presence of multiple disulfide linkages, however, limits the structural information that can be derived from its MS/MS spectrum.

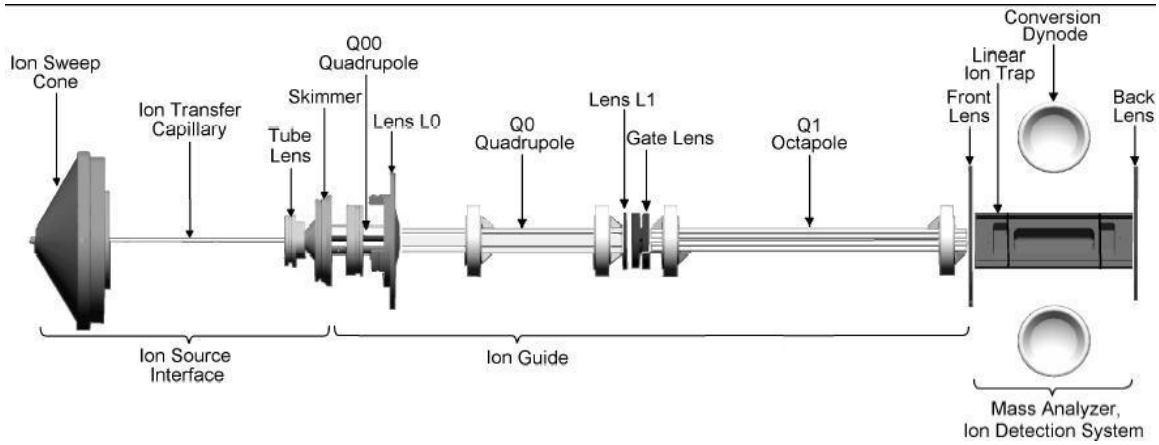

Figure 2-1. Internal components of the LTQ mass spectrometer. Adapted from the Finnigan LTQ Hardware Manual.[45]

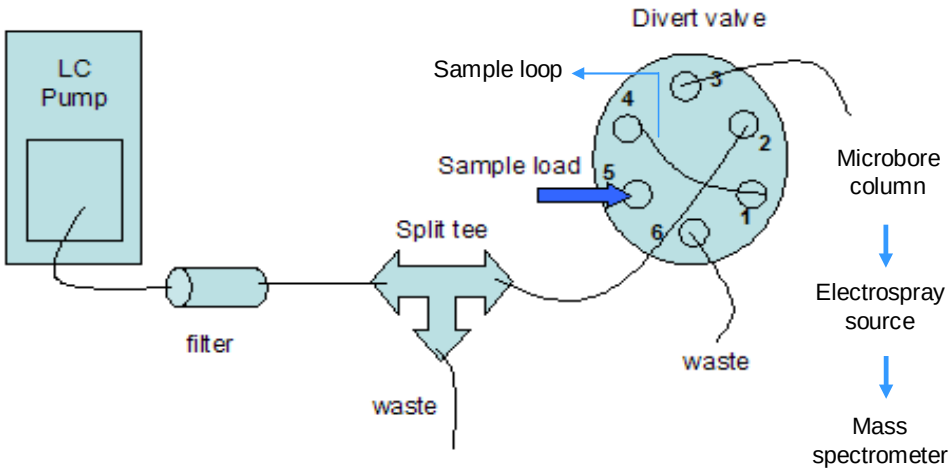

Figure 2-2. Instrument set-up for the HPLC-low flow ESI-MS analysis of ziconotide. Solvent flow from the HPLC is split to achieve optimum flow rates for the Targa C_{18} column (0.3 x 100 mm, 5 µm particle size). Sample is loaded onto a 2 µL sample loop and during injection, solvent flow transports the sample into the column and electrospray source then into the mass spectrometer. Figure is not drawn to scale.

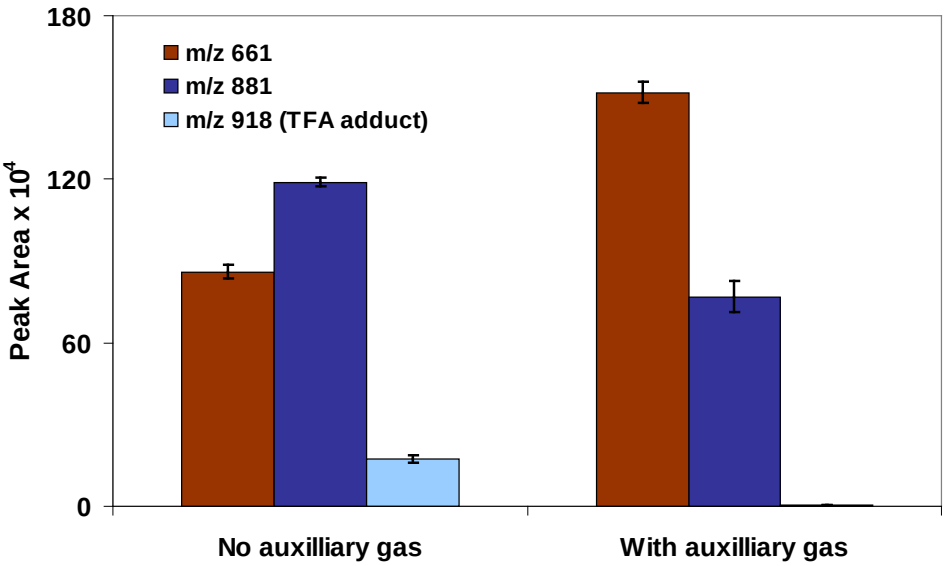

Figure 2-3. Response of ziconotide and TFA adduct with and without auxiliary gas flow. Signal contribution from the predominant TFA adduct of ziconotide was reduced when auxiliary gas was used with the sheath gas. The data are an average of 3 replicate analyses and error bars represent the standard deviation of the replicates.

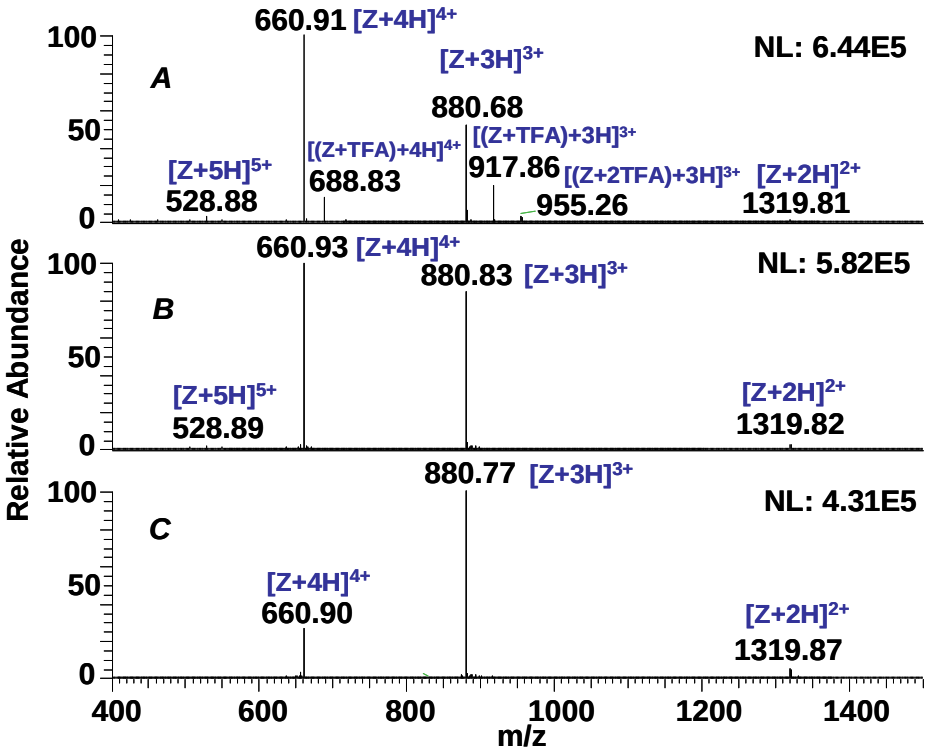

Figure 2-4. Effects of various tube lens offset voltages on the full scan mass spectra of ziconotide: (*A*) 100 V, (*B*) 160 V and (*C*) 200 V. The optimum tube lens offset voltage was determined at 160 V where the signal for both the +3 and +4 ions of ziconotide are abundant and contribution from TFA adducts is minimal. spray voltage: 3.75 kV, capillary temperature: 300 °C, sheath gas: 40, auxiliary gas: 20, NL: normalized level

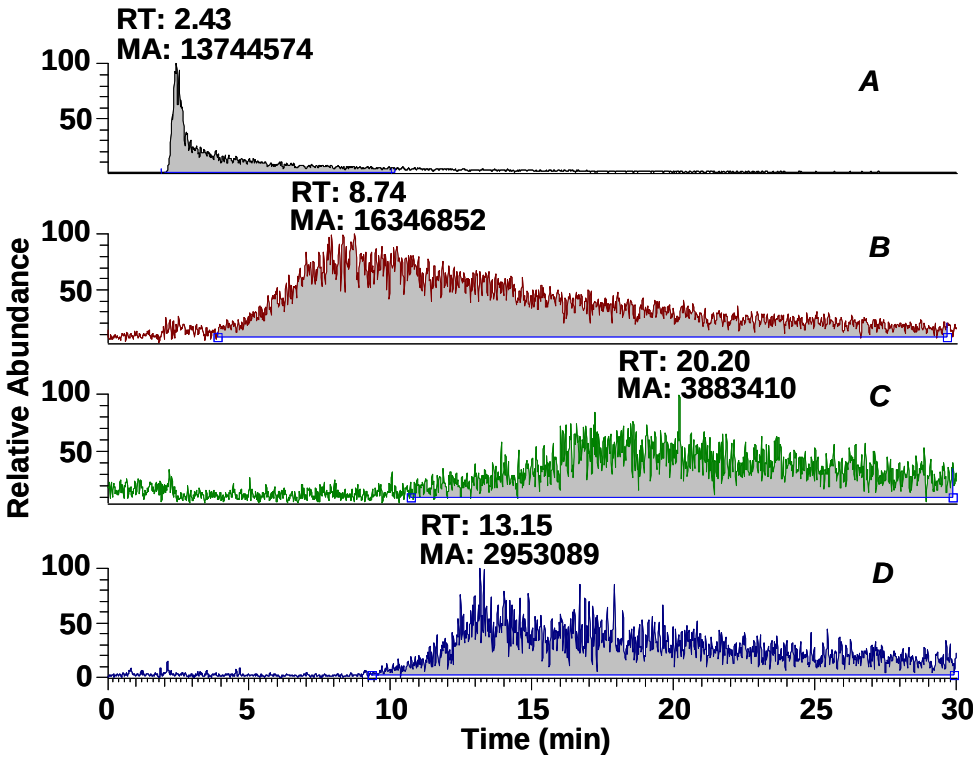

Figure 2-5. Extracted ion chromatograms of *m/z* 661 from low flow isocratic elution of ziconotide using 0.5% HAc in (*A*) 70:30, (*B*) 50:50, (*C*) 20:80 and (*D*) 10:90 MeOH: H_2O mixtures. The best peak shape was obtained with 0.5% HAc in 70:30 MeOH:H_2O as the mobile phase. The peak, however, elutes early in the chromatographic run. RT: retention time, MA: manually integrated area

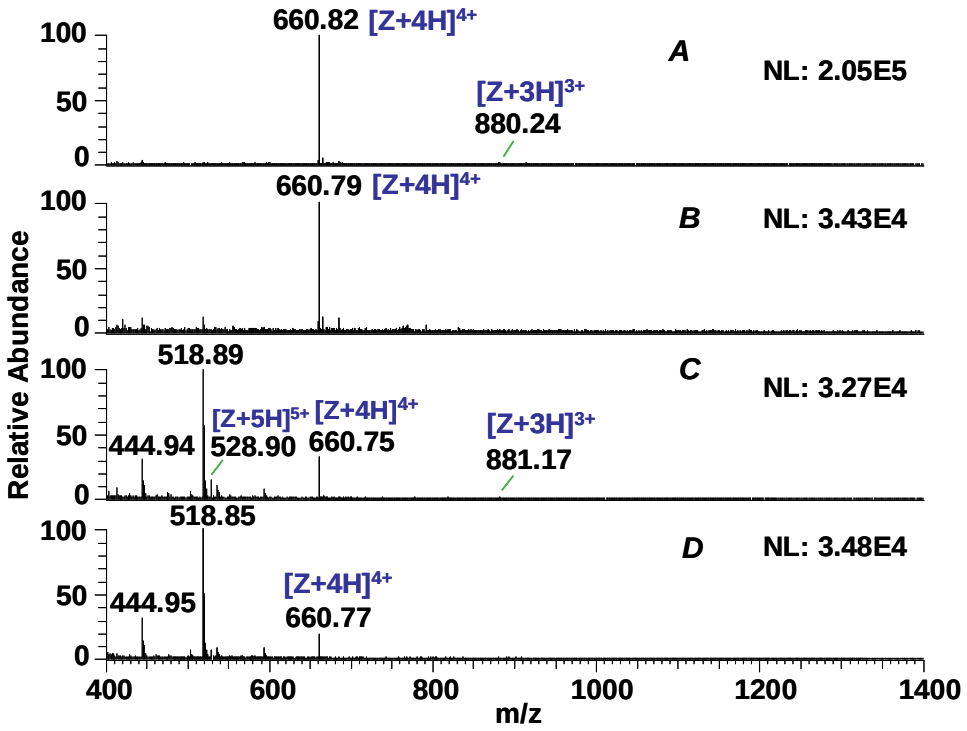

Figure 2-6. Mass spectra of ziconotide peaks that were eluted isocratically with 0.5% HAc in (*A*) 70:30, (*B*) 50:50, (*C*) 20:80 and (*D*) 10:90 MeOH: H_2O mixtures.

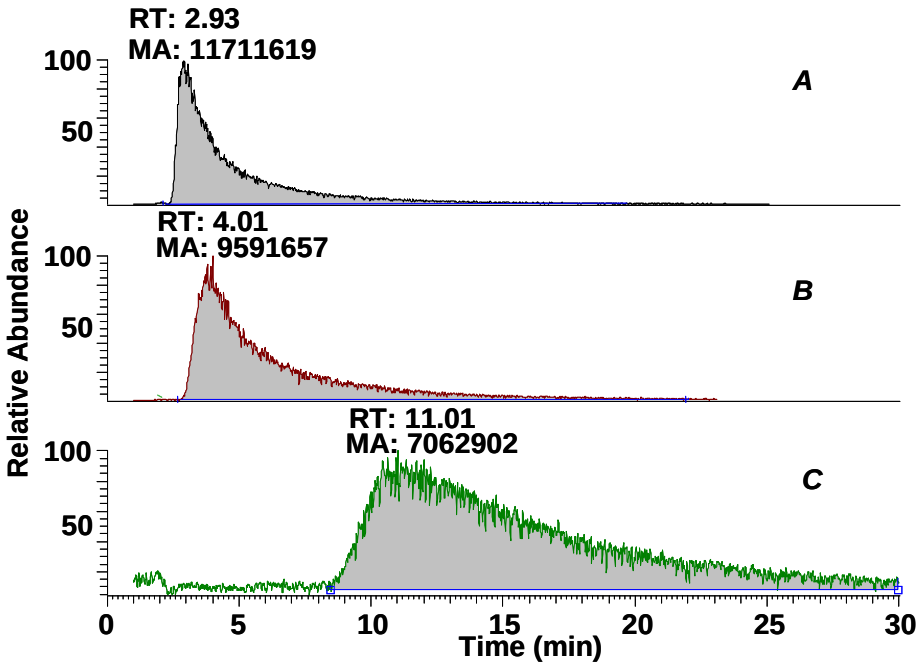

Figure 2-7. Extracted ion chromatograms of *m/z* 661 from low flow gradient elution of ziconotide with 0.5% HAc in (*A*) 70:30, (*B*) 20:80 and (*C*) 10:90 MeOH: H_2O mixtures as starting mobile phase compositions. Better peak shape was obtained with 0.5% HAc in 70:30 and 20:80 MeOH:H_2O compared to acidified 10:90 MeOH: H_2O. All peaks, however, exhibited tailing. RT: retention time, MA: manually integrated area

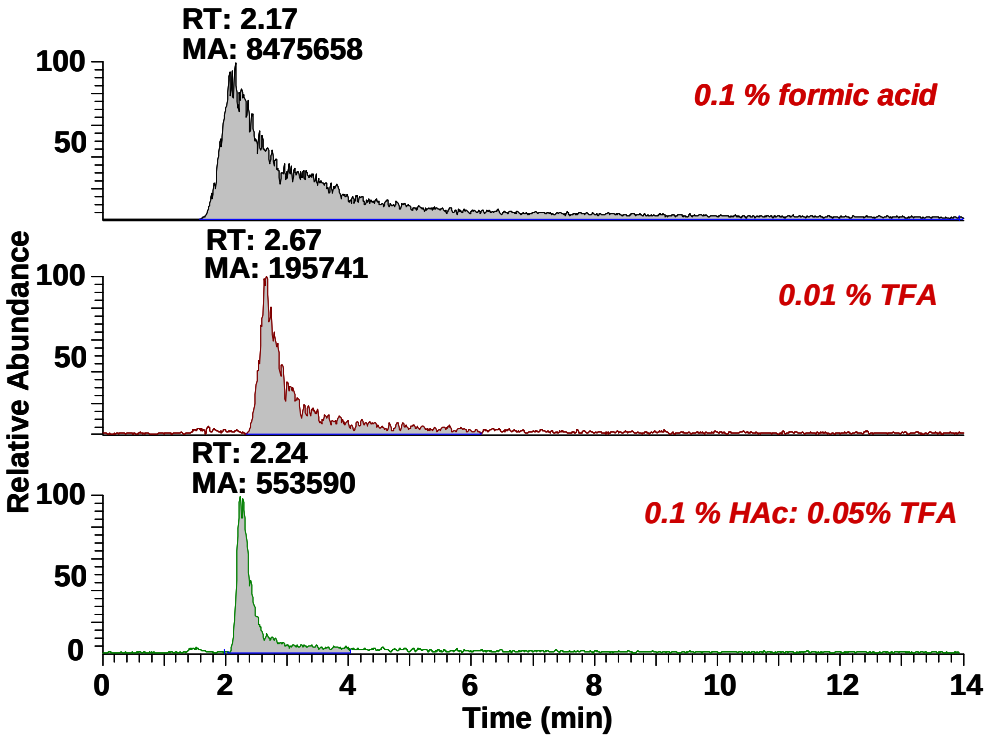

Figure 2-8. Extracted ion chromatograms of *m/z* 661 from low flow isocratic elution of ziconotide using 15:85 ACN:H_2O with various acidic components. The best peak shape was obtained with 0.1% HAc: 0.05% TFA in the mobile phases. Lower peak areas were obtained with solvents containing TFA compared to that with formic acid only. RT: retention time, MA: manually integrated area

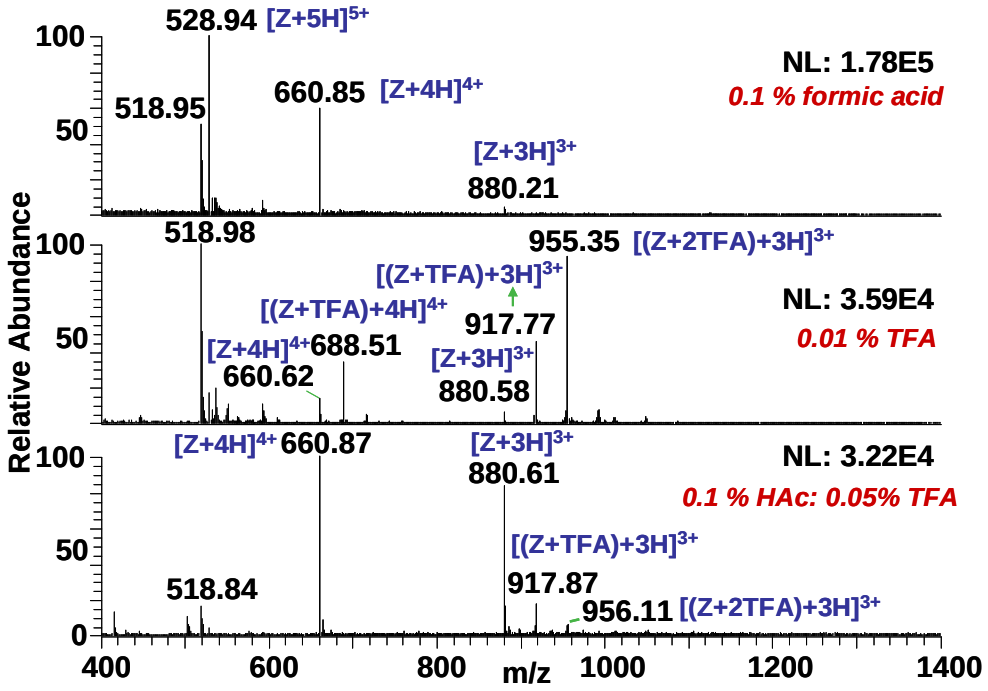

Figure 2-9. Mass spectra of ziconotide peaks from isocratic elutions using 15:85 ACN:H_2O with various acidic components. Differences in the identity and abundance of ions present in each mass spectrum were observed. The use of 0.1% HAc: 0.05% TFA as acid component of the mobile phase yields a good abundance of ziconotide ions and minimal signal contribution from TFA adducts.

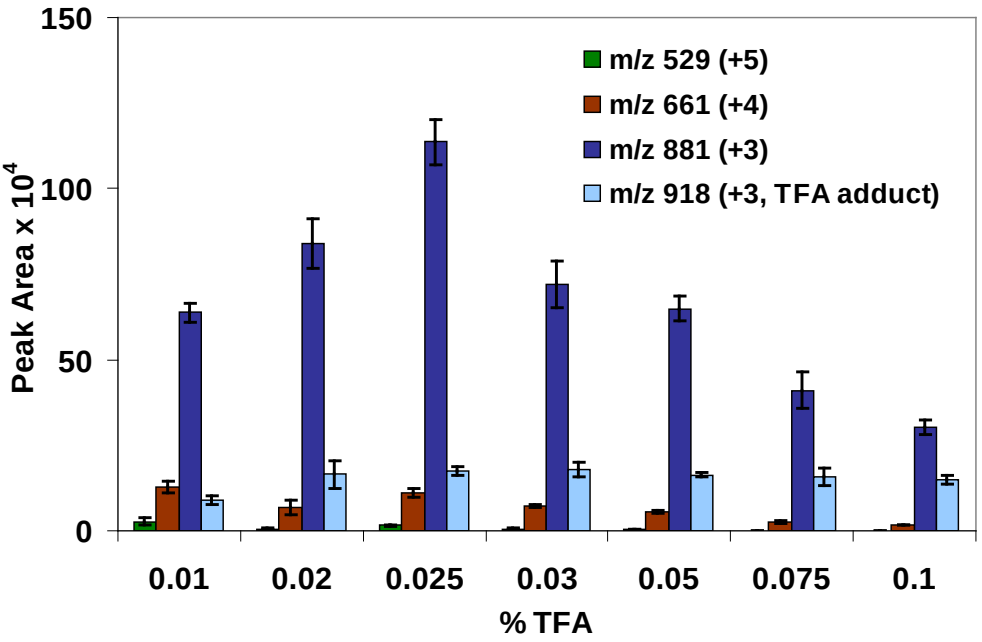

Figure 2-10. Response of ziconotide ions and a TFA adduct with increasing TFA concentration in the mobile phases. The +3 ion of ziconotide at *m/z* 881 was the most predominant charge state. The highest response for this ion was obtained with 0.025% TFA. The data are an average of 3 replicate analyses and error bars represent standard deviation of the replicates.

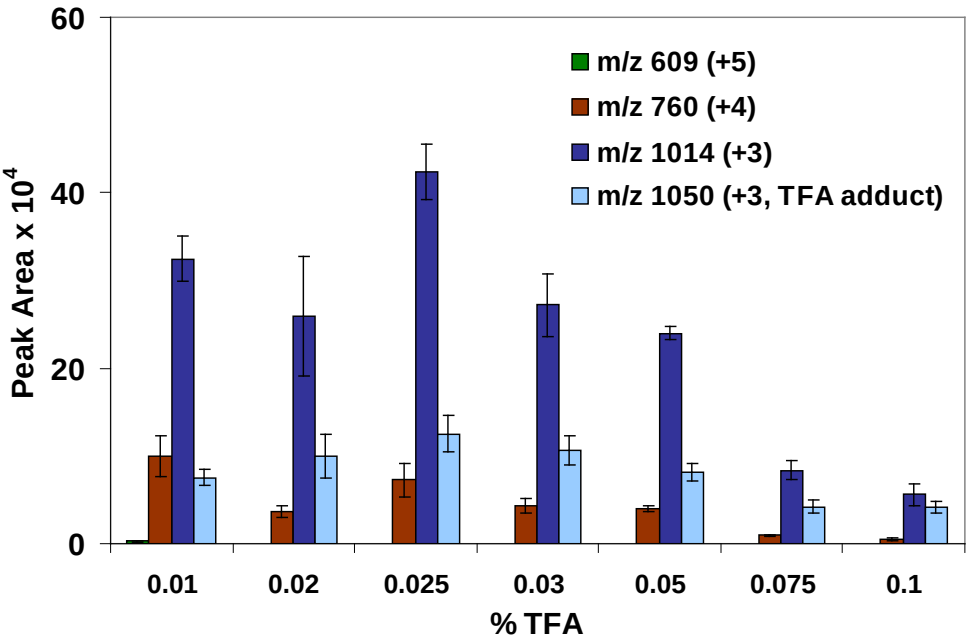

Figure 2-11. Response of ω-conotoxin GVIA ions and a TFA adduct with increasing TFA concentration in the mobile phases. The +3 ion of the IS at *m/z* 1014 was the most predominant charge state. The highest response for this ion was obtained with 0.025% TFA. The data are an average of 3 replicate analyses and error bars represent standard deviation of the replicates.

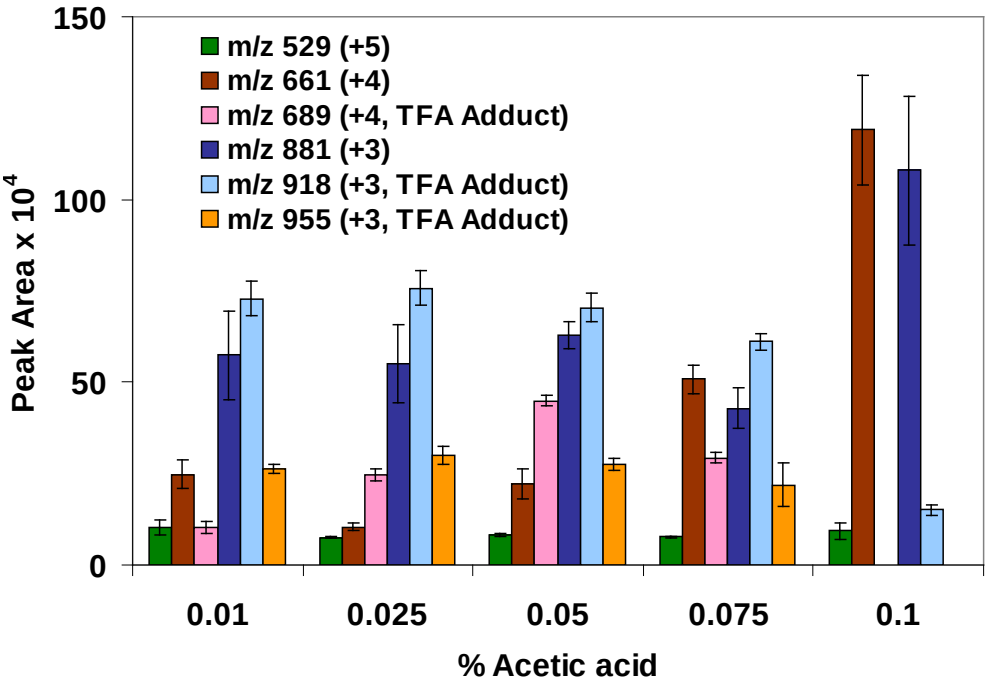

Figure 2-12. Response of ziconotide ions and its TFA adducts with increasing HAc concentration in mobile phases with 0.01% TFA. The highest response for ziconotide with minimum contribution from TFA adducts was obtained with 0.1% HAc. The signal for the +3 and +4 ions of ziconotide were comparable in this case. The data are an average of 3 replicate analyses and error bars represent standard deviation of the replicates.

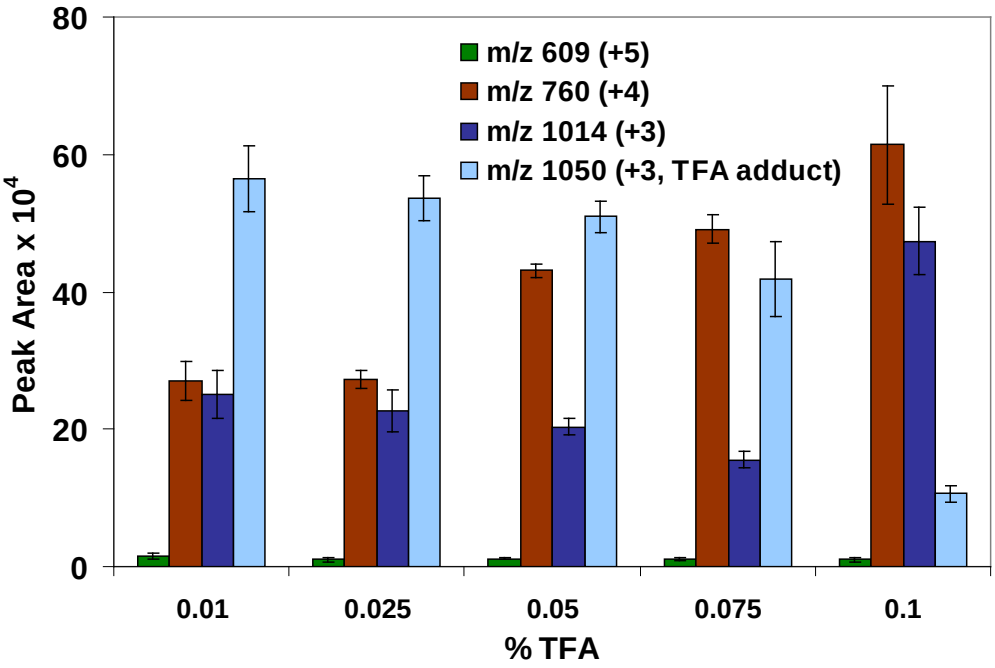

Figure 2-13. Response of ω-conotoxin GVIA ions and a TFA adduct with increasing HAc concentration in mobile phases with 0.01% TFA. The highest response for the +3 and +4 ions of the IS with minimum contribution from the only TFA adduct observed was obtained with 0.1% HAc. The data are an average of 3 replicate analyses and error bars represent standard deviation of the replicates.

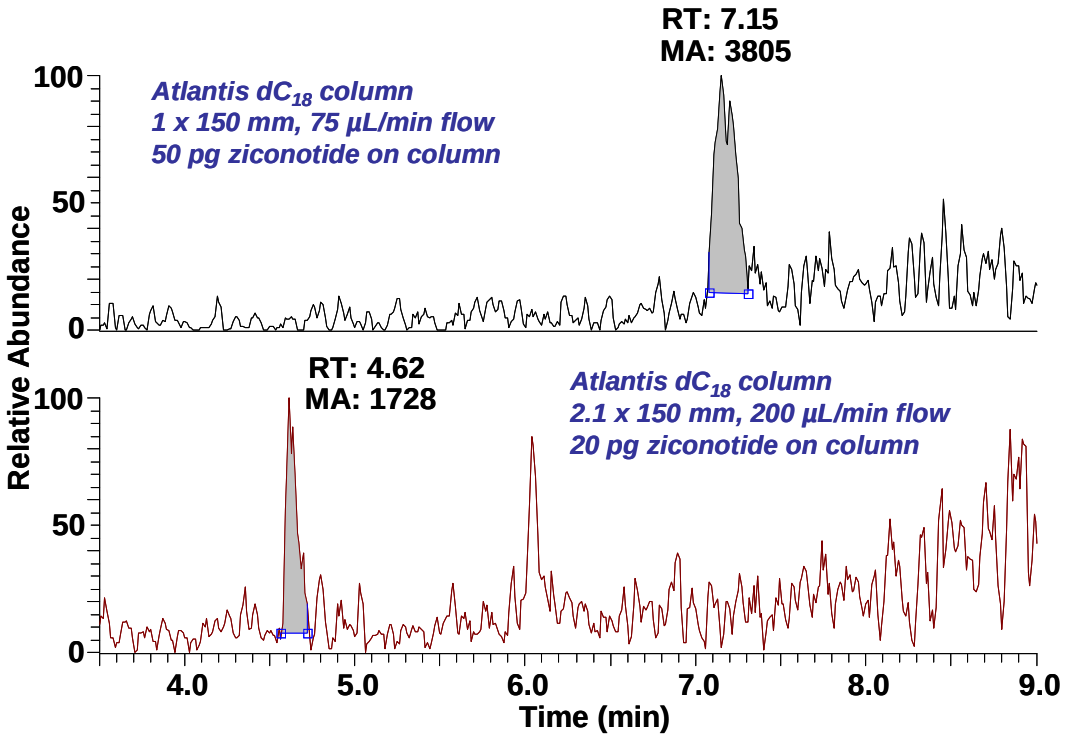

Figure 2-14. Extracted ion chromatograms of *m/z* 661 for the lowest amount of ziconotide that can be detected on Atlantis dC_{18} columns with the same length but varying internal diameters. Improvement in the detection sensitivity of ziconotide was not observed with use of a smaller diameter column (*top panel*), in this case. The limit of detection obtained with the larger diameter column (*bottom panel*) was less than that of the small diameter column.

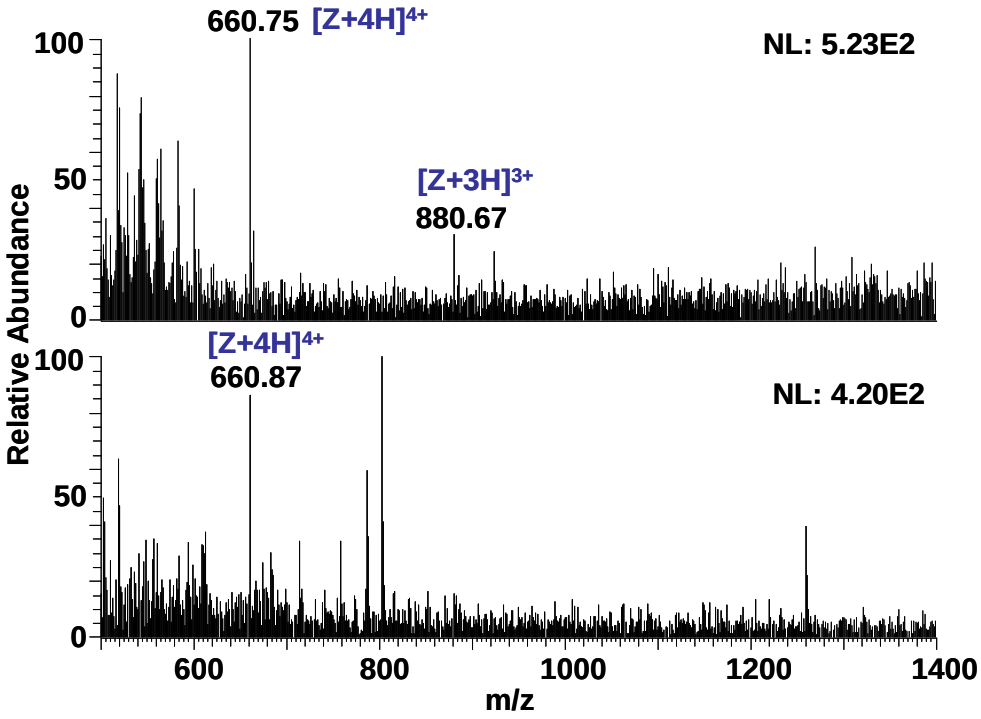

Figure 2-15. Mass spectra of peaks corresponding to the lowest amount of ziconotide that can be detected on 150 mm Atlantis dC_{18} columns with internal diameters of 1 mm (*top panel*) and 2.1 mm (*bottom panel*).

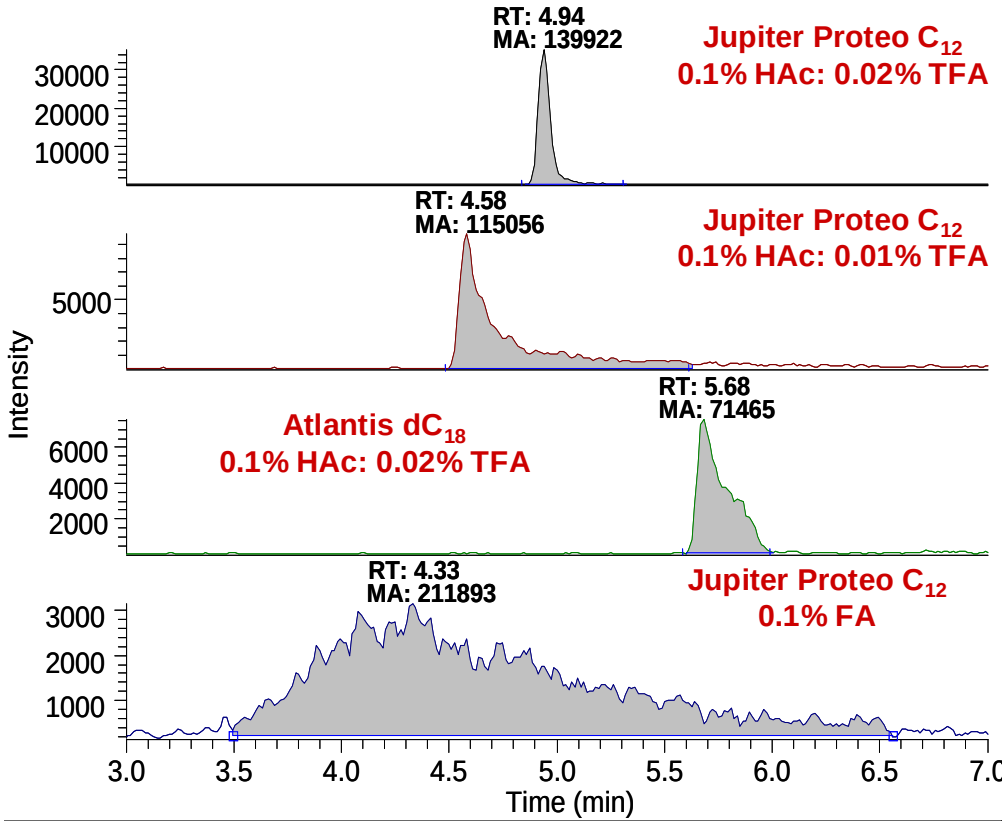

Figure 2-16. Comparison of the peak shape of ziconotide obtained with various columns and acid composition of the HPLC solvents.

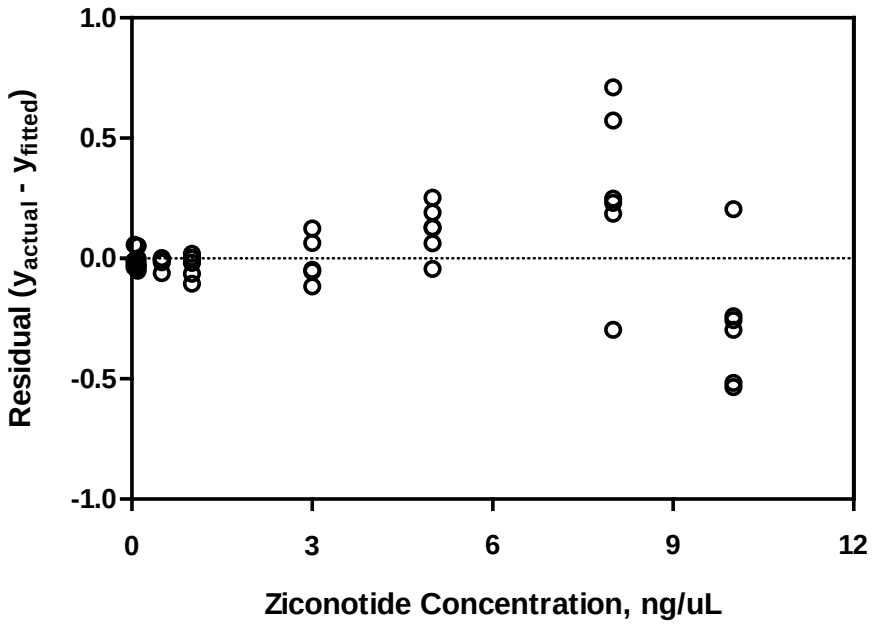

Figure 2-17. Plot of y-residual vs. ziconotide concentration. Data from the inter-day assay of ziconotide standards were used. The greater variance of the standards with higher concentrations compared to those with lower concentrations supported the need for weighting.

Table 2-1. Test for homoscedasticity using the F-test.

[Ziconotide Standard] ng/µL	**A_{zic}**	**A_{IS}**	**Response (A_{zic}/A_{IS})**	**s^2**
0.05	58891	951096	0.0479	5.44×10^{-6}
	68344	917115	0.0530	
	66233	911003	0.0507	
	59962	787271	0.0533	
	67539	913997	0.0541	
	67095	937598	0.0504	
10.0	15627335	977477	10.001	9.40×10^{-2}
	15686759	955908	9.972	
	15417215	962997	9.605	
	14488562	837191	10.395	
	14553122	938112	9.704	
	15233215	936254	9.607	
$F_{exp} = s_{10.0}^2/s_{0.05}^2 = 9.40 \times 10^{-2}/5.44 \times 10^{-6} = 1.73 \times 10^4$				
F_{tab} (5, 5, 0.99) = 10.97				

A_{zic}: peak area of the +4 ion of ziconotide (*m/z* 661)

A_{IS}: peak area of the +4 ion of ω-conotoxin GVIA (*m/z* 760)

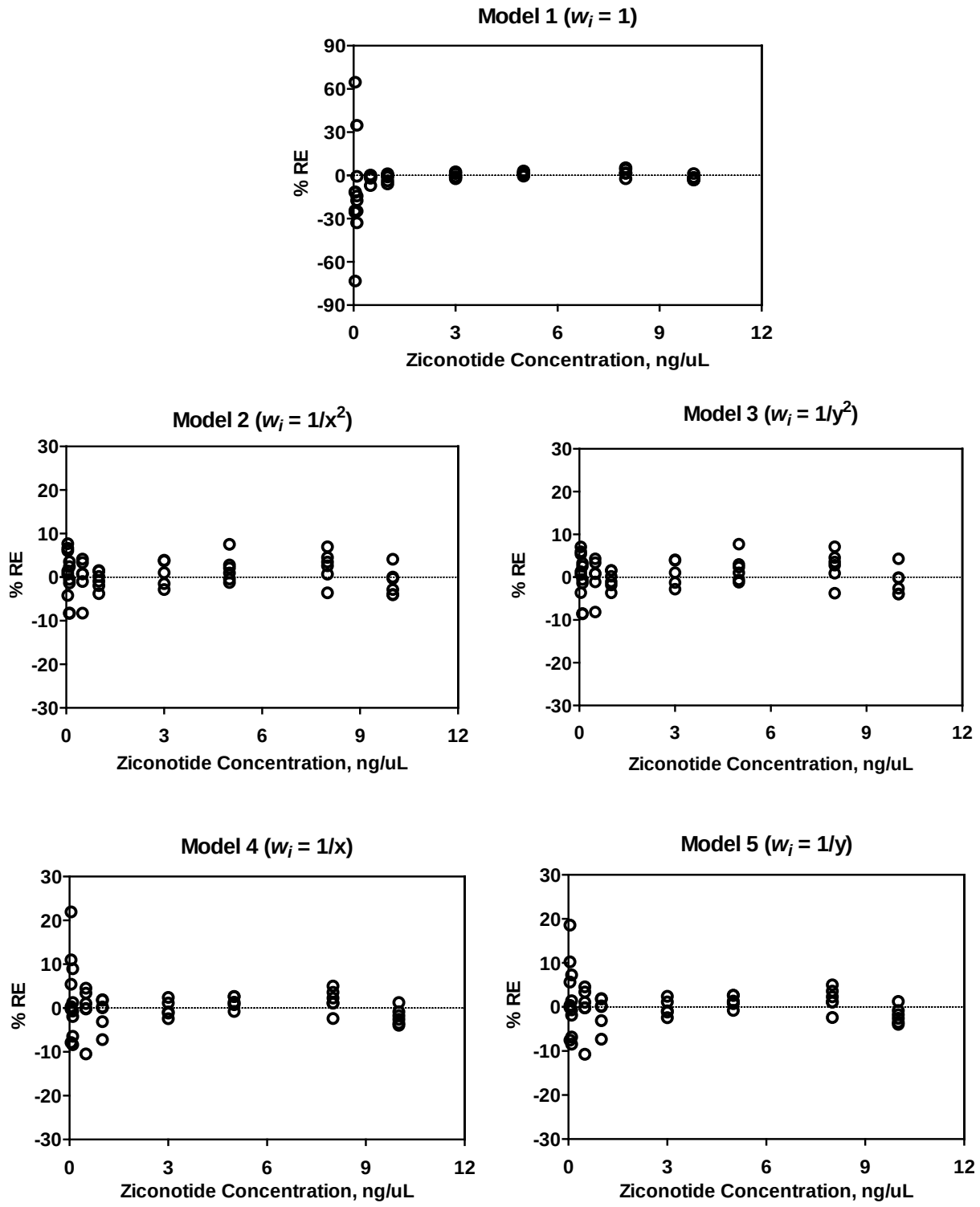

Figure 2-18. Plots of percent relative error (%RE) vs. ziconotide concentration for unweighted (Model 1) and weighted (Models 2-5) linear regressions of ziconotide standards. Data from the inter-day assay of ziconotide standards were used. The best accuracy and %RE distribution scatter was achieved with $1/x^2$ (Model 2) as the weighting model.

Table 2-2. Regression parameters of the calibration curves generated for each weighting factor (w_i) and the respective sum of the relative errors (Σ%RE) for the inter-day assay data.

Model	w_i	**m ± std. error**	**b ± std. error**	$\mathbf{R^2}$	**Σ%RE**
1	1	1.653 ± 0.012	0.001 ± 0.050	0.997	598.16
2	$1/x^2$	1.647 ± 0.012	-0.0132 ± 0.0015	0.997	243.76
3	$1/y^2$	1.645 ± 0.013	-0.0128 ± 0.0015	0.997	245.00
4	1/x	1.659 ± 0.010	-0.016 ± 0.007	0.997	252.75
5	1/y	1.659 ± 0.010	-0.016 ± 0.007	0.997	251.22

n = 65, m = slope, b = y-intercept, R^2 = correlation coefficient

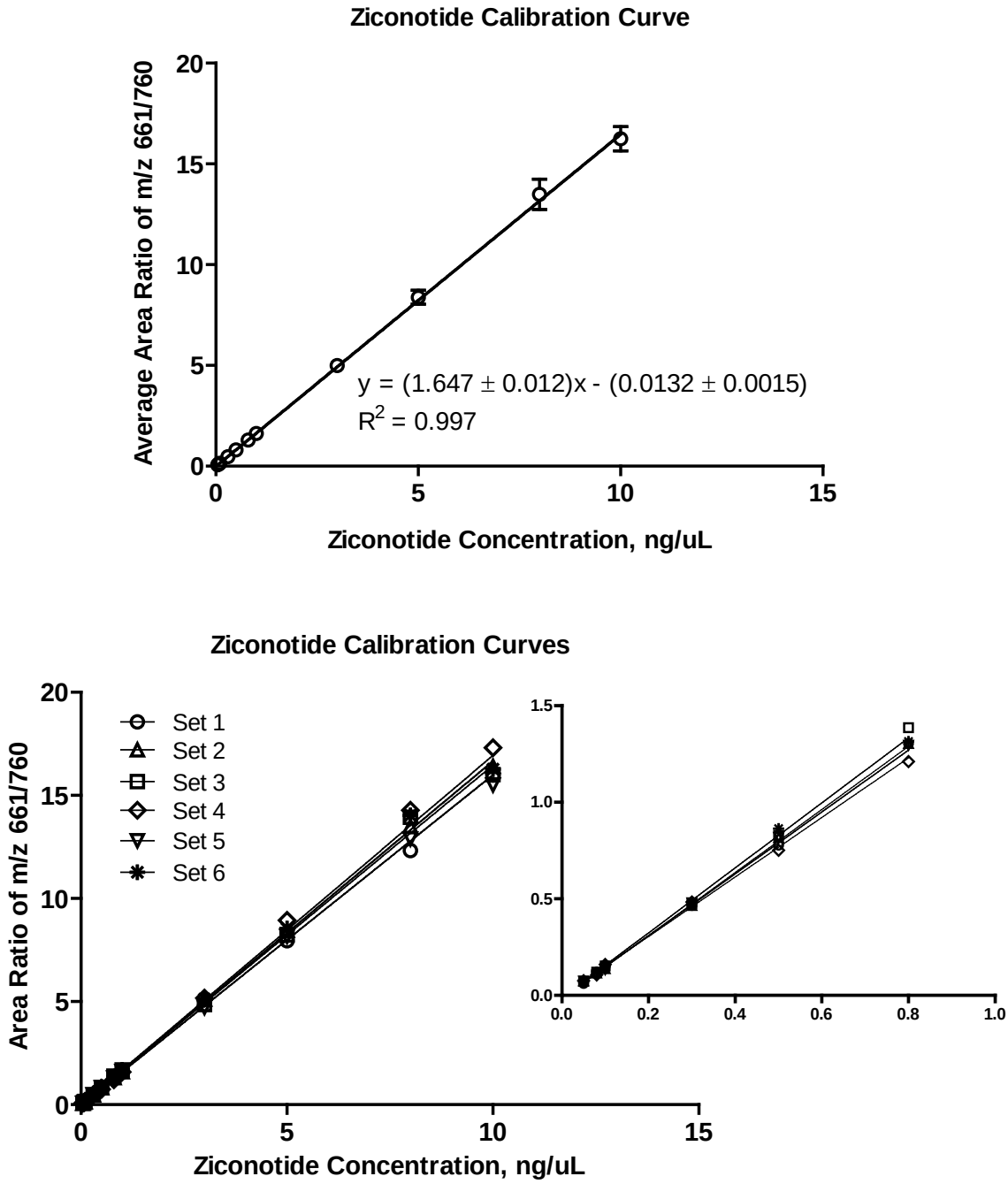

Figure 2-19. Graphical representations of the area ratio of the +4 ions of ziconotide to ω-conotoxin GVIA vs. ziconotide concentration. The top panel shows the average of six separate dilutions and the error bars represent standard deviation of the measurements. The line equation and standard deviation of the slope and y-intercept are shown. The bottom panel shows each of the six response curves, results of which were averaged to generate the first plot. The inset shows a blow-up of the calibration range from 0.05 to 0.8 ng/µL.

Table 2-3. Regression parameters for the six calibration curves of ziconotide.

Calibration Curve	m ± std. error	b ± std. error	R^2
1	1.600 ± 0.019	-0.0147 ± 0.0023	0.9993
2	1.647 ± 0.026	-0.013 ± 0.003	0.9994
3	1.668 ± 0.019	-0.0119 ± 0.0024	0.9976
4	1.67 ± 0.05	-0.013 ± 0.006	0.9901
5	1.60 ± 0.03	-0.013 ± 0.004	0.9991
6	1.695 ± 0.016	-0.0138 ± 0.0020	0.9981

n = 11 except for CC4 with n=10, m = slope, b = y-intercept, R^2 = correlation coefficient

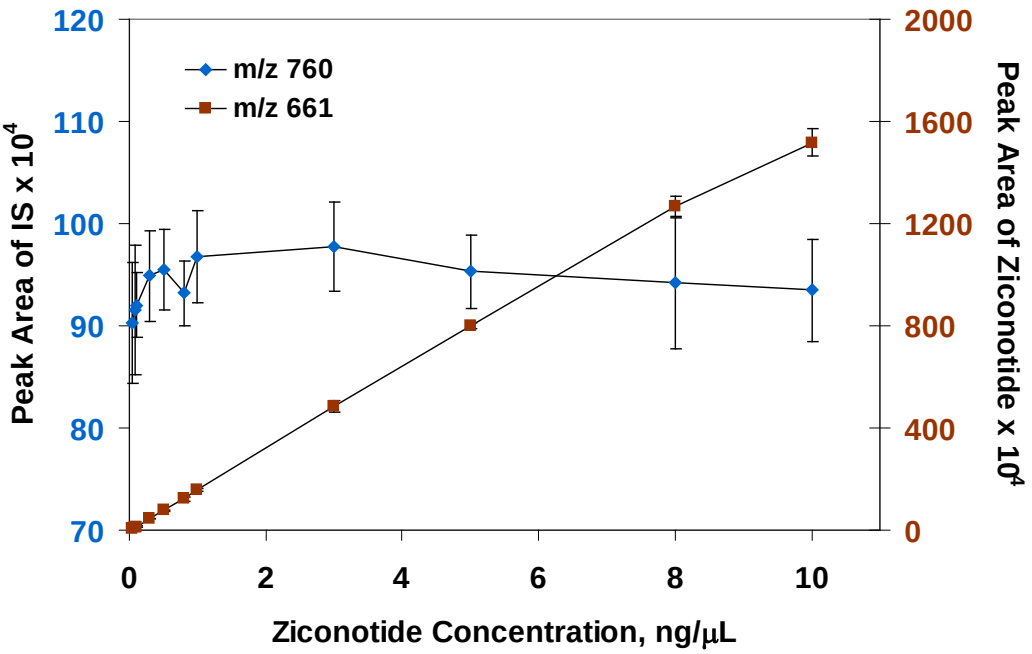

Figure 2-20. Response of ziconotide and ω-conotoxin GVIA (IS) across the calibration curve. The data are an average of 6 separate dilutions corresponding to each of the calibrator analyzed in 6 separate days. The error bars represent the standard deviation of the measurements.

Table 2-4. Precision and accuracy of ziconotide calibration standards assayed during a six-day period.

Nominal Concentration, ng/µL	n	Average Calculated Concentration, ng/µL	%RSD	%RE
0.050	6	0.051_6	4.5	3.2
0.080	6	0.077_6	5.8	-3.0
0.10	6	0.097_9	5.3	-2.1
0.30	6	0.29_6	2.2	-1.2
0.50	6	0.49_9	4.4	-0.075
0.80	6	0.79_9	4.7	-0.91
1.0	6	0.99_4	2.1	-0.62
3.0	5	3.0_3	3.0	0.84
5.0	6	5.1_0	3.0	2.0
8.0	6	8.2_0	3.6	2.5
10	6	9.8_8	3.1	-1.2

%RSD = (SD/ $\overline{X}$) x 100 where SD: standard deviation and $\overline{X}$: mean

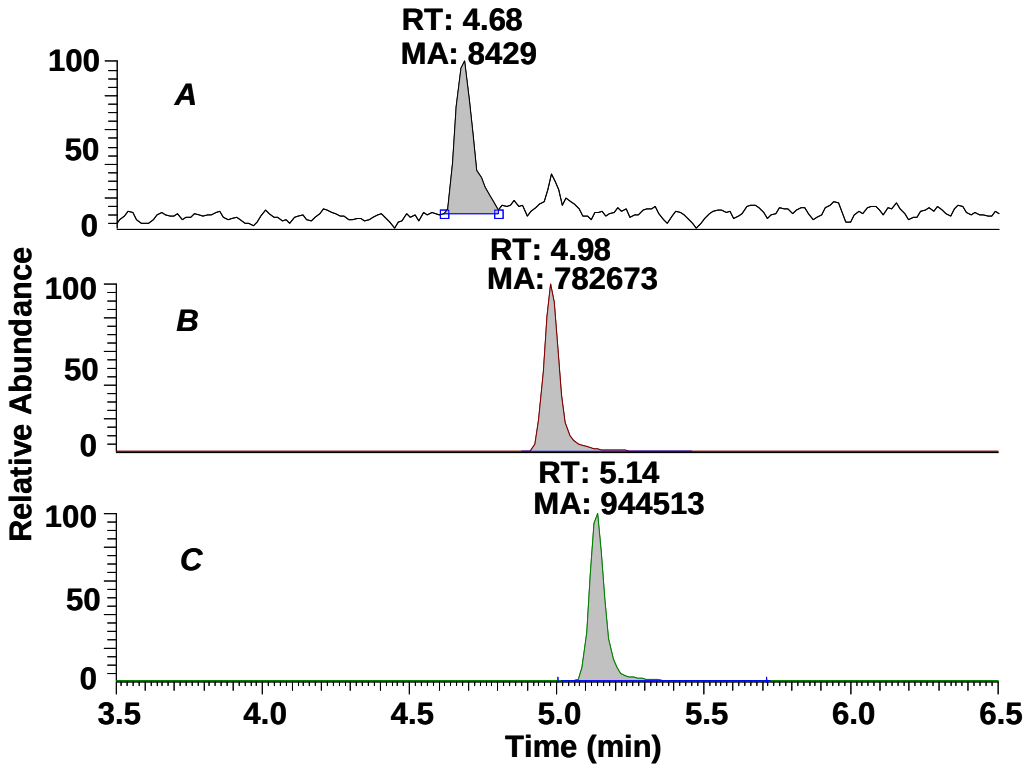

Figure 2-21. Extracted ion chromatograms (*A*) oxidized ziconotide, (*B*) ziconotide and (*C*) ω-conotoxin GVIA for the 0.5 ng/µL calibration standard. Chromatograms were processed using a 3-point boxcar smoothing calculation. RT: retention time in min, MA: manually integrated area

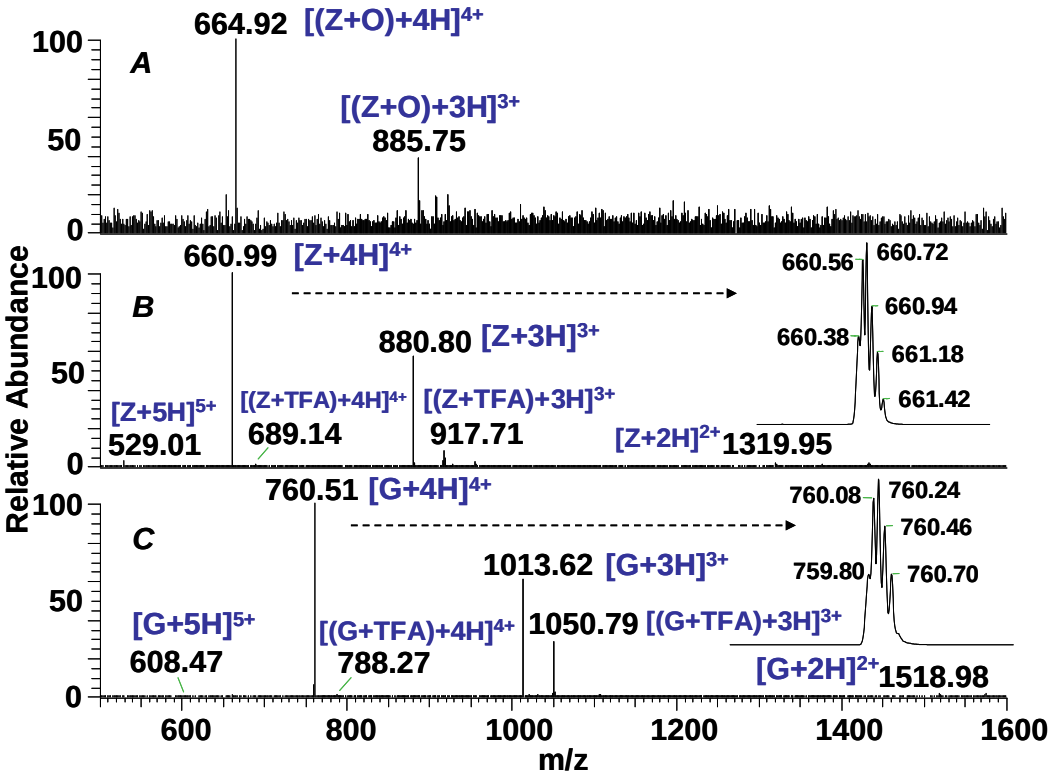

Figure 2-22. Full-scan mass spectra of (*A*) oxidized ziconotide, (*B*) ziconotide and (*C*) ω-conotoxin GVIA. Insets show the isotopic distributions of the +4 charge state of ziconotide (Z) and ω-conotoxin GVIA (G) obtained with zoom scan.

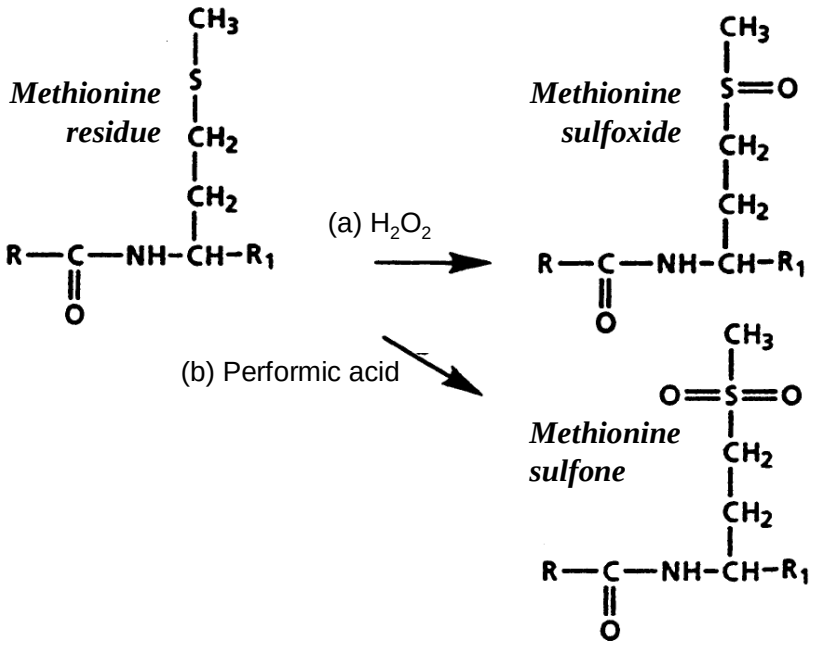

Figure 2-23. Methionine oxidation under (a) mild and (b) strong oxidizing conditions. Hydrogen peroxide, iodine and dimethylsulfoxide are examples of mild oxidants while 95% performic acid is a strong oxidant.[58] Adapted from Reubsaet *et al*.[57]

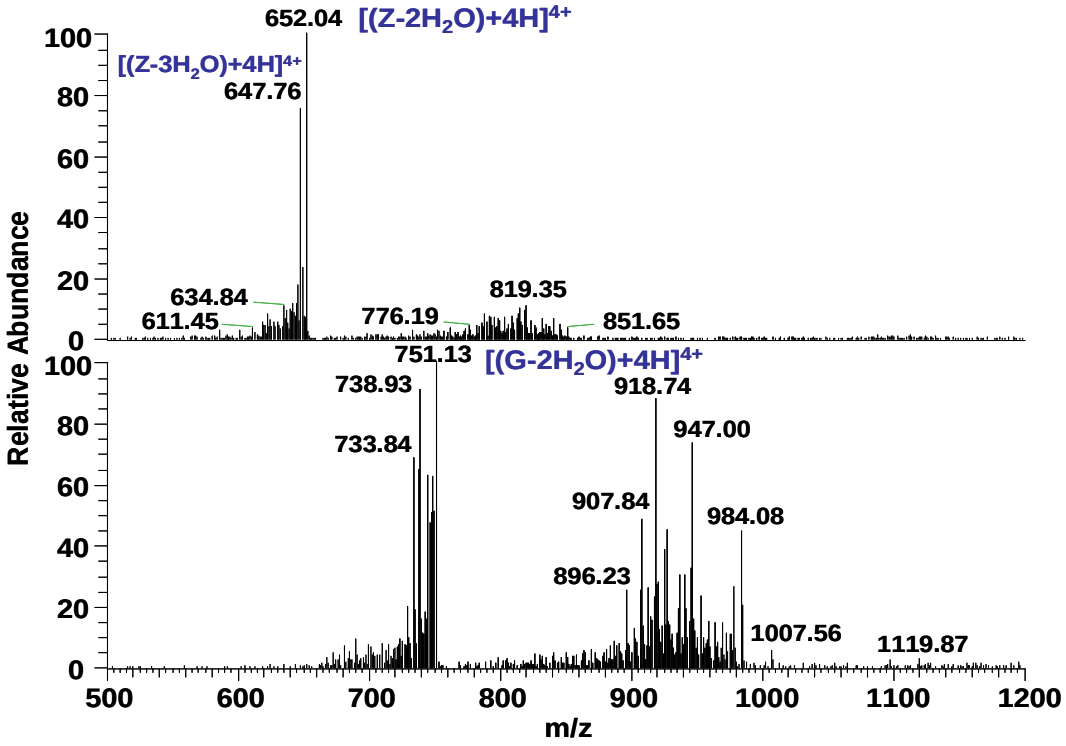

Figure 2-24**.** Product ion spectra of the +4 ions of ziconotide at *m/z* 661.0 (*top*) and ω-conotoxin GVIA at *m/z* 760.4 (*bottom*) at 30% collision energy. The product ions identified were mostly due to water losses.

CHAPTER 3
HPLC-ESI-MS^n ANALYSIS OF REDUCED AND ALKYLATED ZICONOTIDE

Introduction

The extensive cross-linking of ziconotide and the internal standard (IS), ω-conotoxin GVIA, via the six cysteine residues in each molecule, reduces the structural information that can be derived from their collision-induced dissociation (CID) spectra. Experiments which involved reduction of disulfide bonds linking the cysteine residues of the conopeptides and alkylation of the resulting sulfhydryl groups in order to eliminate cross-linking and increase the likelihood of fragmentation during CID will be reported in this chapter.

The presence of six cysteine residues, which form three disulfide bridges with a distinct pattern, is a common structural feature of ω-conopeptides.[2, 12, 20, 59] Disulfide bond formation is a post-translational modification that plays an important role in imparting stability to the peptide conformations and maintaining certain biological functions such as specific receptor interactions.[18, 48, 60] This modification is especially abundant in some hormones, enzymes, plasma proteins and venoms such as those from spiders, snakes or cone snails.[7, 61]

Techniques employed to elucidate the structure of these disulfide-rich peptides include conventional methods[8] such as Edman degradation and amino acid analysis, cDNA sequencing[1, 49] and mass spectrometry (MS).[1, 16, 18, 48, 62]. High energy CID, in particular, has been used to characterize and sequence disulfide-linked peptides.[63, 64] Results for low energy CID conditions, however, indicate that the presence of disulfide bonds makes the peptides less susceptible to collisional fragmentation, making reduction and alkylation prior to MS-based structure confirmation essential.[49, 65, 66]

Reduction, which is typically performed with dithiothreitol (DTT) or tris-(2-carboxyethyl)-phosphine (TCEP), involves the cleavage of disulfide bonds and addition of hydrogen to the

thiolate anion resulting in 2 sulfhydryl groups per disulfide bond. Dithiothreitol, which is the reducing agent used in the experiments described in this chapter, react as the thiolate ion and reduce disulfide bridges through a thiol interchange.[67] The mechanism involved in the reduction process involving dithiols is illustrated in Figure 3-1. Thiols, like DTT, work best for these reactions at high pH compared to TCEP, which can be employed at low pH.[61, 68] Thiol-disulfide exchange, which is responsible for disulfide scrambling in peptides with tightly clustered disulfides, however, is minimized in acidic conditions.[61] It is for this reason that the use of TCEP was explored and evaluated in various applications.[18, 60, 61]

In order to minimize disulfide scrambling for reduction conducted with DTT at basic pH, alkylation is performed immediately after reduction. Alkylating agents like iodoacetamide (IAM) attack the thiolate ion and in the process, compete with disulfide exchange.[61] Alkylation protects the sulfhydryl groups formed and prevents them from reforming disulfide bonds. The alkylation process is also favored in basic conditions.[60, 68] A general representation of reduction and alkylation is shown in Figure 3-2.

Reduction and alkylation combined with high performance liquid chromatography (HPLC)-mass spectrometric analysis has emerged as an important technique in the analysis of conopeptides. Jakubowski *et al*. compared the mass profiles and CID spectra before and after the global reduction and alkylation of unpurified cone snail venom to determine the amino acid sequence of several conopeptides and ascertain those which contain cysteine.[48] Using the same global reduction and alkylation procedure and HPLC/MS, screening for post-translational modifications in conotoxins was achieved by the same group.[19] A differential alkylation procedure using substituted maleimides followed by HPLC and tandem mass spectrometric

(MS/MS) analysis was used by Jones *et al*. to establish disulfide bond connectivity in a group of conopeptides.[18]

The optimization of parameters (*e.g.*, reagent concentration, reaction time, temperature) affecting reduction and alkylation will be discussed in the sections that follow. Analysis of the major products of reduction and alkylation of the conopeptides by HPLC/MS/MS was carried out in order to identify potential fragment ions for quantitation. The optimized reduction and alkylation method was then evaluated for the analysis of ziconotide plasma extract.

Experimental Section

Chemicals and Reagents

The conopeptides ω-conotoxin MVIIA (0.1 mg, ≥ 95% purity by HPLC) and ω-conotoxin GVIA (0.1 mg, 98.3% purity by HPLC), DL-dithiothreitol, and iodoacetamide were purchased from Sigma-Aldrich (St. Louis, MO). Glacial acetic acid (HAc), ammonium hydroxide (NH_4OH), trifluoroacetic acid (TFA), HPLC-grade acetonitrile (ACN), methanol (MeOH) and isopropanol (IPA) were obtained from Thermo Fisher (Fair Lawn, NJ). Water used for solution preparation was purified by RiOs™ reverse osmosis and Milli-Q polishing systems (Millipore, Billerica, MA). Water used for peptide solution preparation was also vacuum-degassed to remove dissolved oxygen in order to minimize possible oxidation of ziconotide.

Evaluation of Ziconotide Extraction Recovery with ZipTip C_{18} Pipette Tips

The extraction recoveries of a ziconotide standard solution from ZipTip C_{18} pipette tips (Millipore, Billerica, MA) using various elution solvents were evaluated. Prior to sample loading, the resin in the tip was wet with 20 μL of 100% ACN and equilibrated with 20 μL of 0.02% (v/v) TFA in water. The sample, 10 μL of 0.234 μM ziconotide in 0.02% $TFA_{(aq)}$, was applied to the resin bed by aspirating and dispensing 5 times to ensure maximum binding of the

peptide. Contaminants were removed by washing the resin with 10 μL of 0.02% TFA in water, 4-5 times. The purified conopeptide was eluted with 10 μL of solvent, aspirated and dispensed 3 times. Ten microliters of 0.183 μM of the internal standard (IS), ω-conotoxin GVIA, in the corresponding elution solvent was added before final dilution to 40 μL. Percent extraction recoveries from elution with 0.02% TFA in 15:85, 20:80, 25:75, 50:50 and 80:20 ACN: H_2O and 0.02% TFA in 50:50 IPA: H_2O mixtures were then compared. To avoid peak-splitting on analysis, the final ACN concentration from elution with 0.02 % TFA in 50:50 ACN:H_2O was adjusted to 25% before final dilution.

ZipTip extract of 10 μL of 0.02% TFA in water mixed with 10 μL each of 0.234 μM ziconotide and 0.183 μM ω-conotoxin GVIA in the appropriate elution solvent, and 10 μL of elution solvent, constituted the control solution. Ten microliters of 0.02% TFA in water was added to the control solution for extraction with 0.02% TFA in 50:50 ACN: H_2O, instead of 10 μL of elution solvent, to adjust the ACN concentration to 25%. Responses of the ziconotide extracts were compared to the average response of the control solutions to determine percent recoveries. The solvent that yielded the best recovery was used for the elution of reduced and alkylated ziconotide from the ZipTip resin.

Optimization of Parameters Affecting Reduction

The effects of reducing agent (DTT) concentration, reduction time and temperature on the response and identity of ziconotide reduction products were investigated. Reduction of 30 μL of 2.95 μM aqueous ziconotide solution with 20 μL of aqueous DTT solution at various concentrations (*i.e.*, 0.60, 1.2, 2.4, 4.8 and 9.6 mM) was carried out in a water bath held at 60 °C for 30 min. The mixture was allowed to equilibriate to room temperature for 1 min. Six

microliters of 0.1% TFA in water was then added to a 30-μL aliquot of the reduction mixture to quench the reaction and reduce disulfide scrambling.

Thirty microliters of the reduction mixture treated with 0.1% TFA in water were applied to the resin bed of pre-conditioned C_{18} ZipTips by aspirating and dispensing 10 μL at a time of the 30 μL sample for 5 times. The resin bed was washed with 10 μL of 0.02% TFA in water, 4-5 times to remove remaining contaminants. The purified conopeptide was then eluted with 30 μL of 0.02% TFA in 50:50 ACN:H_2O, by aspirating and dispensing 10 μL thrice each time. Finally, the organic composition in the final solution was adjusted to 25% by adding 30 μL of 0.02% TFA in water to the extract before LC-MS analysis.

Following the same reduction and ZipTip extraction procedures described above, the effect of carrying out reduction at 5, 10, 30 and 60 min to the extent of reaction was explored. The effect of various temperatures (*i.e.*, 30, 45, 60 and 75 °C) on the extent of reduction and formation of unwanted side products was also tested. Reduction time for ω-conotoxin GVIA was also optimized.

Blank and control solutions analyzed with each run were processed identically to the ziconotide samples. Blank solutions contained all reagents present in the sample except ziconotide. Control solutions contained all reagents present in the sample except DTT. The blank, in this case, was composed of 30 μL of degassed, deionized water mixed with 20 μL of the appropriate $DTT_{(aq)}$ solution while the control was made up of 2.95 μM ziconotide solution mixed with 20 μL of degassed, deionized water. Both were extracted with ZipTips which were eluted with 0.02% TFA in 50:50 ACN:H_2O with the final ACN concentration adjusted to 25%. Blank, control and sample solutions were processed and analyzed one after the other to minimize response differences due to time variability.

Optimization of Parameters Affecting Alkylation

Using the optimal conditions determined for the reduction of ziconotide, parameters that may affect the results of alkylation were also optimized. These include the concentration of the alkylating agent, iodoacetamide, alkylation time and temperature. Reduction of 30 μL of 2.95 μM aqueous ziconotide solution with 20 μL of 0.60 mM $DTT_{(aq)}$ was carried out at 60 °C for 10 min. A 30-μL aliquot of the reduction mixture was made basic with 0.1 M NH_4OH (2 μL, pH 10.5) before alkylation. Ten microliters of 3.2 mM $IAM_{(aq)}$ was then added and alkylation proceeded for 15, 30, 45, and 60 min in the dark at room temperature. The reaction was quenched with the addition of 8 μL of 0.1% TFA in water and exposure to light. The resulting products were extracted using pre-conditioned C_{18} ZipTips with 0.02% TFA in 50:50 ACN:H_2O as eluent. The final ACN concentration in the extract was adjusted to 25% prior to HPLC-MS analysis. The same procedures for sample loading, washing away of contaminants and sample elution used in the optimization of reduction parameters were followed. Alkylation reactions without NH_4OH and without 0.1% TFA in water for quenching the reaction were also performed.

The alkylation temperature (*i.e.*, 22, 30, and 60 °C) and IAM concentrations (*i.e.*, 3.2, 6.4, 12.8 and 25.6 mM) were also varied to assess the effects of these variables on the response and identity of the products of reduction and alkylation of ziconotide. Blank and control solutions were processed identically to the ziconotide samples. The blank consisted of 30 μL of degassed, deionized water mixed with 20 μL of 0.60 mM $DTT_{(aq)}$ solution while the control had 2.95 μM ziconotide solution mixed with 20 μL of degassed, deionized water. Reduction, alkylation, extraction and analysis of all solutions were conducted one after the other to minimize response differences due to variations in time.

Generation of the Response Curve for Reduced and Alkylated Ziconotide

Six standard solutions of aqueous ziconotide with concentrations ranging from 0.035 to 1.8 μM were prepared and mixed with a fixed amount of internal standard. Thirty microliters of each solution and 30 μL of 0.66 μM ω-conotoxin GVIA were reduced with 40 μL of 0.60 mM DTT for 20 min at 60 °C. The mixture was allowed to equilibrate to room temperature for one minute. Sixty microliters of the reduction mixture were made basic with the addition of 4 μL of 0.1 M NH_4OH. Twenty microliters of 3.2 mM IAM were then added and alkylation proceeded for 15 min in the dark at room temperature. The alkylation mixture was exposed to light and 30 μL of it was applied to the resin bed of a pre-conditioned C_{18} ZipTip by aspirating and dispensing 10 μL at a time of the 30 μL sample for 5 times. Contaminants were washed away with 10 μL of 0.02% TFA in water, aspirated and dispensed 4-5 times. The purified conopeptide was then eluted with 30 μL of 0.02% TFA in 25:75 ACN:H_2O, by aspirating and dispensing 10 μL thrice each time. Ten microliters more of 0.02% TFA in 25:75 ACN:H_2O was added to provide sufficient sample volume for LC-MS analysis. Blank and control solutions were analyzed identically to the ziconotide samples.

Application of the Reduction and Alkylation Method to Ziconotide Plasma Extract

The optimized reduction and alkylation method was used for a preliminary analysis of blank horse plasma supplemented with ziconotide. The extraction method developed for ziconotide in horse plasma at Dr. Laszlo Prokai's laboratory in the University of North Texas Health Science Center was slightly modified and employed in this experiment.[69] One hundred microliters of 25 ng/μL aqueous ziconotide solution was added to 1 mL of blank horse plasma and diluted to 2.5 mL with 0.5% acetic acid before loading onto a pre-conditioned PD-10 desalting column (GE Healthcare, Piscataway, NJ). The column was washed with 3.5 mL of

0.5% HAc to remove high molecular weight compounds, followed by 5 mL of 0.5% HAc to elute the low molecular weight fraction containing ziconotide. A Waters C_{18} Sep-Pak® cartridge (Waters Corporation, Milford, MA) was washed with 3 mL ACN and 5 mL of 0.5% HAc for conditioning. The low molecular weight (MW) eluate from the PD-10 column was then loaded onto the C_{18} cartridge and the cartridge was washed with 5 mL of 0.5% HAc. The cartridge was dried for 10 min at a pressure of 20 in Hg. Ziconotide was eluted afterwards with 1% HAc in 40:60 MeOH:H_2O and dried under $N_{2(g)}$ at 60 °C. The residue was dissolved in 100 µL of degassed, deionized water. A portion (50 µL) was placed in a 250 µL, 11 mm polypropylene autosampler vial covered with crimp seals that include Teflon/red rubber septa (National Scientific, Rockwood, TN) for LC-MS analysis.

Another portion (30 µL) was reduced with 20 µL of 0.60 mM DTT for 10 min at 60 °C. The mixture was allowed to equilibrate to room temperature for a minute. The reduction mixture (30 µL) was then made basic with 2 µL of 0.1 M NH_4OH and alkylated with 10 µL of 3.2 mM IAM for 15 min in the dark at room temperature. The alkylation mixture was exposed to light and 30 µL was extracted with a pre-conditioned C_{18} ZipTip following the optimized sample loading, washing and sample elution procedure described in the analysis of calibration standards. Considering 100% recovery and taking into account the dilutions in the sample treatment, 100 µL of 15 ng/µL ziconotide solution was added to 3 mL of 1% HAc in 40:60 MeOH:H_2O, dried under $N_{2(g)}$ at 60 °C and reconstituted with 100 µL of degassed, deionized water to estimate extraction recovery. This resulting solution served as the control solution and the amount of ziconotide in solution is equivalent to the ideal amount (1.5 µg) present in the extract before drying the sample.

HPLC-ESI-MS/MS Analysis

A Surveyor Autosampler/HPLC system interfaced to a Thermo Finnigan (San Jose, CA) linear ion trap (LTQ) mass spectrometer equipped with an electrospray ionization source (ESI) was employed for LC-MS analyses. Chromatographic separation was achieved with a Jupiter Proteo C_{12} column (2 x 150 mm, 4 µm particle size, 90 Å pore size) from Phenomenex (Torrance, CA) with a Security Guard™ cartridge (2 x 4 mm, C_{12}) to protect the analytical column. The column oven was set to 30 °C while the autosampler was maintained at 12 °C. Mobile phase A was 0.1% HAc: 0.02% TFA in water while mobile phase B was 0.1% HAc: 0.02% TFA in acetonitrile. Gradient elution with solvent B raised from 2 to 70% in 9 minutes was employed for the ZipTip extraction recovery and reduction and alkylation analyses. A longer gradient, with solvent B raised from 2 to 60% in 20 min was used to resolve the reduction products of ziconotide. Both gradients were followed by a 6.5 min column equilibration to initial solvent conditions. A flow rate of 200 µL/minute was used. Using the partial loop injection mode, 10 µL of the sample was loaded onto the column. External and internal syringe needle washes with 50:50 ACN: water were incorporated in the autosampler method to prevent carry-over from previous injections.

Electrospray ionization in the positive mode was employed. The spray needle voltage was set at 3.75kV while the capillary voltage was at 45 V. The capillary temperature was maintained at 300 °C. Sheath gas flow was set to 40 and that of the auxiliary gas to 10 arbitrary units. The LTQ mass spectrometer was set to acquire data for 10 min for the 9-min gradient and 20 min for the longer gradient used to resolve the products of ziconotide reduction. Sample from the chromatography column during the first 2 min and last 0.5 min was diverted to waste. The LTQ was programmed for full-scan MS then full-scan MS/MS (*m/z* 500 – 1400) of *m/z* 661 and *m/z*

760, the quadruply-charged ions of ziconotide and ω-conotoxin GVIA, respectively. The precursor ion isolation width in full-scan MS/MS mode was set to 3 *m/z* with collision energy (CE) at 30% and activation energy (q) at 0.250.

Full-scan MS and full-scan MS/MS (*m/z* 400 – 1500) of *m/z* 748 and *m/z* 848, the +4 ions of the reduced and alkylated ziconotide and ω-conotoxin GVIA, respectively, were also performed. Collision energy of 35% and activation energy of 0.250 were employed for its analysis. A precursor ion isolation width of 2 *m/z* was used. The same scan modes and MS/MS parameters were used for analyzing the reduction products of ziconotide. An nth order triple play (full scan, zoom scan, CID at 35% CE) data dependent acquisition mode was employed for charge state confirmation and MS^3 analysis was performed to identify product ions whose *m/z* correspond to more than 1 ion when compared to theoretical values.

MS Data Analysis

Base peak chromatograms (BPCs) of the products of ziconotide reduction and extracted ion chromatograms (EICs) of intact and modified ziconotide and ω-conotoxin GVIA were generated using the Xcalibur software. Chromatograms were processed using a 3-point boxcar smoothing calculation. Extracted ion chromatograms were generated by plotting the response of each charge state or product ion versus time using the full-scan MS or MS/MS filters, resulting in a peak area for each ion. Peak areas for the various ions were then manually integrated. The area ratios of the sum of the +3 and +4 ions of ziconotide to IS were used for ZipTip extraction recovery evaluation. The response of the reduction products of ziconotide was obtained from base peak chromatograms while those of reduction and alkylation were from the sum of the peak areas for the +3, +4 and +5 ions of modified ziconotide and ω-conotoxin GVIA.

The ratio of the peak area of the +4 ion of modified ziconotide to that of the IS was plotted against ziconotide concentration to generate the response curve. Weighted least squares linear regression was used for data fitting, with $1/x^2$ as the weighting scheme of choice. GraphPad Prism® Version 5.01 (San Diego, CA) was used for data processing. One-or two-way analysis of variance (ANOVA) in Microsoft Excel (Redwood, WA) established statistical differences at 95% confidence level for the experimental parameters. Two-way ANOVA with replication was used in this study.

Results and Discussion

Comparison of Extraction Recoveries with ZipTip C_{18} Pipette Tips

Extraction recoveries of intact ziconotide from ZipTip C_{18} resin using the following elution solvents were compared: 0.02% TFA in 15:85, 20:80, 25:75 and 50:50 ACN: H_2O mixtures. Response of the ziconotide extracts was compared to the average response of the control solutions and percent recoveries were calculated according to Equation 3-1. The ratio of the total areas of the peaks for the +3 and +4 charge states of ziconotide to those for the +3 and +4 charge states of the IS was used to determine the response of the extract and control solutions.

$$\text{Percent recovery} = \frac{\left(\text{Area ratio of } m/z \ \frac{661+881}{760+1014}\right)_{\text{extract}}}{\left(\text{Average area ratio of } m/z \ \frac{661+881}{760+1014}\right)_{\text{control}}} \times 100 \qquad (3\text{-}1)$$

A graph of the average extraction recoveries obtained from the different solvents is presented in Figure 3-3. The average percent recovery with 0.02% TFA in 50:50ACN:H_2O was slightly higher (88.3 ± 17.5) compared to that of 0.02% TFA in 25:75 ACN:H_2O (81.1 ± 5.2). The final organic composition in extracts eluted with 0.02% TFA in 50:50ACN:H_2O was adjusted to 25% before analysis because splitting of the ziconotide peak was observed at ACN

concentrations of more than 40% in the reconstitution solvent (data not shown). Values obtained for the seven extractions with 0.02% TFA in 50:50 ACN:H_2O, however, were less precise as indicated by the higher standard deviation of its percent recovery. Average percent recoveries with 0.02% TFA in 15:85 and 20:80 ACN:H_2O were lower at 65.3 ± 7.1 and 68.0 ± 3.5, respectively, compared to that obtained with 0.02% TFA in 25:75 ACN:H_2O. The use of 0.02% TFA in 80:20 ACN: H_2O and 50:50 IPA: H_2O, a more non-polar solvent, for ziconotide elution was also evaluated but no improvement in percent recoveries was observed for either. Since the highest recovery was obtained with 0.02% TFA in 50:50ACN:H_2O, it was chosen as the elution solvent for the succeeding experiments in optimizing reduction and alkylation parameters.

Optimized Conditions for Ziconotide Reduction

The starting amounts of reagents used in the reduction and alkylation experiments for this study were based from the work of Yen *et al.*.[60] The same reference was used as the basis for the reduction and alkylation procedure employed by Moller *et al.* in the determination of a novel framework or pattern of cysteine residues in conotoxins.[21] Yen and co-workers used a 25-fold molar excess of DTT and a 75-fold molar excess of IAM versus cysteine residues for reduction and alkylation of 5 to 30 µL of 2-20 pmol/µL peptide or protein solution (0.01 to 0.6 nmol).[60]

The identity and response of the products of ziconotide reduction were determined and compared at the various reaction conditions investigated. The net reactions undergone by ziconotide (Z) during reduction and alkylation are represented in Figure 3-4. The *m/z* of the various charge states of ziconotide after reduction of 1, 2, or 3 disulfide bonds were calculated and summarized in Table 3-1. The *m/z* of the corresponding oxidation products of the intact and reduced ions are shown in Table 3-2. The resulting *m/z* after the addition of 1 or 2 oxygen atoms were determined to account for all the possible products of oxidation. Knowing the expected *m/z*

for the various reduction and oxidation products of ziconotide helped in the identification of the ions observed from the mass spectra of the reduced peptide.

Reductions of 2.95 µM ziconotide with increasing DTT:Z molar ratios at 136, 271, 542, 1085 and 2169, for 30 minutes at 60 °C were compared. These molar ratios correspond to DTT concentrations of 0.60, 1.2, 2.4, 4.8 and 9.6 mM, respectively. The plot of average peak area versus DTT: Z molar ratio for the products of ziconotide reduction is shown in Figure 3-5. The peak areas obtained for the product of interest, the triply-reduced ziconotide, were not significantly different across the various concentrations used. Doubly-reduced and oxidized ziconotide were observed as side products. The peak areas for the doubly-reduced ziconotide were also not significantly different but those for oxidized ziconotide decreased with increasing DTT concentrations. Since no statistical difference was established for the response with increasing DTT:Z molar ratios, the lowest DTT concentration (0.60 mM), was used for subsequent analysis. Statistical difference at the 95% confidence level of the various responses being compared was established with one-way ANOVA. When the results of the analysis showed P-value > 0.05 and $F < F_{critical}$, the group averages for the particular parameter being investigated are not significantly different, while P-value < 0.05 and $F > F_{critical}$ signify that the group averages are statistically different.

The results for reduction with 0.60 mM DTT performed at 5, 10, 30 and 60 min at 60 °C are illustrated in Figure 3-6. Peak areas of the triply-reduced ziconotide were not statistically different at various reduction times but contribution from the oxidized product was less at 5 and 10 min. Peak areas of the doubly-reduced peptide were not significantly different at the reduction times investigated. Since a good yield for the desired product and minimal contribution from side products were obtained with reduction at 10 min, subsequent experiments

were performed at this reaction time. The choice between 5- and 10-min reduction times was based on ensuring a more complete reaction at 10 versus 5 min.

Comparison of the response for reduction conducted at various temperatures showed that yields for the desired product were comparable at 60 and 75 °C but the least amount of side products was obtained at 60 °C (Figure 3-7). Reduction carried out at 30 °C only showed the unreduced ziconotide while reduction at 45 °C yielded some unreduced, doubly- and triply-reduced peptide. Based on the results of this evaluation, 60 °C was chosen as the reduction temperature.

Finally, results of reduction conducted for 10 min at 60 °C with increasing DTT:Z molar ratios were compared to those obtained at 30 min (Figure 3-8). Two-way ANOVA was used to determine if there is interaction between DTT concentration and reduction time that could affect the response of the various products. Average peak areas of the triply-reduced ziconotide at various DTT concentrations (0.60, 1.2, 2.4, 4.8 and 9.6 mM) were significantly higher for reduction at 30 min compared to those at 10 min. However, the average peak areas for the doubly-reduced and oxidized products were also higher at 30 min. When responses for the various DTT concentrations used were compared, results showed no significant differences. Considering the effect of concentration and reduction time, results from the two-way ANOVA of the response for the completely reduced peptide showed no interaction between the two variables. Results from this study supported further the choice of 10 min as the reduction time. Analysis with the internal standard, ω-conotoxin GVIA, required the alkylation time to be adjusted to 20 min due to incomplete reduction of the IS at 10 min.

The base peak chromatogram and mass spectra of the products of ziconotide reduction are shown in Figures 3-9 and 3-10, respectively. Reduction was conducted with 20 µL of 0.60 mM

DTT, for 10 min at 60 °C, which are the optimal conditions determined. The *m/z* of the +3 and +4 ions of the oxidation product observed corresponds to the *m/z* of ziconotide ions with a singly-reduced disulfide bond and an additional 16 daltons (Da), which is attributed to oxygen. The base peak chromatogram of blank solutions did not show any peaks at the retention times where the products of ziconotide reduction elute, while that of the control solutions showed a peak at 6.57 min that corresponds to the intact ziconotide. The blank solution consisted of the ZipTip C_{18} extract of 30 μL of degassed, deionized water mixed with 20 μL of 0.60 mM $DTT_{(aq)}$ while the control was the extract of 2.95 μM ziconotide solution mixed with 20 μL of degassed, deionized water. Both were processed and analyzed identically as the ziconotide samples.

Optimized Conditions for Ziconotide Alkylation

Optimization of alkylation time, temperature and concentration of the alkylating agent, iodoacetamide were also carried out. The addition of ammonia solution before alkylation was carried out to enhance alkylation efficiency. The use of ammonia at this step was reported by Yen and co-workers.[60] To aid in the identification of the alkylation products, *m/z* of the various ions of ziconotide after reduction and addition of 2, 4, and 6 carbamidomethyl moieties were calculated and summarized in Table 3-3. The *m/z* of the corresponding oxidation products of modified ziconotide ions are presented in Table 3-4.

Using the optimal conditions for reduction, alkylation at different times was performed with 3.2 mM IAM in the dark and at room temperature. The response of the completely reduced and alkylated ziconotide was comparable at 15, 30, 45 and 60 min. alkylation times (Figures 3-11). Response of the completely reduced and alkylated ziconotide, in all the optimization studies, pertains to the sum of the peak areas of the +3, +4 and +5 ions of the completely modified peptide. These ions correspond to *m/z* 997, 748 and 599, respectively and are

represented as $[ZA_6+3H]^{3+}$, $[ZA_6+4H]^{4+}$ and $[ZA_5+5H]^{5+}$. Contribution from the TFA adduct of the oxidation product of modified ziconotide ($[(ZA_6+O+112)+4H]^{4+}$, *m/z* 780), was highest at 60 min. Its signal, however, was quite variable as indicated by the error bar on the plot.

The response of two other side products of the reduction and alkylation of ziconotide were also plotted against alkylation time; these are the doubly-reduced and alkylated ziconotide ($[ZA_6+4H]^{4+}$, *m/z* 719) and the oxidation product of the modified peptide ($[(ZA_6+O)+4H]^{4+}$, *m/z* 752). The signals from these two were found to be small. Responses of the side products were also plotted separately from the most predominant signal to provide a better illustration of their abundance and any trends in response (Figure 3-12). Since the response of the desired product at 15 min was not significantly different from that at 1 hr, 15 min was used as the alkylation time for the succeeding analyses.

The effect of alkylation temperature on the extent of reaction and identity of products formed was investigated next. Alkylation was carried out with 3.2 mM IAM, for 15 min. in the dark at 21, 30 and 60 °C. There was no statistical difference in the peak areas obtained for the completely reduced and alkylated ziconotide at the temperatures evaluated (Figure 3-13). The average peak area for the major product at 30 °C seemed higher than at room temperature (21 °C) but variability in its signal was also greater. Ions corresponding to the doubly-reduced and alkylated peptide and oxidation product of the completely modified ziconotide were observed at all temperatures. The signal due to the doubly-reduced and alkylated ziconotide at 30 °C was also highly variable. The TFA adduct of $[(ZA_6+O)+4H]^{4+}$, in this case, was only detected at 60 °C. The better precision of the response for the completely reduced and alkylated ziconotide and the absence of TFA adduct at room temperature supported the choice for alkylation temperature.

The major reduction and alkylation product was not included in the plot shown on Figure 3-14 to illustrate the response of the side products more clearly.

The responses of triply-reduced and alkylated ziconotide obtained with increasing IAM:Z molar ratios at 15-min alkylation time was plotted and compared against the results at 60-min (Figure 3-15). Results from the two-way ANOVA showed that no significant difference was observed among the average peak areas for the desired product at various IAM:Z molar ratios and at the two alkylation times considered. Responses were also not statistically different when the effect of both IAM:Z molar ratios and alkylation times were considered together. These results suggest that no interaction between the two variables being investigated exists.

A plot of the average peak areas for the side products observed with increasing IAM:Z molar ratios and at the two alkylation times being compared is presented in Figure 3-16. The signals for both $[ZA_4+4H]^{4+}$ and $[(ZA_6+O)+4H]^{4+}$ were low and not significantly different across the various iodoacetamide concentrations used. The responses obtained at 15- and 60-min. alkylation times for these two side products were also similar. Greater variability was observed, however, for the response of the TFA adduct of the oxidation product of modified ziconotide ($[(ZA_6+O+TFA)+4H]^{4+}$) at both 15- and 60-min. alkylation times. The TFA adduct signal was generally lower across the different IAM: Z ratios at 15-min. than 60-min except at IAM concentration of 6.4 mM (1205 IAM: Z molar ratio). The highest signal for the TFA adduct was observed at the highest IAM concentration used (*i.e.*, 25.6 mM). Standard deviation of these data was also the greatest. Since the response for the major product, triply-reduced and alkylated ziconotide, did not change significantly at increasing IAM concentrations and alkylation times of 15- and 60-min., the optimized conditions for alkylation were determined to be 3.2 mM IAM at

15 min. in the dark and at room temperature. Contributions from side products were also minimal at these conditions.

Reduction and alkylation reactions were also conducted without adding NH_4OH to make the solution basic and without adding 0.1% TFA in water to quench the reaction. The responses of the major and side products at these two conditions were compared to the products of reduction and alkylation carried out with NH_4OH and with TFA added (Figure 3-17). The response of modified ziconotide obtained without NH_4OH was significantly lower compared to that with NH_4OH. This result showed that making the reaction mixture basic with NH_4OH before alkylation helped enhance the efficiency of the reaction. On the other hand, the response of modified ziconotide without the addition of TFA was slightly higher than that with TFA present. The TFA adduct of the oxidation product of modified ziconotide was also not observed when alkylation was conducted without adding 0.1% TFA to quench the reaction. The importance of adding NH_4OH to the reaction mixture before alkylation and the improvements observed without quenching the alkylation process with TFA were established from the results of the analyses described.

Identification of Potential Fragment Ions for Quantitation

The extracted ion chromatograms and full-scan mass spectra of modified ziconotide and ω-conotoxin GVIA are shown in Figures 3-18 and 3-19, respectively. The +3, +4 and +5 charge states of the completely reduced and alkylated conopeptides were observed in each mass spectrum with the +4 ion as the most predominant. The net reactions undergone by ω-conotoxin GVIA during reduction and alkylation followed the representation adapted for ziconotide (Figure 3-4). The inclusion of other ions in the mass spectrum of the reduced and alkylated ziconotide such as the doubly-reduced and alkylated ions of the peptide at *m/z* 719 (+4) and 958 (+3) and

the oxidation product of the modified peptide at *m/z* 752 (+4) could have resulted from co-elution of the peaks for these products and that of the product of interest. The ion at *m/z* 775 (+4) with a corresponding +3 ion at *m/z* 1033 was not successfully identified. The use of a shorter gradient for the chromatographic separation of reduction and alkylation products shortened the analysis time but limited the complete resolution of the various products. Obtaining the peak areas of the ions of interest from extracted ion chromatograms circumvented some of the issues associated with co-elution and facilitated the determination of the response solely from the ion or ions of interest. The presence of other reduction and alkylation products was not observed in the mass spectrum for the internal standard. A small contribution from the +4 ion of modified ziconotide was observed in the mass spectrum of the IS due to some degree of overlap of the peaks of the 2 conopeptides.

Isolation and fragmentation of the +4 charge states of modified ziconotide and ω-conotoxin GVIA through CID at 35% collision energy were performed to identify potential fragment ions for quantitation. The product ion spectra for the +4 ions of the modified conopeptides are shown in Figure 3-20. The MS/MS product ions were identified with the aid of ProteinProspector's MS-Product software[70] that provided theoretical average masses for peptide fragments which are needed for reliable mass assignment. The majority of the fragment ions were b and y ions from peptide bond cleavage. Table A-1 summarizes the observed and theoretical *m/z* of the various product ions of modified ziconotide together with their relative intensities and calculated mass differences (see Appendix A). The same information for the product ions of modified ω-conotoxin GVIA is summarized in Table A-2 (see Appendix A). The difference between the observed and theoretical *m/z* (Δm) was limited to ≤ 0.5 Da for identification of the fragment ions. The 3 most intense product ions of *m/z* 748, the +4 ion of

modified ziconotide, were *m/z* 900.42, 937.32, and 716.30, corresponding to y_{23}^{3+}, y_{24}-H_2O^{3+}, and y_{12}-NH_3^{2+}, respectively while those of *m/z* 848, the +4 ion of modified ω-conotoxin GVIA, were *m/z* 1004.21, 1033.22 and 1033.92, corresponding to y_{24}^{3+}, a_{18}-NH_3^{2+}, and y_{25}^{3+}, respectively. These ions could be used as diagnostic ions for the qualitative and quantitative determination of ziconotide and ω-conotoxin GVIA.

When the *m/z* of a product ion corresponded to that predicted for several possible CID products, the fragment ion actually responsible for the observed peak was confirmed by performing MS^3 analysis. As an example, the ion at *m/z* 900.42, the most abundant one seen following CID of *m/z* 748 might be attributed to 3 different product ions: b_{15}-H_2O^{2+} (*m/z* 900.09, $\Delta m = 0.33$), b_{15}-NH_3^{2+} (*m/z* 900.59, $\Delta m = 0.17$), and y_{23}^{3+} (*m/z* 900.73, $\Delta m = 0.31$). Comparison of the product ions obtained after MS^3 analysis of *m/z* 900.42 with theoretical *m/z* values generated using ProteinProspector's MS-Product software confirmed its identity as y_{23}^{3+}.

Generation of the Response Curve for Modified Ziconotide

Six ziconotide standards with concentrations ranging from 0.035 to 1.8 µM containing a fixed concentration of 0.20 µM ω-conotoxin GVIA (IS) in the reduction mixture were alkylated, extracted and analyzed using HPLC-ESI-MS and MS/MS. Peak areas of the most abundant ions (*i.e.*, +4 charge states) in the full scan mass spectra of the modified conopeptides were obtained from corresponding extracted ion chromatograms. The ratios of the area of the +4 ion of ziconotide to that of the IS were plotted against ziconotide concentrations, using a weighted linear fit, to generate the calibration curve for modified ziconotide (Figure 3-21).

Since each solution had to be reduced, alkylated, extracted and analyzed one after the other, only 8 solutions including blank and control solutions were processed in duplicate and included in the run. Out of the 6 standard solutions, only 4 yielded quantifiable signal. No

signal was detected for the +4 ion of modified ziconotide in the lowest calibrator (0.035 µM) while its signal to noise ratio (S/N) was less than 10 in the next calibration standard (0.059 µM). Analysis of back-calculated concentrations of calibration standards yielded absolute values of ≤ 4.0% for the % relative error (%RE) and % relative standard deviation (%RSD) of 1.0 to 16.3% (Table 3-5). With a %RSD of 16.3%, the standard at 1.2 µM failed to satisfy the Food and Drug Administration's (FDA) 15% acceptance criteria for %RSD. The limited number of replicates analyzed for each standard contributed to the high %RSDs obtained for some calibrators.

Using the results from back-calculation of the calibration standard concentrations and the FDA guidelines, the lower limit of quantitation (LLOQ) for the reduced and alkylated ziconotide was found to be 0.50 ng on column. This corresponds to the lowest calibration standard analyzed that yielded a quantifiable signal (%RE ≤ 20%, %RSD ≤ 20%). The limit of detection (LOD) was determined from the ziconotide concentration that exhibited a signal to noise ratio (S/N) of at least 3. As mentioned in Chapter 2, the constant 3 represents a confidence level of detection of 89% or greater, and is the value recommended in literature.[52-54] The LOD, in this case, corresponds to 0.25 ng on column.

The LOD and LLOQ determined from peak areas of the +4 ions of modified ziconotide (*m/z* 748) and IS (*m/z* 848), which were recorded from 10 blank analyses were also evaluated for comparison. The average (S_{bl}) of the area ratios of *m/z* 748 to *m/z* 848 and the resulting standard deviation (s_{bl}) from the blank measurements were calculated and incorporated into equation 3-1, where S_{LOD} corresponds to the signal required for the LOD.

$$S_{LOD} = S_{bl} + 3(s_{bl}) \qquad (3\text{-}1)$$

The signal at LOD is then incorporated into equation 3-2 to determine the concentration at LOD (C_{LOD}), where m is the slope obtained from the plot shown in Figure 3-21.

$$C_{LOD} = (S_{LOD} - S_{bl})/m \quad (3\text{-}2)$$

The LOD for the reduced and alkylated ziconotide was found to be 0.13 µM or 0.57 ng on column.

The lower limit of quantitation was calculated as 10 times the standard deviation of the blank measurement, s_{bl} (Equation 3-3).

$$C_{LLOQ} = (10 \times s_{bl})/m \quad (3\text{-}3)$$

The LLOQ for modified ziconotide obtained by using the above equation was determined to be 0.42 µM or 1.8 ng on column. This calculated value, however, was higher than the LLOQ obtained from the experimental results (0.50 ng) using the FDA guidelines. The LOD (0.57 ng) from the blank measurements was also higher than 0.25 ng, which corresponds to the concentration with a S/N of at least 3.

Using the ratio of the blank signals for *m/z* 748 to *m/z* 848 could have contributed to the difference in LOD and LLOQ values obtained from calculations and experimental results. The equations presented above which include the signal and standard deviation of blank measurements are intended for LOD and LLOQ determination involving linear response curves.[71] The area ratio of *m/z* 748 to *m/z* 848 was used for calculations since plot of the area of *m/z* 748 versus ziconotide concentration did not yield a linear plot. A quadratic fit best describes the relationship between peak area and modified ziconotide concentration, in this case.

The ratio of the total peak areas of the 3 major fragment ions of modified ziconotide (*m/z* 716, 900.5, 937.5) to that of the IS (*m/z* 1004, 1033, 1034) against ziconotide concentration was also plotted and considered for the determination of LLOQ and LOD. However, using the line equation for the plot described, the %RSD calculated for 2 of the calibration standards (0.59 and 1.8 µM) failed the FDA acceptance criterion of 15%. There was also no improvement in the

LOD and LLOQ when the response of product ions of modified ziconotide and IS were used. This is contrary to what was expected since isolation and fragmentation of a precursor ion should result to improved signal to noise ratio which helps increase the sensitivity of a method.[72] This improvement, however, is associated with applications involving analyses of compounds in complex sample matrices where MS/MS facilitates the reduction of chemical noise contribution.

Base peak chromatograms of blank and control solutions for reduction and alkylation are shown in Figure 3-22. The absence of any distinct peak in the blank chromatogram at the elution times of the modified conopeptides indicates the absence of possible interference from the blank solution. The peak that is starting to appear at 6 min in the blank chromatogram corresponds to a polyethyleneglycol (PEG) contaminant peak. The peak observed in the control chromatogram corresponds to the unmodified or intact ziconotide. Difference in peak areas observed for the modified and unmodified ziconotide could be attributed to differences in ionization efficiency (see Figures 3-18 and 3-22).

Reduction and Alkylation of Ziconotide Plasma Extract

A preliminary analysis of ziconotide extract from blank horse plasma using the reduction and alkylation method developed was conducted. Extraction of the peptide from blank horse plasma using a PD-10 desalting column and C_{18} cartridge was shown to be fairly successful. Comparison of the total peak area of the +3 (*m/z* 881), +4 (*m/z* 661), and +5 (*m/z* 529) charge states of intact ziconotide from the actual extract and control solution showed an average percent recovery of 71.41% ± 26.21% for a supplemented concentration of 2.5 µg/mL ziconotide in 1 mL of horse plasma. This average was only from duplicate analysis of both extract and control solutions. Representative extracted ion chromatograms of the 3 major ions of intact ziconotide for the extract, control and blank matrix and their respective mass spectra are shown in Figures

3-23 and 3-24. A sample of blank horse plasma processed in the same way as the extract constituted the matrix blank.

The full-scan mass spectra of the extract and control solution showed the +3 and +4 ions of intact ziconotide as the most abundant ions. The presence of other ions, specifically *m/z* 627 and 835, was also observed. The masses of these ions when compared to *m/z* 661 and 881, respectively, differ by 136 Da. This mass difference could correspond to the loss of 8 ammonia (17 Da) groups. The acidic conditions used during extraction would easily favor protonation and cleavage of the amine groups from the 4 lysine and 2 arginine residues, N-terminal and amidated C-terminal of ziconotide, thus accounting for the loss observed. The pH of peptide or protein solutions is said to greatly affect unfolding and denaturation.[17] The possible unfolding of ziconotide, in this case, provides access to the basic amine groups for protonation. The presence of these ions (*i.e.*, *m/z* 627, 835) in the extracted matrix blank, however, may indicate contamination.

Results from the HPLC/MS analysis of the reduction and alkylation product of the solid phase extraction (SPE) extract showed the presence of reduced and alkylated ziconotide (Figures 3-25 and 3-26). However, the response for modified ziconotide was low. Failure to account for changes in peptide concentration during reduction and alkylation led to the use of the same DTT and IAM concentrations as those used during optimization wherein the peptide concentration was lower than that present in the extract analyzed. The low signal for modified ziconotide could also indicate the need to optimize reduction and alkylation in the actual sample matrix.

Other ions of significant abundance (*i.e.*, *m/z* 705, 940) were also present in the mass spectra of the reduced and alkylated extract. These ions were found to correspond to the completely reduced and alkylated forms of *m/z* 627 and 835, respectively, which further lose 2

water molecules. The *m/z* of the completely reduced and alkylated species of *m/z* 627 and 835, are 714 and 952. The detection of *m/z* 705 and 940 in the mass spectra of the blank could be due to contamination.

Conclusion

The reduction and alkylation conditions for ziconotide were systematically optimized. The reduction conditions were found to be optimal at 10 min and 60 °C with the use of 0.60 mM dithiothreitol while complete alkylation was achieved with 3.2 mM iodoacetamide at room temperature for 15 min in the dark. Reduction time had to be adjusted to 20 min when the internal standard, ω-conotoxin GVIA was added to the reaction mixture. The optimized conditions for alkylation were used for the analysis of a mixture of ziconotide and the IS with the volume of reagents doubled. Reduction of the disulfide bonds and alkylation of the resulting sulfhydryl groups eliminate cross-linking and increase the probability of fragmentation during CID of the conopeptides.

Tandem HPLC/MS/MS analyses of modified ziconotide yielded structurally relevant fragment ions (*i.e.*,b and y ions) as compared to that of the intact peptide. The availability of software such as ProteinProspector's MS Product software aided in the reliable assignment of masses to the fragment ions generated. The 3 most intense product ions of the CID of ziconotide could be used as diagnostic ions for the qualitative and quantitative determination of the conopeptide.

The limit of quantitation obtained for modified ziconotide, however, restricted the application of the method to complex sample matrices. Because of the low effective dose of ziconotide, concentrations of the peptide in biological samples are expected to be in the ng/mL or pg/mL range. Nevertheless, the feasibility of analyzing ziconotide from blank horse plasma

extracts supplemented with ziconotide standard using the reduction and alkylation method developed was tested and positive results were obtained. Ziconotide was detected from the plasma extract although the intensity of the signal obtained was low compared to what was actually expected from the amount supplemented. Further optimization of the extraction, reduction and alkylation methods using plasma samples is recommended to improve product yield.

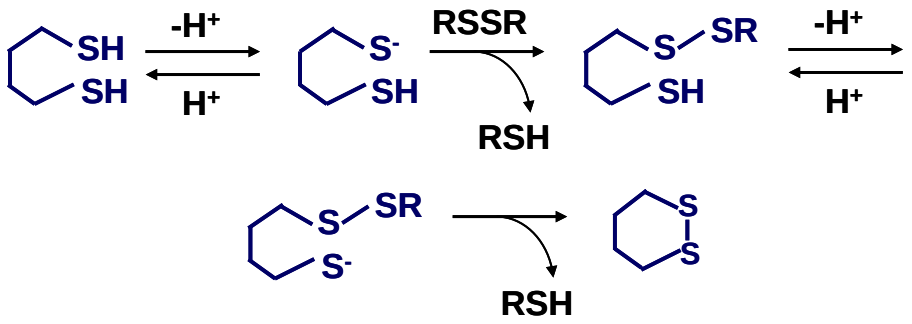

Figure 3-1. Mechanism involved in the reduction of disulfide bridges by dithiols. The dithiol undergoes deprotonation forming a thiolate anion. The anion then attacks a disulfide bond, cleaving the disulfide bond in the process and forming sulfhydryl groups. Overall, the oxidation of the dithiol to the cyclic disulfide facilitates the reduction of other disulfides in solution. Adapted from Lamoureux, *et al*.[67]

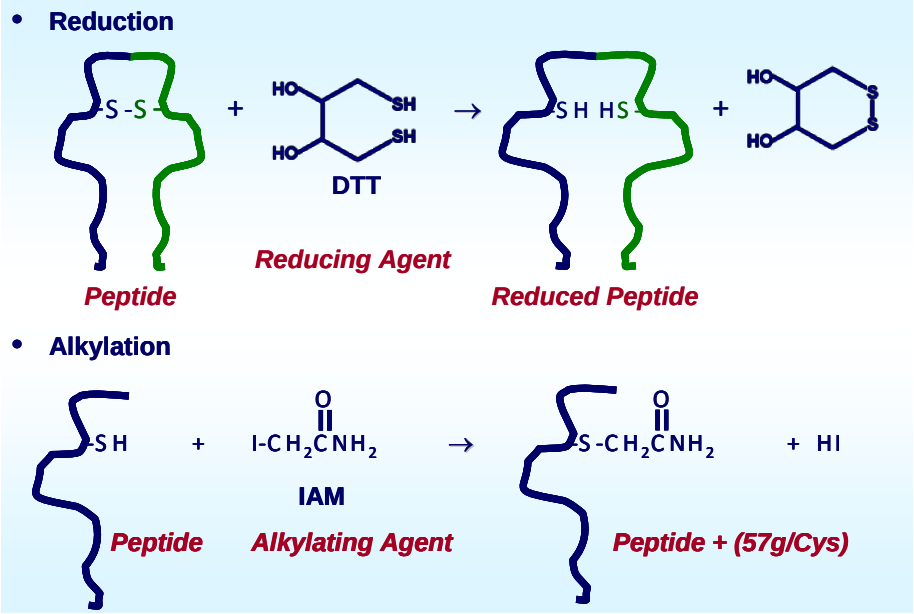

Figure 3-2. Representation of disulfide bond reduction and alkylation of the resulting sulfhydryl groups.

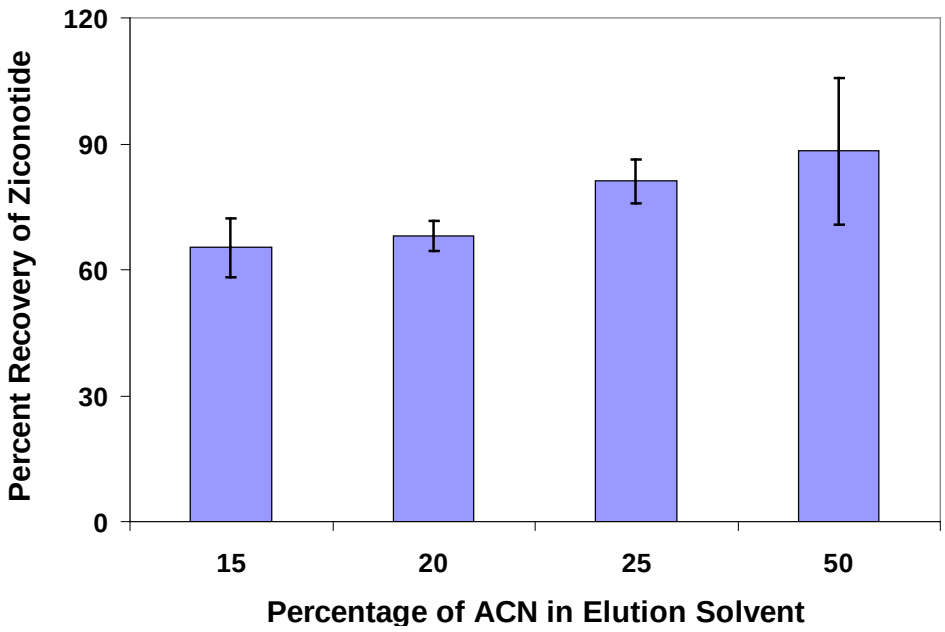

Figure 3-3. Extraction recoveries of ziconotide from ZipTip C_{18} pipette tips using various elution solvents. Mixtures of acetonitrile and water with 0.02% TFA constituted the solvents. The 0.02% TFA in 50:50 ACN: H_2O elution solvent exhibited a higher but comparable extraction recovery with 0.02% TFA in 25:75 ACN: H_2O. The data are an average of 7 separate extractions and error bars represent standard deviation of the extractions.

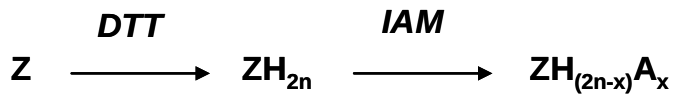

***n*: number of disulfide bonds reduced**
***x*: number of carbamidomethylated cysteine residues**
***A*: carbamidomethyl group**

Figure 3-4. Representation of the net reactions for the reduction and alkylation of ziconotide .

Table 3-1. The *m/z* of the various charge states of ziconotide after reduction of its disulfide bonds.

Ave. MW of Z	Charge State (CS)	*m/z* of CS	Added Mass per -S-S- Reduced	*m/z* of CS after Reduction of "X" -S-S-		
				1	2	3
2639.1	1+	2640.1	2.02	2642.2	2644.2	2646.2
	2+	1320.6		1321.6	1322.6	1323.6
	3+	880.7		881.4	882.1	882.7
	4+	660.8		661.3	661.8	662.3
	5+	528.8		529.2	529.6	530.1

X: number of disulfide bonds -S-S-: disulfide bond

m/z of CS = (Ave. MW of Z + CS*1.01)/CS

m/z of CS after reduction = (*m/z* of CS*CS + 2.02*X -S-S- reduced)/CS

Table 3-2. The *m/z* of the oxidation products of the various ions of intact and reduced ziconotide.

CS	*m/z* of CS	*m/z* after Oxidation		*m/z* of CS after Reduction of "X" -S-S- and Oxidation					
		Add'n of 1 O	Add'n of 2 O	Addition of 1 O			Addition of 2 O		
				1	2	3	1	2	3
1+	2640.1	2656.1	2672.1	2658.2	2660.2	2662.2	2674.2	2676.2	2678.2
2+	1320.6	1328.6	1336.6	1329.6	1330.6	1331.6	1337.6	1338.6	1339.6
3+	880.7	886.1	891.4	886.7	887.4	888.1	892.1	892.7	893.4
4+	660.8	664.8	668.8	665.3	665.8	666.3	669.3	669.8	670.3
5+	528.8	532.0	535.2	532.4	532.9	533.3	535.6	536.1	536.5

X: number of disulfide bonds -S-S-: disulfide bond O: oxygen

m/z of CS after addition of 1O = (*m/z* of CS*CS + 16)/CS

m/z of CS after addition of 2O = (*m/z* of CS*CS + 32)/CS

m/z of CS after reduction and addition of 1O = (*m/z* of CS*CS + 2.02*X -S-S- reduced + 16)/CS

m/z of CS after reduction and addition of 2O = (*m/z* of CS*CS + 2.02*X -S-S- reduced + 32)/CS

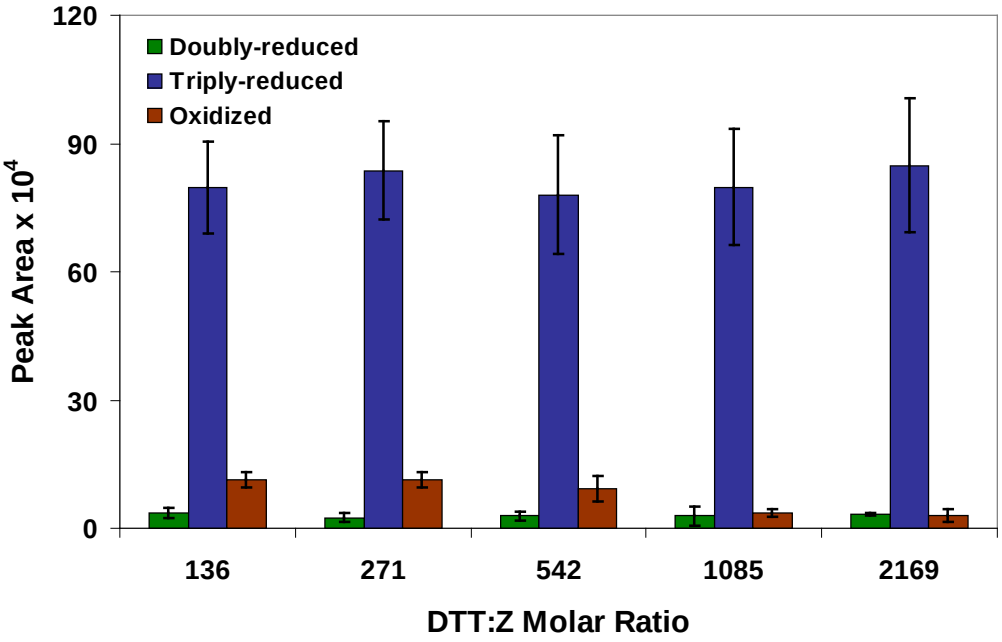

Figure 3-5. Response of the various products of ziconotide reduction with increasing DTT:Z molar ratio. Reduction of 2.95 µM ziconotide was conducted for 30 minutes at 60°C. There was no statistical difference in the peak areas for the triply- and doubly-reduced peptide but lower response was observed for the oxidized product at higher DTT: Z molar ratios. The data are an average of 6 replicate analyses and error bars represent standard deviation of the measurements.

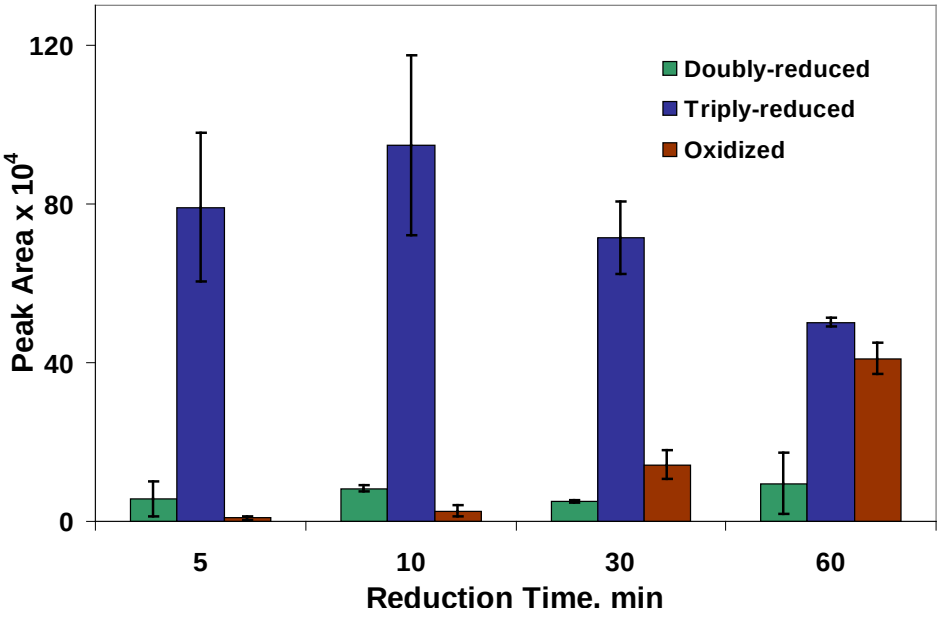

Figure 3-6. Response of reduced and oxidized ziconotide with increasing reduction times. Average (n = 6) peak areas of the completely reduced ziconotide for 5, 10 and 30 minutes showed no significant difference but contribution from the oxidized product was minimal at 5 and 10 minutes. Error bars represent the standard deviation of the replicates.

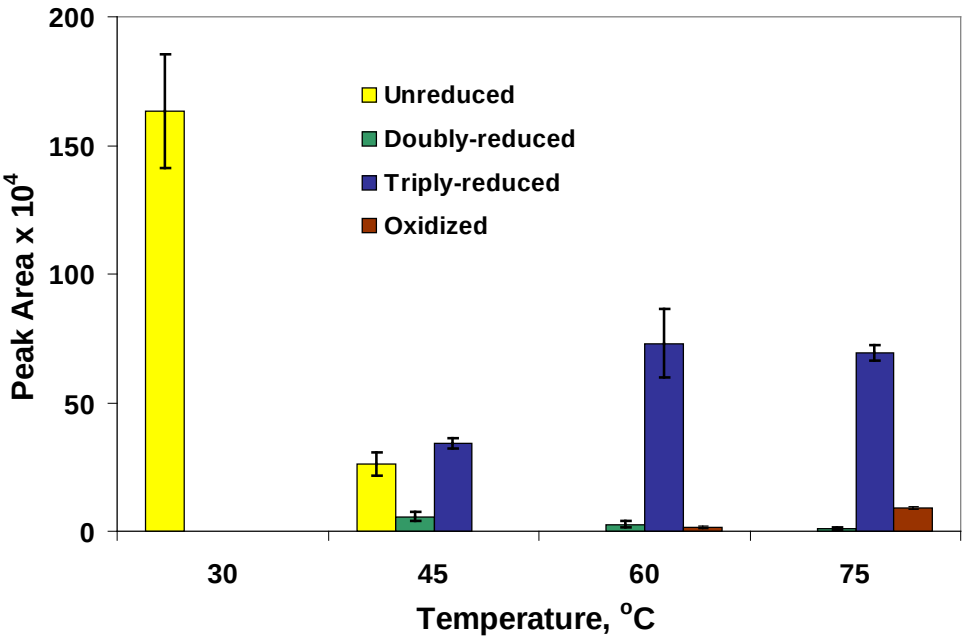

Figure 3-7. Response of reduced and oxidized ziconotide with increasing reduction temperatures. Good yields of the desired product were observed at 60 and 75°C but the least amount of side products was obtained at 60°C. The data are an average of 6 replicate analyses and error bars represent standard deviation of the measurements.

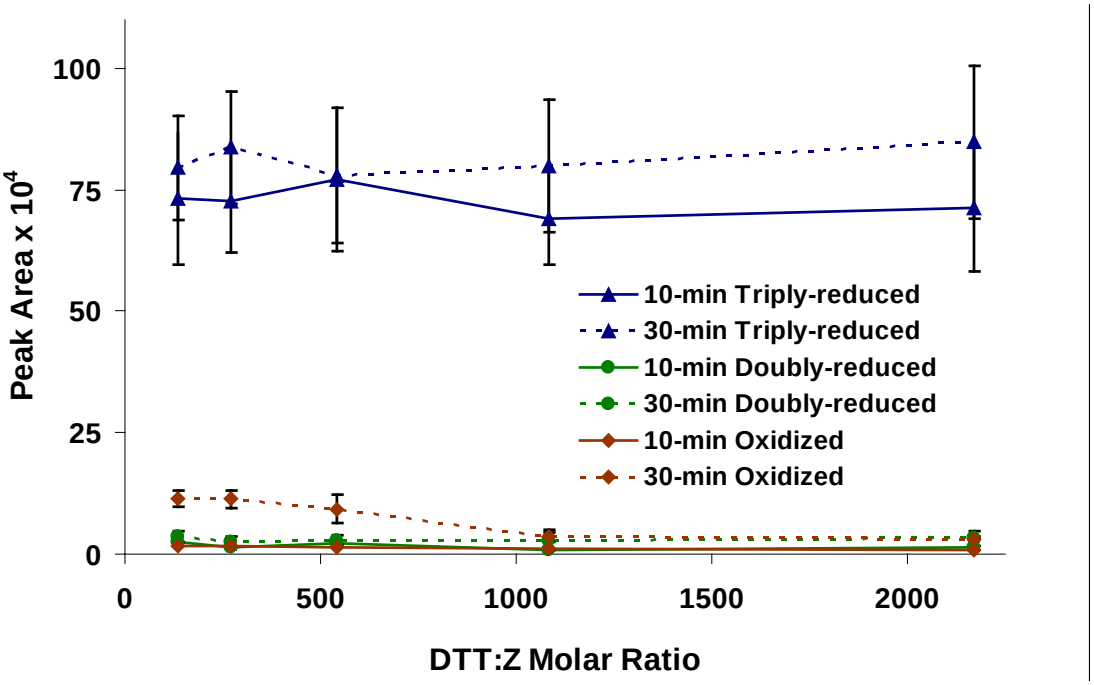

Figure 3-8. Response of reduced and oxidized ziconotide at 10- and 30-minute reduction times with increasing DTT concentrations. Responses (n = 6) of the triply-reduced ziconotide at 10- and 30-minute reduction times were statistically different while there were no significant difference at various DTT concentrations. There was no interaction between the two variables based on statistical analysis.

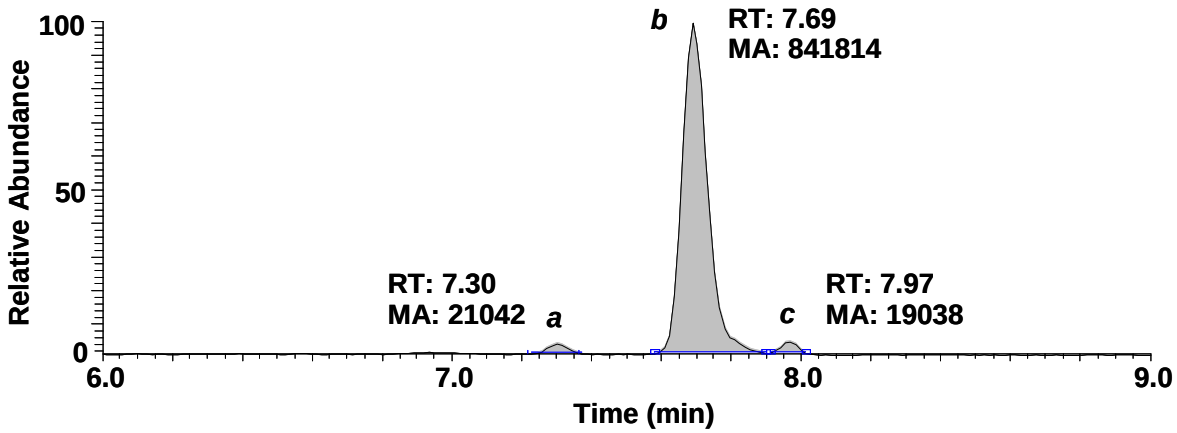

Figure 3-9. Base peak chromatogram of the various products of ziconotide reduction. Reduction was carried out with 0.60 mM DTT for 10 min at 60 °C, the optimum conditions determined. Peaks *a, b, and c* correspond to mass spectra *A, B* and *C,* respectively. RT: retention time, MA: manually integrated area

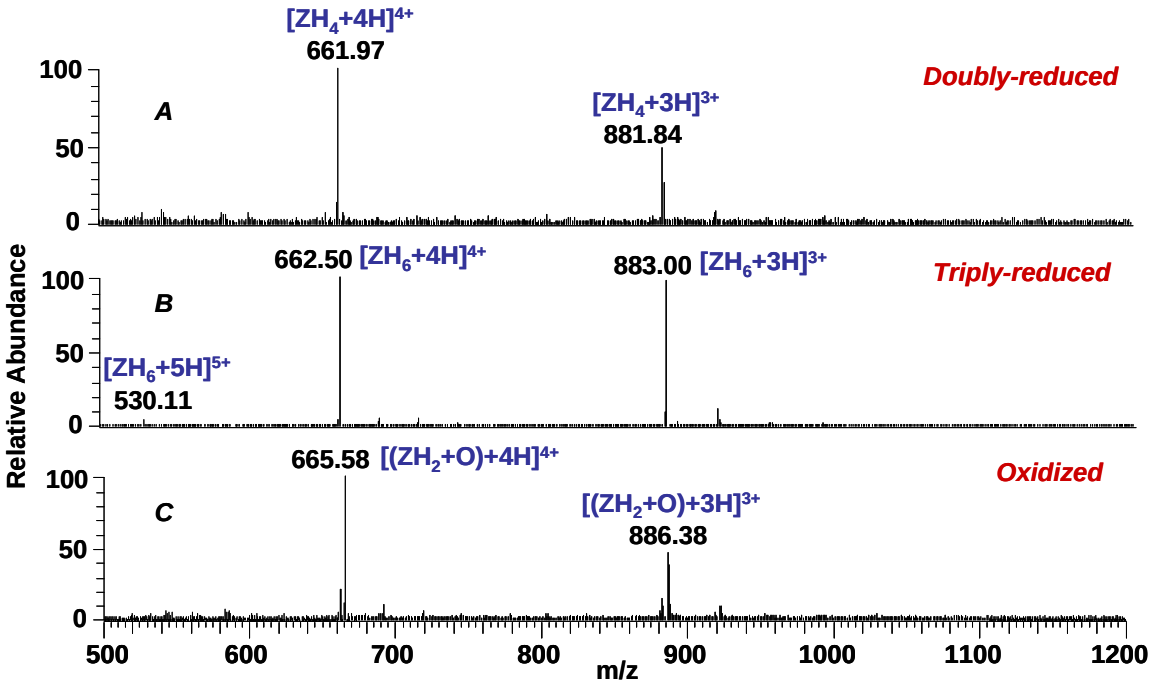

Figure 3-10. Full-scan mass spectra of reduced and oxidized ziconotide(*A*-*C*). The average molecular mass of the oxidation product corresponds to the addition of 16 Da to the mass of a singly-reduced peptide. A gradient of 2-60% B in 20 min was used to resolve the various products.

Table 3-3. The *m/z* of the various charge states of ziconotide after reduction and alkylation of its disulfide bonds.

CS	*m/z* of CS	*m/z* of CS after Reduction of "X" -S-S-			m/z of CS after Addition of "Y" IAM		
		1	2	3	2	4	6
1+	2640.1	2642.2	2644.2	2646.2	2756.3	2872.4	2988.6
2+	1320.6	1321.6	1322.6	1323.6	1378.7	1436.7	1494.8
3+	880.7	881.4	882.1	882.7	919.4	958.2	996.9
4+	660.8	661.3	661.8	662.3	689.8	718.9	747.9
5+	528.8	529.2	529.7	530.1	552.1	575.3	598.5

X: number of disulfide bonds -S-S-: disulfide bond

Y: number of carbamidomethyl moieties

m/z of CS after reduction = (*m/z* of CS*CS + 2.02*X -S-S- reduced)/CS

m/z of CS after alkylation = (*m/z* of CS after reduction*CS + 57.06*Y IAM added)/CS

Table 3-4. The *m/z* of the oxidation products of the various ions of reduced and alkylated ziconotide.

CS	*m/z* of CS after Addition of "Y" IAM			*m/z* of CS after Addition of "Y" IAM and Oxidation					
				Addition of 1 O			Addition of 2 O		
	2	4	6	2	4	6	2	4	6
1+	2756.3	2872.4	2988.6	2772.3	2888.4	3002.5	2788.3	2904.4	3018.5
2+	1378.7	1436.7	1494.8	1386.7	1444.7	1502.8	1394.7	1452.7	1510.8
3+	919.4	958.2	996.9	924.8	963.5	1002.2	930.1	968.8	1007.5
4+	689.8	718.9	747.9	693.8	722.9	751.9	697.8	726.9	755.9
5+	552.1	575.3	598.5	555.3	578.5	601.7	558.5	581.7	604.9

Y: number of carbamidomethyl moieties

m/z of CS after alkylation = (*m/z* of CS after reduction*CS + 57.06*Y IAM added)/CS

m/z of CS after alkylation and addition of 1O = (*m/z* of CS after reduction*CS + 57.06*Y IAM added + 16)/CS

m/z of CS after alkylation and addition of 2O = (*m/z* of CS after reduction*CS + 57.06*Y IAM added + 32)/CS

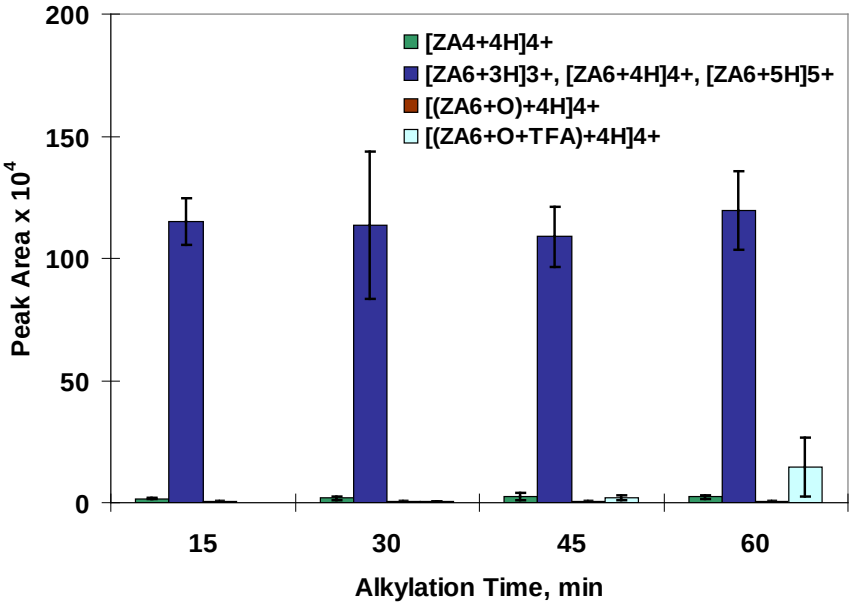

Figure 3-11. Average peak area (n = 6) for the reduction and alkylation products of ziconotide at increasing alkylation times. Responses for the completely reduced and alkylated product at various alkylation times were comparable. Error bars represent standard deviation of the replicates.

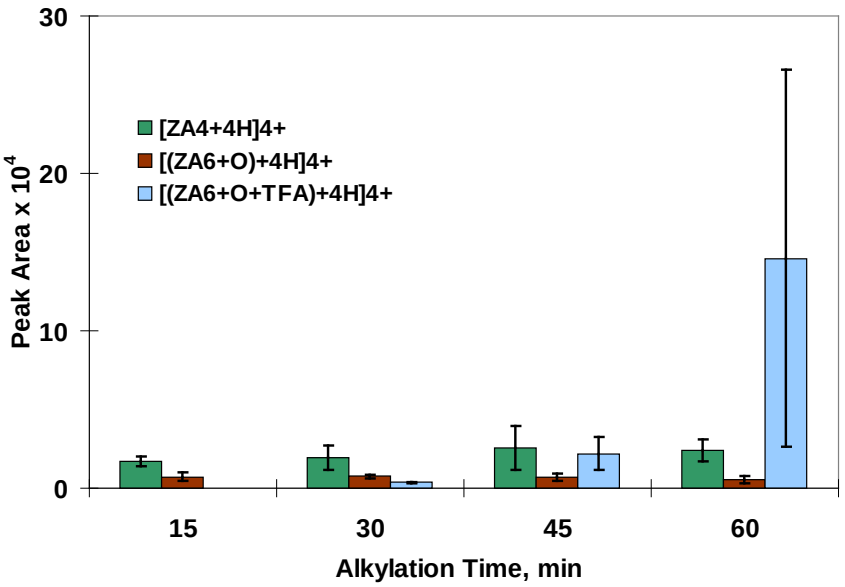

Figure 3-12. Response of the side products of modified ziconotide at different alkylation times. Contribution from the TFA adduct of the oxidation product of modified ziconotide was highest at 60 min. but its signal was irreproducible.

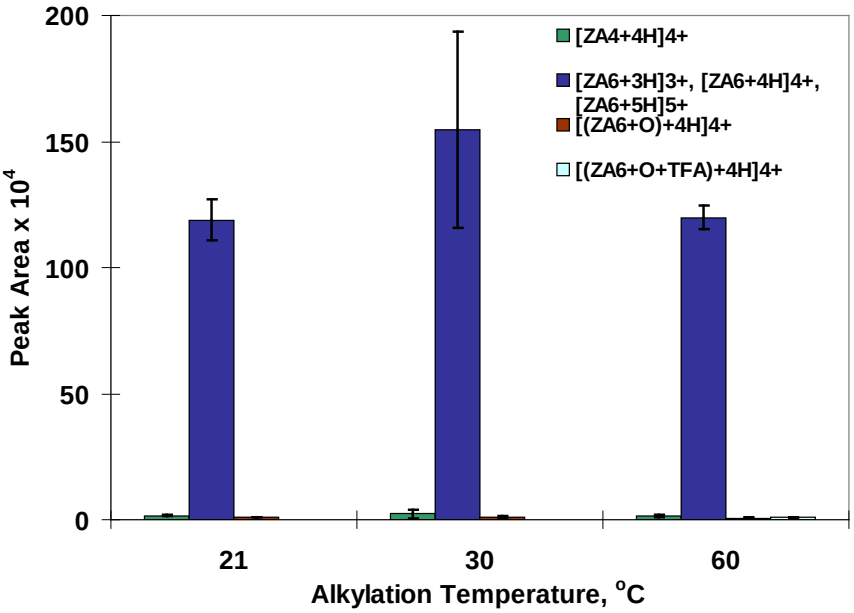

Figure 3-13. Response of the various ions of reduced and alkylated ziconotide at different alkylation temperatures. There was no significant difference in the peak areas (n = 6) obtained for the major product at the temperatures evaluated. Response at 30 °C seemed higher than at room temperature but the greater variability in signal resulted to the choice of room temperature for alkylation. Error bars represent SD.

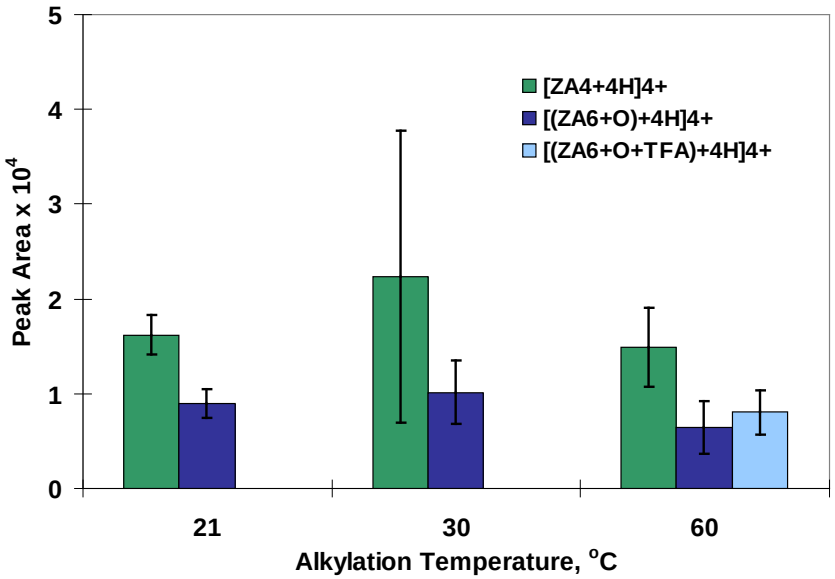

Figure 3-14. Response of the side products of modified ziconotide at various alkylation temperatures. The average peak area for $[ZA_4+4H]^{4+}$ at 30 °C was also variable. The TFA adduct of $[(ZA_6+O)+4H]^{4+}$ was only observed at 60 °C.

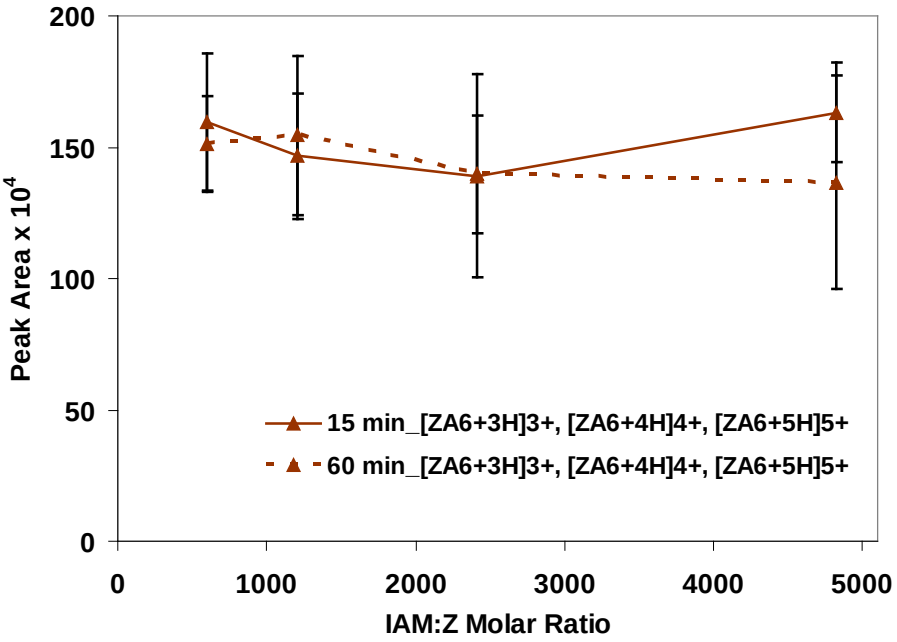

Figure 3-15. Average peak areas (n = 6) of the triply-reduced and alkylated ziconotide with increasing IAM: Z molar ratios at 15- and 60-min. alkylation times. The responses were not significantly different at various IAM: Z molar ratios and at the alkylation times considered. Results from two-way ANOVA did not indicate interaction between the two variables.

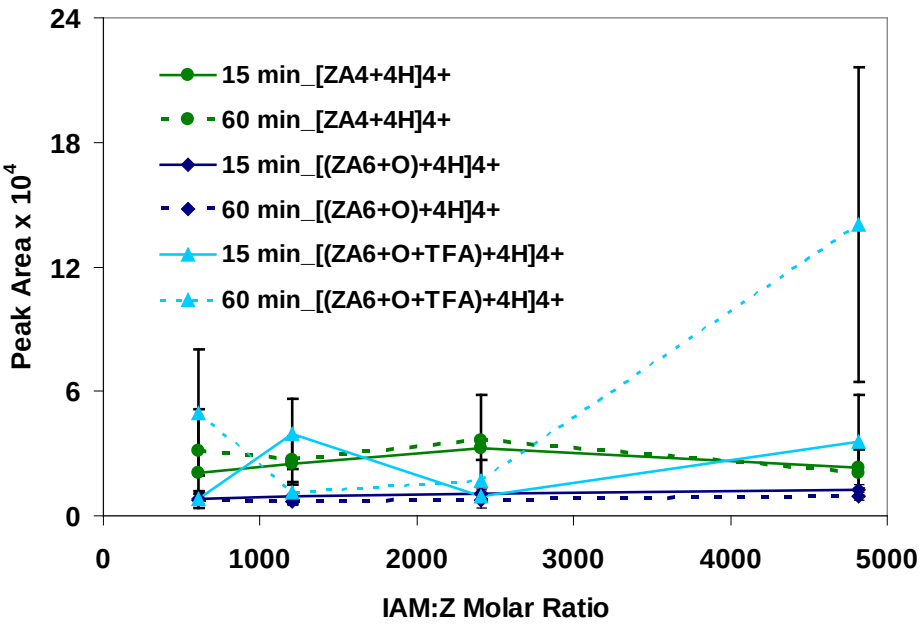

Figure 3-16. Signal contributions of the side products of ziconotide modification with increasing IAM: Z molar ratios at 15- and 60-min. alkylation times. The responses (n = 6) for $[ZA_4+4H]^{4+}$ and $[(ZA_6+O)+4H]^{4+}$ were low and not significantly different at various IAM: Z molar ratios and at the alkylation times considered. Response for $[(ZA_6+O+TFA)+4H]^{4+}$ was generally variable and its highest contribution was observed at the highest IAM concentration used. Variability of this data was also the highest. Error bars represent standard deviation.

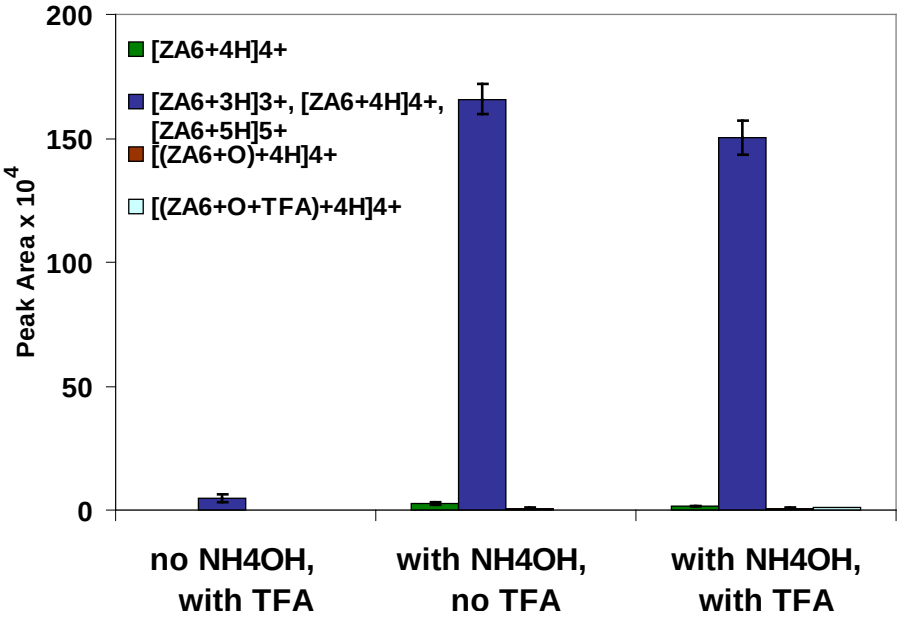

Figure 3-17. Response comparison of the major and side products of modified ziconotide with and without the addition of NH_4OH to enhance alkylation efficiency and the addition of TFA to quench the reaction. The data are an average of 3 replicate analyses and error bars represent standard deviation of the measurements.

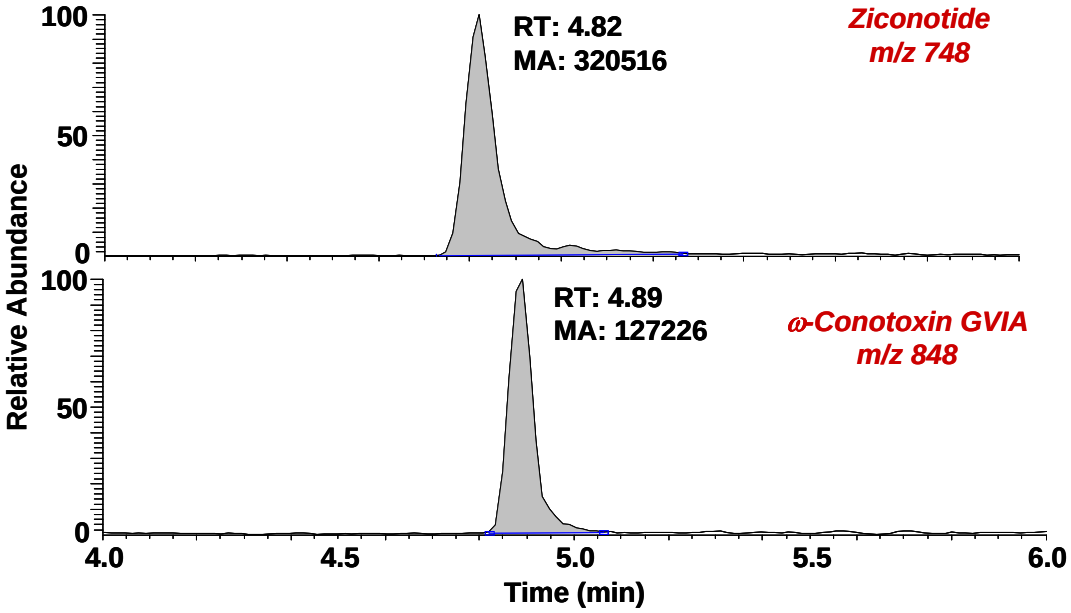

Figure 3-18. Extracted ion chromatograms of the +4 charge states of the reduced and alkylated ziconotide (*top*) and ω-conotoxin GVIA (*bottom*). These data correspond to initial concentrations of 1.8 µM for ziconotide and 0.66 µM for ω-conotoxin GVIA.

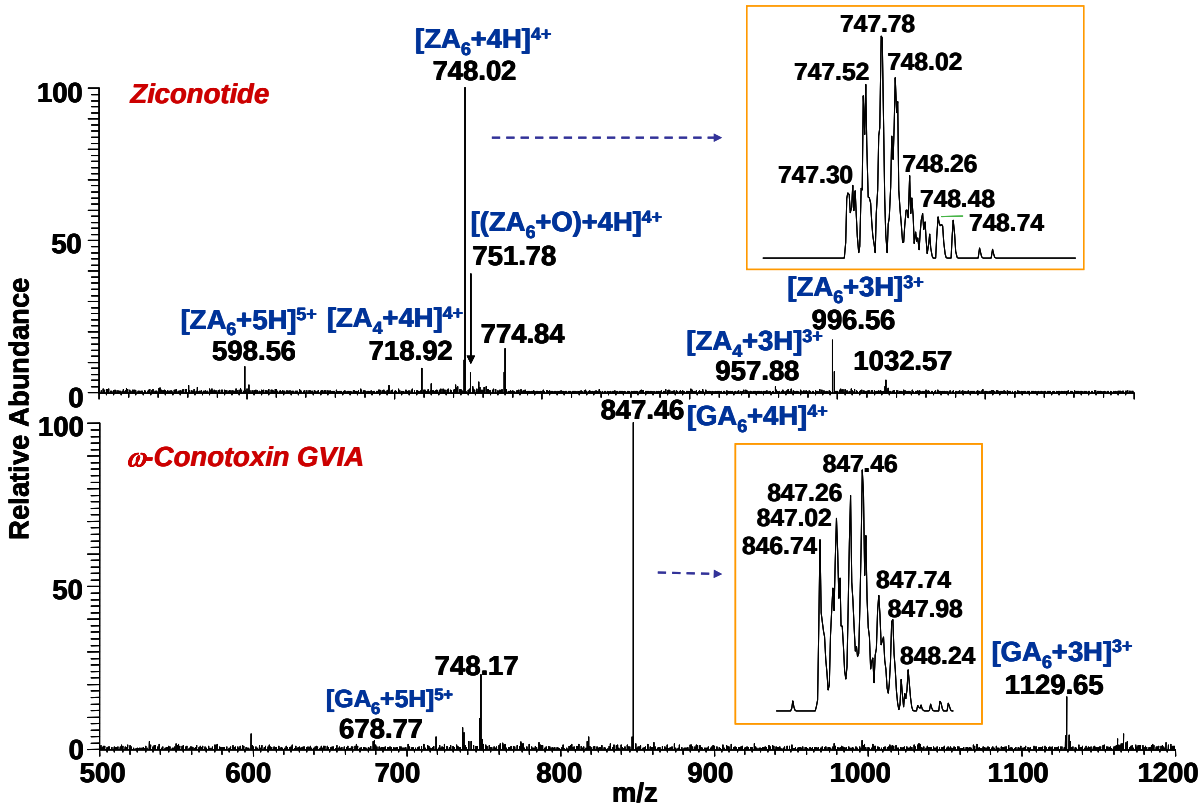

Figure 3-19. Full-scan mass spectra of the modified conopeptides, ziconotide (*top*) and ω-conotoxin GVIA (*bottom*). The +4 charge states of the completely reduced and alkyalted conopeptides were the most aboundant ions. The +3 and +5 ions of the modified conopeptides were also present. The doubly-reduced and alkylated ziconotide ($[ZA_4+4H]^{4+}$, $[ZA_4+3H]^{3+}$) and the oxidation product of the completely modified ziconotide were also observed in its mass spectrum. Insets show the isotopic distributions of the +4 ions of the modified ziconotide and ω-conotoxin GVIA.

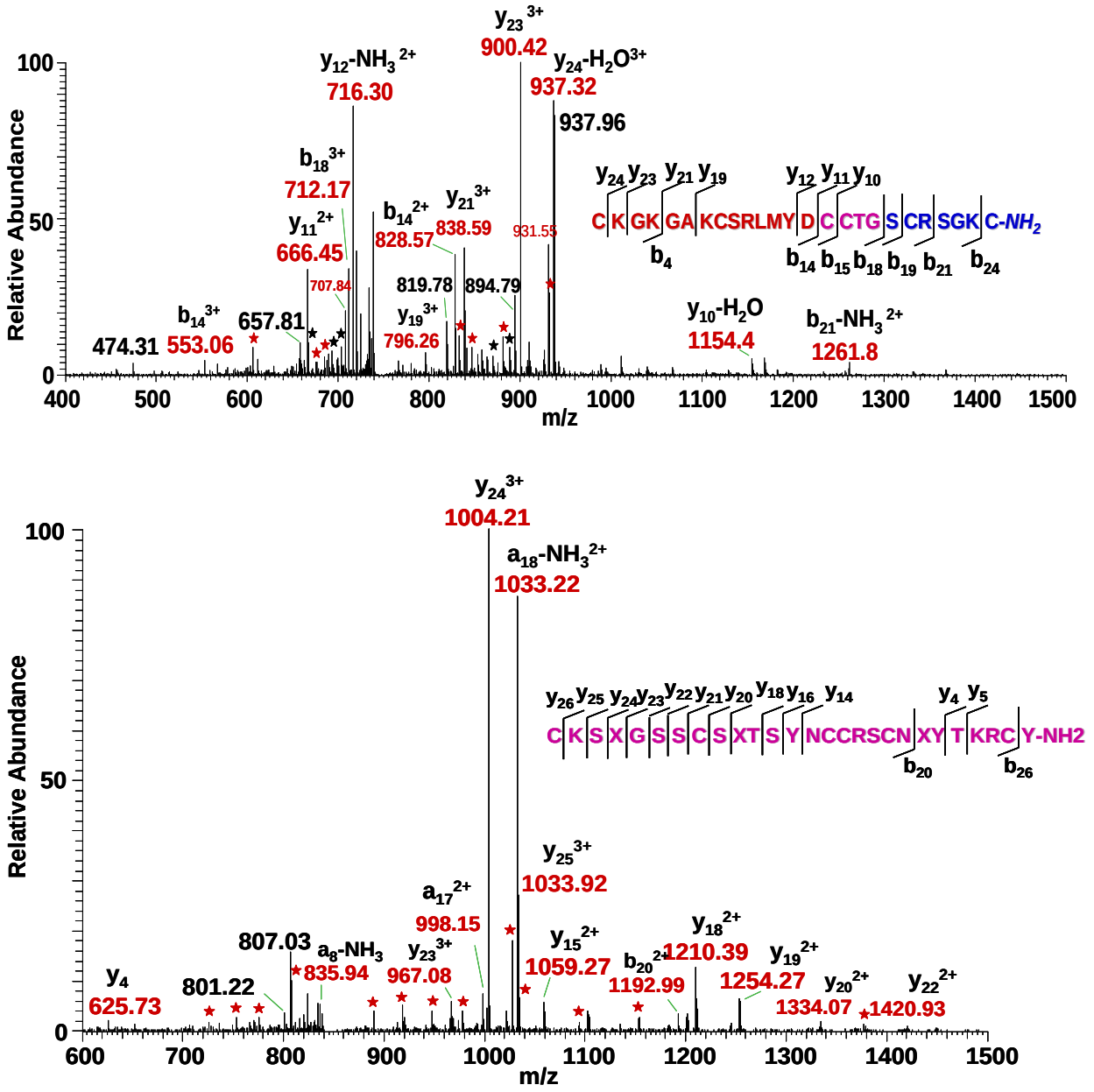

Figure 3-20. Full-scan MS/MS spectra of the +4 ions of modified ziconotide at *m/z* 748 (*top*)and ω-conotoxin GVIA at *m/z* 848 (*bottom*). Product ions matching the theoretical product ions proposed for the peptides are labeled in red and marked with red stars; those in black and marked with black stars correspond to more than one product ion. The observed b and y ions are also shown in the amino acid sequences.

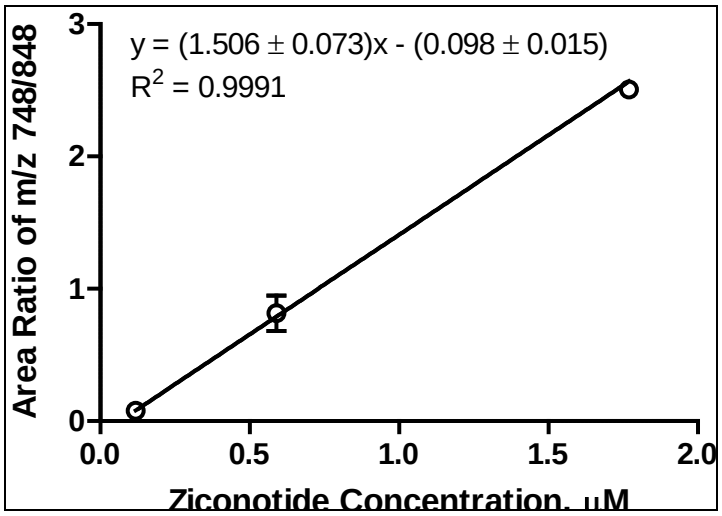

Figure 3-21. Graphical representation of the area ratio of the +4 ions of modified ziconotide to ω-conotoxin GVIA versus ziconotide concentration. The data are an average of two separate extractions and the error bars represent standard deviation of the duplicate extractions. The line equation and standard deviation of the slope and y-intercept are shown.

Table 3-5. Precision and accuracy of calibration standards for the analysis of reduced and alkylated ziconotide.

[Ziconotide] µM	Amt. on Column ng	Peak Area of *m/z* 748/848	Calculated [Z] µM	% Relative Error	%RSD
0.035	0.15	nd			
0.059	0.25	0.03704*			
0.12	0.50	0.07935	0.118	-0.39	4.6
0.59	2.5	0.8152	0.593	1.9	14.7
1.2	5.0	1.757	1.22	5.3	16.3
1.8	7.5	2.505	1.70	-2.4	0.9

- nd: not detected *: S/N < 10
- Amt. on Column = [Z] x $\frac{\text{Z sol'n vol.}}{\text{total vol. of reduction mix}}$ x $\frac{\text{reduction mix vol.}}{\text{total vol. of alkylation mix}}$ x $\frac{\text{vol. of alkylation mix extracted}}{\text{total vol. of extract}}$ x injection vol. x MW of Z x 1/1000
- Amt. on Column = $0.12 \frac{\text{pmol}}{\mu\text{L}} \times \frac{30\ \mu\text{L}}{100\ \mu\text{L}} \times \frac{60\ \mu\text{L}}{84\ \mu\text{L}} \times \frac{30\ \mu\text{L}}{40\ \mu\text{L}} \times 10\ \mu\text{L} \times \frac{2639.13\ \text{pg}}{\text{pmol}} \times \frac{1\ \text{ng}}{1000\ \text{pg}}$
- A 100 percent recovery at each step of the extraction was considered when the amount of peptide on column was calculated.

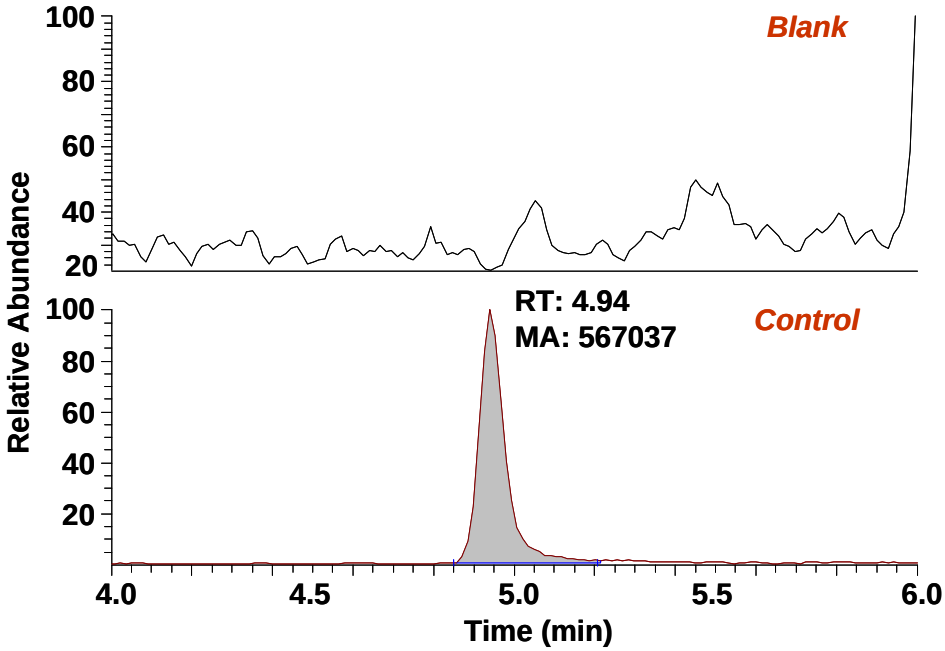

Figure 3-22. Representative base peak chromatograms of reduction and alkylation blank (*top*) and control (*bottom*) solutions. The blank contained all components of the reduction and alkylation mixture except the conopeptides while the control contained all reagents used in the modification except DTT and IAM. Only the time window where the modified conopeptides eluted is shown. The peak that is starting to appear at 6 min in the blank chromatogram corresponds to PEG contaminant. The peak in the control chromatogram corresponds to the unmodified ziconotide.

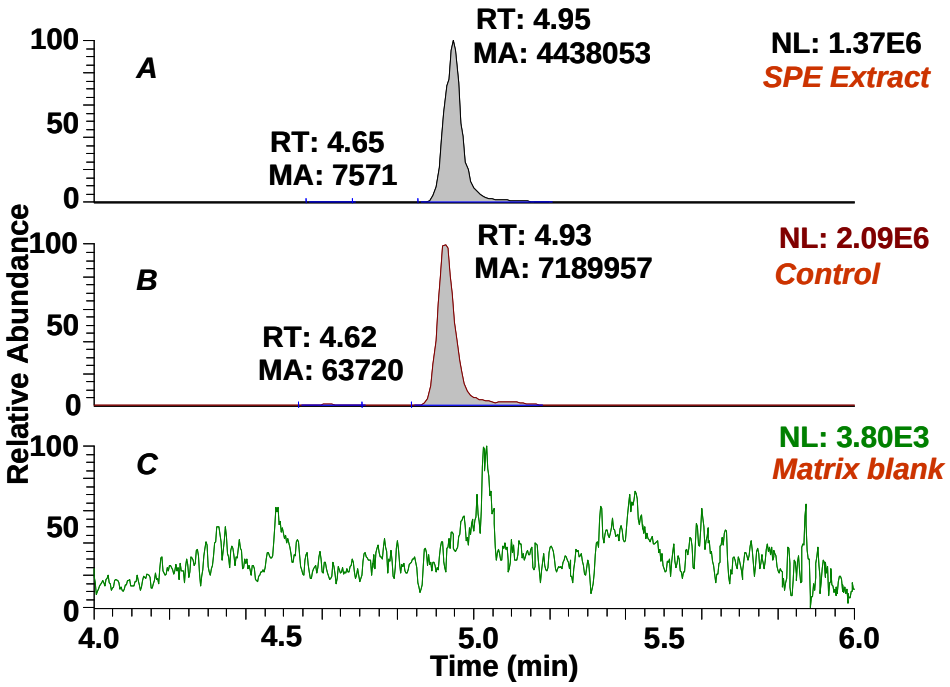

Figure 3-23. Extracted ion chromatograms (EIC) of the 3 major ions of intact ziconotide for the (*A*) C_{18} solid phase extraction (SPE) extract, (*B*) control and (*C*) matrix blank. A 1-mL blank horse plasma supplemented with 2.5 µg ziconotide and diluted to 2.5 mL with 0.5% $HAc_{(aq)}$ was loaded onto a PD-10 desalting column. The low MW eluate was then loaded onto a pre-conditioned C_{18} SPE cartridge and eluted with 1% HAc in 40:60 MeOH: H_2O. The extract was dried and the residue was dissolved in 100 µL of degassed, deionized water. An aqueous solution containing 1.5 µg of ziconotide added to 3 mL of 1% HAc in 40:60 MeOH: H_2O and processed identically as the extract comprised the control solution. The peaks at 4.65 and 4.62 min correspond to oxidized ziconotide. RT: retention time, MA: manually integrated area

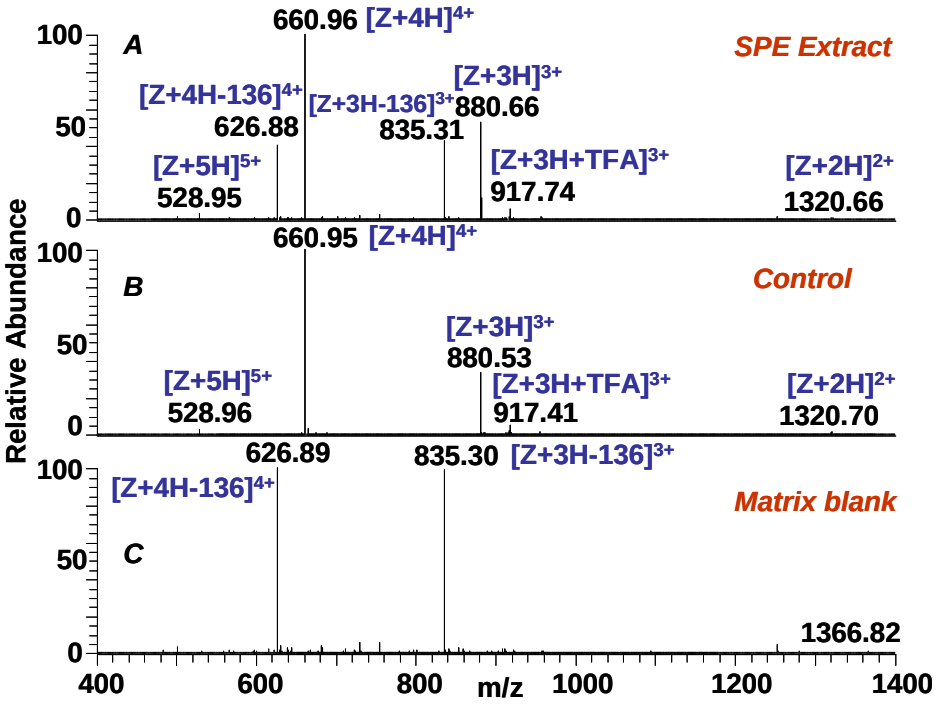

Figure 3-24. Full-scan mass spectra of the major peaks in the EIC of (*A*) ziconotide SPE extract, (*B*) control and (*C*) matrix blank. The most abundant ions in the mass spectra of the extract and control solution correspond to the +3 and +4 charge states of ziconotide. Ions corresponding to loss of 136 Da from *m/z* 661 and 881 were also observed. The presence of these ions in the mass spectrum of the blank could indicate contamination.

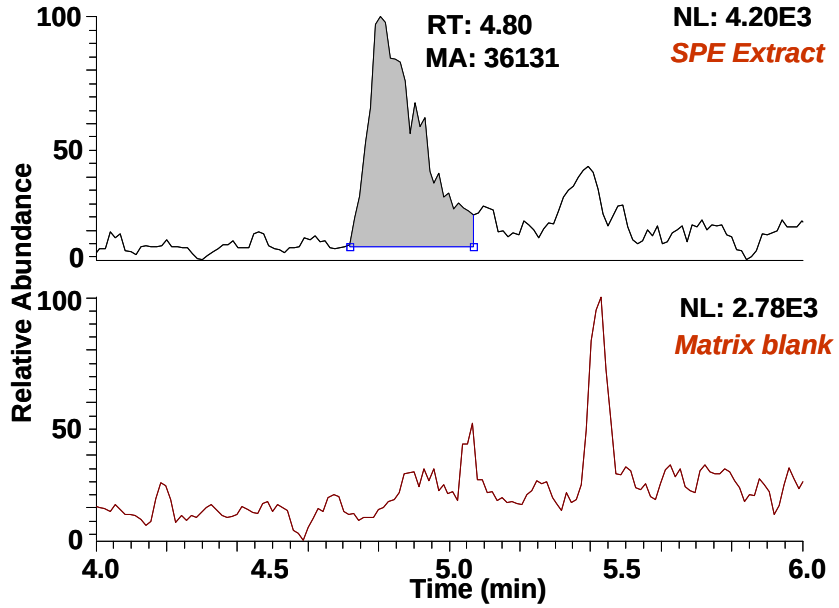

Figure 3-25. Extracted ion chromatograms of the 3 major ions (*m/z* 599, 748, and 997) of reduced and alkylated ziconotide from plasma extract (*top*) and matrix blank (*bottom*). A supplemented concentration of 2.5 µg/mL ziconotide in 1 mL of horse plasma was extracted, reduced and alkylated, then analyzed. Peak for the modified ziconotide was detected but its response was low.

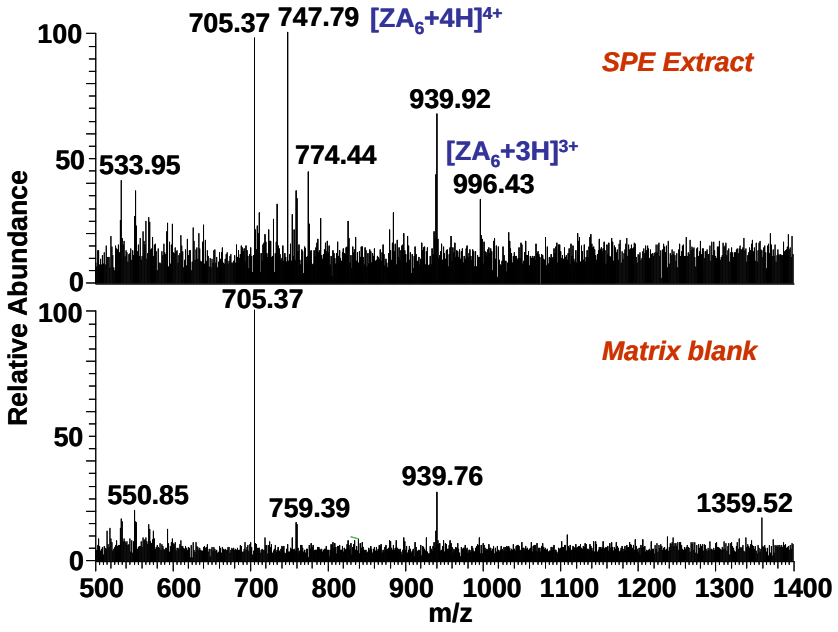

Figure 3-26. Full-scan mass spectra of modified ziconotide from plasma extract (*top*) and matrix blank (*bottom*). The +3 and +4 charge states of the completely reduced and alkylated ziconotide were present in the mass spectra of the extract. The presence of ions at *m/z* 705 and 939 in the mass spectrum of the blank could be due to contamination.

CHAPTER 4
DEVELOPMENT OF A STABILITY-INDICATING METHOD FOR ZICONOTIDE IN COMMERCIAL-TYPE FORMULATIONS

Introduction

The limited sensitivity of the reduction and alkylation procedure employed with the high performance liquid chromatography (HPLC)-electrospray ionization (ESI)-mass spectrometry (MS) method for detecting modified ziconotide, described in the last chapter, led us to pursue the development of a stability-indicating assay for intact ziconotide in commercial-type formulations.

In order to establish that the performance characteristics of the HPLC-ESI-MS method developed were reliable and suitable for the analysis of intact ziconotide, the method had to be validated. The Biopharmaceutics Coordinating Committee in the Center for Drug Evaluation and Research, in cooperation with the Center for Veterinary Medicine at the Food and Drug Administration (FDA), has prepared a guidance for industry document that provides general recommendations for bioanalytical method validation.[55] The important parameters in a validation study include accuracy, precision, sensitivity, selectivity, reproducibility and stability.[55]

Accuracy describes the closeness of the measured value (M_v) to the true value (T_v) (*i.e.*, concentration) and is often reported as percent relative error or % RE (see equation below).[42, 73]

$$\% \text{ RE} = [(M_v - T_v)/T_v] \times 100 \quad (4\text{-}1)$$

Precision, on the other hand, describes the closeness of the results obtained from replicate measurements. It is commonly expressed as the percent coefficient of variation (%CV) or percent relative standard deviation (%RSD) (see Equation 4-2).[42, 73]

$$\% \text{ CV} = \%\text{RSD} = (\text{SD}/\overline{X}) \times 100 \quad (4\text{-}2)$$

where SD: standard deviation and $\overline{X}$: mean

The guidance document recommends analyzing a minimum of three concentrations within the method's linear dynamic range, with at least five replicates per concentration, to determine accuracy and precision.[55] The mean value for each set of quality control (QC) samples should have a difference of ≤ 15% from the actual value except at the lower limit of quantitation (LLOQ), where a deviation of ≤ 20% is allowable.[55] At least 67% of the QC samples should satisfy the acceptance criteria for the analysis to be considered successful.[55] Accuracy and precision during a single run are assessed as intra-day statistics while values from analyses performed on different days are considered as inter-day statistics.

The highest and lowest concentrations that can be determined with acceptable accuracy and precision define the limits of quantitation (LOQ) or working dynamic range of an analytical method.[55, 73] The acceptance criteria are set at ≤ 20% for LLOQ and ≤ 15% for the upper limit of quantitation (ULOQ).[55] The limit of detection (LOD) is the lowest concentration or weight of analyte that can be detected at a known confidence level.[52, 73] A simplified definition of this limit which is often encountered in literature is the analyte concentration with a signal to noise ratio (S/N) of at least three.[74]

A selective analytical method allows for the differentiation and quantitation of an analyte in the presence of other components in the sample.[55, 73] A method is said to be sensitive if it can detect small differences in analyte concentration or if small changes in concentration produce great changes in the response function.[52, 73] Chemical stability refers to the extent to which a compound retains its chemical integrity.[75] Environmental factors such as temperature, light, air and humidity influence stability as well as other factors like nature of the container, pH of the solution and presence of other chemicals.[75, 76]

The effects of harsh oxidative conditions like exposure to high temperature and presence of oxygen on the degradation of ziconotide were investigated in the work reported in this chapter. The conditions chosen were aimed at simulating actual situations to which ziconotide drug formulations might be exposed during transit by personnel who are unaware of the stability considerations for the drug. In the commercially available Prialt formulation of ziconotide (25 or 100 µg/mL) which contains l-methionine as a protective oxygen scavenger at a concentration of 50 µg/mL, one of this formulation's identified degradation pathways involves oxidation of its methionine residue.[56] As discussed in Chapter 2, methionine is first oxidized to its sulfoxide and under strong oxidizing conditions, to a sulfone.[57]

Stability studies on ziconotide drug formulations or admixtures with other analgesics have employed HPLC with ultraviolet-visible (UV-Vis) spectrophotometry for ziconotide detection.[56, 77] In these studies, stability was defined as the time period during which the samples retained at least 90% of the initial ziconotide concentration. Generally, 90% of the labeled potency is recognized as the minimum level of acceptable potency for drugs.[76]

UV-Vis spectrophotometric detection relies on the absorption of light by certain functional groups known as chromophores.[52] The lesser degree of specificity associated with assigning structures based on their retention times and UV-Vis absorption maxima prompted us to evaluate HPLC-ESI-MS as a stability-indicating method for ziconotide analysis. Mass spectrometry enhances detection specificity through its ability to identify structures based on mass-to-charge (*m/z*) ratios and mass shifts following modification.

The validation of an ESI-HPLC-MS method and its application to the analysis of ziconotide solutions similar in composition to the commercial drug formulation are discussed in

the sections that follow. Calculations involved in determining the rate constant of degradation ofziconotide at 50 °C are also presented and discussed.

Experimental Section

Chemicals and Reagents

The conopeptides, ω-conotoxin MVIIA (0.1 mg, ≥ 95% purity by HPLC) and ω-conotoxin GVIA (0.1 mg, 98.3% purity by HPLC), and the amino acid L-methionine (BioChemika Ultra division) were purchased from Sigma-Aldrich (St. Louis, MO). Glacial acetic acid (HAc), trifluoroacetic acid (TFA), sodium hydroxide (NaOH) pellets, hydrochloric acid (HCl), isopropanol (IPA) and HPLC-grade acetonitrile (ACN) were obtained from Thermo Fisher (Fair Lawn, NJ). A sterile, preservative-free, saline solution (0.9% w/v sodium chloride) was acquired from Baxter Healthcare Corporation (Deerfield, Il). Water used for solution preparation was purified by RiOs™ reverse osmosis and Milli-Q polishing systems (Millipore, Billerica, MA). Water used for peptide solution preparation was also vacuum-degassed to remove dissolved oxygen in order to minimize possible oxidation of ziconotide.

Method Validation

Quality control samples at concentrations of 0.06, 0.6, and 6 ng/µL (n = 5) were analyzed with each of the 6 calibration curves discussed in Chapter 2. Eleven calibration standards with ziconotide concentrations ranging from 0.05 to 10 ng/µL, and containing 1 ng/µL of the internal standard (IS), ω-conotoxin GVIA, were included in each calibration curve. The intra- and inter-day accuracy and precision of the optimized HPLC-ESI-MS method for intact ziconotide were evaluated from the results of the QC samples and the 6 calibration curve runs. Results from analyses conducted within 24 hr constituted the intra-day statistics while those from six

independent experiments constituted the inter-day statistics. Concentrations were calculated from the equation of the line derived from the corresponding calibration curve.

Effect of Time in Autosampler Rack on Ziconotide Stability in Simple Solution

The effect of time spent in the autosampler (thermostatted to12 °C) on the concentration of ziconotide was determined to assess for post-preparative stability. The formation of degradation products was also monitored. The calibrators and quality control samples were recapped at the end of the first set of injections and those from the first 3 sets of calibration curves were re-analyzed after sitting in the autosampler for 12 hr while those from the last 3 sets were re-analyzed after 24 hr.

Effect of Harsh Oxidative Conditions on Ziconotide Stability in Commercial-type Formulations

A ziconotide solution similar in composition to the commercially available drug formulation, Prialt® (Elan Pharmaceutical, Inc.), was prepared and used for evaluating the effect of harsh oxidative conditions on the degradation of ziconotide. Prialt® is formulated as a sterile, preservative free, isotonic solution for intrathecal administration.[78] Prialt has to be delivered directly to the spinal fluid via an external or implanted pump due to the potential adverse effects of intravenous administration.[10] A 20 mL vial of Prialt® contains 25 µg/mL of ziconotide acetate, 50 µg/mL of L-methionine (a protective oxygen scavenger) and 9 mg/mL of sodium chloride with the pH adjusted to between 4.0 and 5.0.[56, 78]

L-methionine (5 mg) was first dissolved in sterile, preservative-free 0.9% (w/v) saline solution to prepare a 50 µg/mL methionine solution. Preparation of the test solution involved dissolution of 0.1 mg ziconotide standard in 4.0 mL of sterile, preservative-free 0.9% (w/v) saline solution containing 50 µg/mL L-methionine. The pH of the solution was adjusted to 4.0-5.0 with the addition of a drop of 0.01 M HCl. An aseptic technique that involved wiping the

opening of a container with an alcohol (70% IPA) swab prior to solution transfer was conducted to prevent bacterial contamination. Sampling and appropriate dilution of the test solution to 0.5 ng/µL ziconotide were performed within minutes of preparation to determine the initial ziconotide concentration. A fixed amount of the IS was added to the test solution samples to achieve a final concentration of 1 ng/µL in solution. The solution was diluted with 0.1 % HAc: 0.01% TFA in 1:99 ACN: H_2O. Concentration of ziconotide in this sample was quantified against a calibration curve determined using 9 standards ranging in concentration from 0.05 to 0.60 ng/µL. Quality control samples at concentrations of 0.10, 0.30 and 0.50 ng/µL were prepared in duplicate and analyzed with the calibration curve.

Using aseptic technique, 250 µL aliquots of the test solution were pipetted into limited volume glass inserts with polypropylene bottom spring (Restek, Bellefonte, PA). The inserts were then placed in 4-mL amber screw thread vials (Fisher, Fair Lawn, NJ) and tightly capped with poly(tetrafluoroethylene) or PTFE/silicone closures 13-425 (Fisher, Fair Lawn , NJ). Vials were placed in a calibrated Robbins Scientific hybridization oven model 1000 (SciGene, Sunnyvale, CA) set at 50.0 °C ± 0.2 °C. The glass insert top is designed to be flush with the vial cap. The inserts used in this experiment were smaller than those specified for the vial size, leaving the ziconotide solution in contact with 4.21 to 4.34 cm^3 of air. The volume of air inside the vials was approximated using the volume displacement method. The volume of water displaced by the glass insert and the volume of ziconotide solution in the insert were subtracted from the volume of water in the vial to determine the volume of air.

Vials were removed from the oven at the following time points: 0.5, 1, 2, 4, 6, 8, 16, 24, 48, 72, 96, 120, 144, 168 and 192 hr. The vials were allowed to cool for 5 min before aseptically transferring five 10-µL aliquots into five separate 2 mL plastic microcentrifuge tubes (Thermo

Fisher, Fair Lawn, NJ) containing 440 µL of 1:99 ACN: water with 0.1% HAc: 0.01% TFA. The centrifuge tubes were placed in a refrigerator kept at 5 °C until sample collection and dilution for the vial kept in the oven for 48 hr were completed. Aliquots from a zero hr sample vial were also diluted, refrigerated and submitted for HPLC-MS analysis like the other samples. A fixed amount of the IS was added to each sample before analysis to achieve a final concentration of 1 ng/µL.

HPLC-ESI-MS/MS Analysis

A Surveyor Autosampler/HPLC system interfaced to a Thermo Finnigan (San Jose, CA) linear ion trap (LTQ) mass spectrometer equipped with an electrospray ionization source (ESI) was employed for LC/MS analyses. The same instrument was used in the studies reported in Chapters 2 and 3. Chromatographic separation was achieved with a Jupiter Proteo C_{12} column (2 x 150 mm, 4 µm particle size, 90 Å pore size) from Phenomenex (Torrance, CA) with a Security Guard™ cartridge (4 x 2 mm, C_{12}) to protect the analytical column. The column was set to 30 °C while the autosampler was maintained at 12 °C. Gradient elution with 0.1% HAc: 0.02% TFA in water as solvent A and 0.1% HAc: 0.02% TFA in acetonitrile as solvent B, with solvent B raised from 2 to 70% in 9 min was carried out. This was followed by a 6.5 min column equilibration to initial solvent composition. A flow rate of 200 µL/min was used. Using the partial loop injection mode, 10 µL of the sample was loaded into the column. External and internal syringe needle washes with 0.1% HAc: 0.01% TFA in 50:50 ACN: water were incorporated in the autosampler method to eliminate carry-over.

Electrospray ionization in the positive mode was employed. The spray needle voltage was set at 3.75kV while the capillary voltage was at 45 V. The capillary temperature was maintained

at 300 °C. Sheath gas flow was set to 40 and that of the auxiliary gas to 20 arbitrary units. The use of auxiliary gas was found to lessen the contribution of TFA adducts.

The LTQ mass spectrometer was set to acquire for 10 min. Sample from the chromatographic column during the first 2 min and last 0.5 min was diverted to waste. The LTQ was programmed for full-scan MS then full-scan MS/MS (*m/z* 500 – 1600) of *m/z* 661 and *m/z* 760, the quadruply-charged ions of ziconotide and ω-conotoxin GVIA, respectively. The precursor ion isolation width in full-scan MS/MS mode was set to 3 *m/z* with collision energy at 35% and activation energy (q) at 0.250.

MS Data Analysis

Extracted ion chromatograms (EICs) for the various ions of ziconotide and the internal standard, ω-conotoxin GVIA were generated using the Xcalibur software (Thermo Scientific, San Jose, CA). Chromatograms were processed using a 3-point boxcar smoothing calculation. The peaks for the various charge states of ziconotide and the IS, as well as that of oxidized ziconotide, were manually integrated to determine the area for each. The sum of the contributions of the +3 and +4 ions of oxidized ziconotide was used for its EIC. The ratio of the peak area of the +4 ion of ziconotide to that of the IS was plotted against ziconotide concentration. Weighted least squares linear regression (WLSLR) analysis was used for data fitting, with $1/x^2$ as the weighting scheme of choice.[42, 43] GraphPad Prism® Version 5.01 was used for data processing.

Results and Discussion

Intra- and Inter-day Accuracy and Precision of Quality Control (QC) Samples

The intra- and inter-day accuracy and precision of quality control samples at ziconotide concentrations of 0.06, 0.6 and 6 ng/μL (n =5) analyzed with each of the 6 calibration curves

shown and discussed in Chapter 2 are summarized in Table 4-1. All the QC samples for the six analyses performed yielded %RSDs ≤ 7.3% and %REs ≤ 5.4% except for the 0.06 ng/µL QC in calibration curves 4 and 5 which yielded 12% and 11% absolute relative error, respectively. The higher %REs obtained for the QCs mentioned were due to inclusion in the calculations of a replicate not satisfying the acceptance criterion for %RE of ≤ 15% for the purpose of data set completeness. The inter-day statistics also exhibited very good agreement among all 30 replicate measurements of QC samples (%RSD ≤ 6.5); the concentrations calculated were very close to those of the nominal, as well (% absolute RE ≤ 5.0). Overall, the results of the analysis of QC samples and calibrators signify the accuracy, precision and robustness of the HPLC-ESI-MS method developed for the analysis of intact ziconotide.

Post-Preparative Stability of Ziconotide

The post-preparative stability of ziconotide standards and quality control samples after remaining in the autosampler (thermostatted to 12 °C) for 12 and 24 hr were evaluated. The first three calibration curves used for method validation were re-analyzed 12 hr after initial analysis while the last three curves were re-analyzed after 24 hr. The slopes of the curves from the time-delayed analysis were lower than those analyzed immediately (Table 4-2). This decrease can be attributed to the lower peak areas of ziconotide in the re-injected samples and slight changes in the IS response. The precision and accuracy of all the calibrators and QC samples still pass the FDA criteria of ≤ 15%, even at the LLOQ, signifying that ziconotide prepared in 1:99 ACN: water with 0.1% HAc: 0.01% TFA remains stable for at least 24 hr at 12 °C.

Tables 4-3 and 4-4 summarize the results for the time-delayed analysis of the calibration standards and quality control samples, respectively. The low %RSDs and % REs obtained for the calibrators were comparable to those of the calibration curves analyzed immediately. The

slightly higher %RSDs obtained for the re-injected QCs can be attributed to the oxidation of ziconotide over time. A comparison of the response of oxidized ziconotide from quality control samples which were analyzed immediately and those with time delays in the analysis is shown in Figure 4-1.

Effect of Harsh Oxidative Conditions on Ziconotide Degradation

The validated method was then used to evaluate the degradation of ziconotide in a test solution similar in composition to the commercially available drug formulation. Aliquots of the test solution in smaller glass inserts placed in 4-mL, capped vials were exposed to harsh oxidative conditions (*i.e.*, temperature of 50 °C, presence of atmospheric oxygen) and removed from storage at various times for analysis. Samples were diluted fifty-fold in 1:99 ACN: H_2O with 0.1% HAc: 0.01% TFA and stored at 5 °C before analysis at the end of the second day. Sampling was continued until 192 hr for the initial run and 144 hr for the repeat experiment due to the limited sample available.

Ziconotide concentrations in the samples were quantified against a calibration curve from 0.05 to 0.6 ng/µL. The undiluted ziconotide concentrations were obtained from the average calculated concentrations (n = 5, 9 or 10) with the use of appropriate dilution factor. These were divided by the initial ziconotide concentration which was obtained from a sample analyzed right after preparation of the test solution. The resulting percentages of initial concentration were plotted against storage time using an exponential function (Figure 4-2), specifically at 0.5, 1, 2, 8, 16, 24, 48, 96, 120, and 144 hr. Only those time points with n = 9 or 10 were included in the plot. Q-test at 95% confidence level was performed to determine if a certain replicate would be excluded. The rate constant for the degradation of ziconotide at 50 °C was determined from *k* and it was found to be $4.8 \pm 0.8 \times 10^{-3}$/hr. The time during which the samples retained at least

90% of the initial ziconotide concentration was determined from the intersection of the lower and upper 95% confidence limit (CL) and 90% ziconotide and this was found to be approximately equal to 17 to 48 hr. The 95% confidence limit takes into account the uncertainty associated with the measurements made.[76] This result indicates that it would take 17 to 48 hr of exposure at 50 °C for the concentration of a 25 µg/mL ziconotide solution to be reduced to 90% of the initial, which is generally recognized as the minimum acceptable potency level for a drug. Table 4-5 summarizes the results of monitoring the changes in ziconotide concentration in test solution samples exposed to harsh oxidative conditions at various times. The test solution initially contained 25 µg/mL of ziconotide and 50 µg/mL of L-methionine in sterile, preservative-free 0.9% saline solution with pH adjusted to between 4.0 and 5.0. Calculations were based on the measured initial concentration.

Assuming a first-order rate of decomposition for ziconotide, a plot of the natural logarithm (ln) of the undiluted ziconotide concentration in molarity versus time was constructed (Figure 4-3). The test solutions had to be diluted for analysis but their original concentrations were used for plotting. Figure 4-3 shows several points lying on or near the straight line that described the relationship between ln ziconotide concentration and time. This supports the assumption that the degradation of ziconotide could be a first-order or pseudo first-order reaction. The slope of this plot is the negative of the rate constant (k) of the reaction of interest.[79] Therefore, the rate constant for the degradation of ziconotide at 50 °C was determined to be $4.9 \pm 0.7 \times 10^{-3}$/hr. This value agreed well with the rate constant obtained from the exponential plot, $4.8 \pm 0.8 \times 10^{-3}$/hr. The possibility that the degradation of ziconotide could be a pseudo first-order reaction as well is supported by having an excess of L-methionine in solution. Performing the experiment with a

higher concentration of L-methionine would help establish if the rate of degradation of ziconotide is affected by the amount of L-methionine present in solution.

Using the equation for the half-life ($t_{1/2}$) of a first-order reaction (see Equation 4-3) and the rate constant obtained, the half-life of the degradation of ziconotide was calculated to be 141 hr. The time it takes for the percentage of initial ziconotide concentration to reach 50% was estimated from the intersection of the lower and upper 95% CL and 50% ziconotide (Figure 4-4) and was found to be approximately equal to 120 – 214 hr. Data for time points 168, 192 and 216 hr were calculated using the line equation for the % of initial ziconotide concentration vs. time (Figure 4-2) and included in the plot shown in Figure 4-4 to extend the 95% CL band for extrapolating the time when 50% of the initial ziconotide concentration had been reached. The calculated half-life value of 141 hr is within the range of half-life values estimated from the intersection of the lower and upper 95% confidence limit and 50% of initial ziconotide concentration. This comparability in half-life values also supported the assumption that the degradation of ziconotide could be a first-order or pseudo first-order reaction. The wide range of values obtained was a result of taking the average of the measurements from 2 separate experiments which were conducted several months apart. Effort was undertaken to repeat the exact conditions in the initial experiment but comparison of the results from the 2 experiments suggested that an underlying instrumental or solution preparation condition could account for the differences observed.

$$t_{1/2} = \ln 2/k \qquad (4\text{-}3)$$

In order to estimate the effect of temperature on the shelf-life of a material, $Q_{\Delta T}$ is calculated (Equation 4-4).[76] The $Q_{\Delta T}$ value is a multiplier or divisor used to estimate the changes in the reaction rate constant with changes in temperature (ΔT). The estimate that for every 10°C

decrease in storage temperature, the shelf-life doubles is based on $Q_{\Delta T}$ calculations, for instance. However, this statement is only true if the activation energy (E_a) of the reaction(s) that causes degradation is 15 kcal/mol.[76] The activation energy for many chemical processes involved in the degradation of a drug substance or product is typically within the range of 10 to 25 kcal/mol.[76, 80]

$$Q_{\Delta T} = \exp [E_a/RT (\Delta T/T + \Delta T)] \quad (4\text{-}4)$$

where R: universal gas constant, 1.987 cal/deg mole
T: temperature (in Kelvin) whose effect is being investigated

The stability of ziconotide at room temperature and at various activation energies was determined from calculations involving $Q_{\Delta T}$ and published stability data for ziconotide stored in naïve pumps at 37 °C (Table 4-6).[77] Naïve pumps are pumps that have not been exposed to ziconotide. These results were compared to calculations performed on stability data at 50 °C which were obtained from the experiment described in this chapter (Table 4-7). Since the activation energy of the reaction involved in the degradation of ziconotide is not known, calculations were carried out at activation energies of 10, 15, 20 and 25 kcal/mol. The room temperature used in $Q_{\Delta T}$ calculations is the designated controlled room temperature which is 25 °C.[81]

The stabilities of ziconotide at room temperature obtained from data for a diluted 25 μg/ml ziconotide formulation at 37 °C turned out to be greater than those calculated using the experimental stability data at 50 °C. The stability at room temperature for a degradation reaction with E_a of 25 kcal/mole calculated from data at 37 °C, for example, is 59 days compared to 12 - 35 days if calculations were based from stability data at 50 °C. Comparison of these values yielded an absolute relative error of 44-80%. This difference in results could be attributed to the variability of the results obtained and the possible effects of temperature on peptide

conformation which may result in non-Arrhenius behavior.[82] The prediction of shelf-life using results from stability studies conducted at high temperatures tends to be complicated more by the effect of temperature on protein conformation. Reliance on stability studies carried out at the recommended storage conditions, therefore, is often required for establishing the expiry of biotechnology-derived products.[82] The calculations performed in this chapter involving rate constants and $Q_{\Delta T}$s are based on the assumption that the system under study follows the Arrhenius equation. The Arrhenius equation (Equation 4-5) defines the relationship between the rate at which a reaction proceeds and its temperature.[79]

$$k = A\, exp^{(-Ea/RT)} \quad \text{where k: rate constant} \qquad (4\text{-}5)$$

A: pre-exponential factor or frequency factor
E_a: activation energy
R: universal gas constant, 8.314×10^{-3} kJ/mol K
T: temperature in Kelvin

When the corresponding 90% stability at 50 °C was calculated at various activation energies using the published stability data at 37 °C, a fair agreement between one of the experimental and calculated results at activation energy of 25 kcal/mol was obtained (Table 4-8). Comparison of the calculated and experimental 90% stabilities, 3 vs. 0.71 to 2.0 days, respectively, yielded an absolute relative error of 31 to 75%. This result could indicate that the activation energy for the reaction involved in the degradation of ziconotide at 50 °C is approximately 25 kcal/mol or greater.

A peak that elutes at the same time as oxidized ziconotide was detected on the chromatograms of the test solution samples. Figure 4-5 shows the extracted ion chromatograms for ziconotide, its oxidized form and the internal standard, ω-conotoxin GVIA, for the test solution stored at 50°C for 144 hr while their mass spectra are presented in Figure 4-6. The mass

spectra of the early eluting peak confirmed the presence of oxidized peptide. A mass shift of 16 daltons (Da) was observed for both the +3 and +4 charge states of ziconotide. The addition of 16 Da in mass is commonly associated to oxidation or the incorporation of oxygen to the original structure of a compound. The mass shift observed, in this case, corresponds most likely to the oxidation of the methionine residue of ziconotide to its sulfoxide form.

Changes in response of the oxidized form, reported as percentage of the total ion signal for ziconotide, were plotted with the changes in response of the +3 and +4 charge states of ziconotide (Figure 4-7). The total ion signal was taken as the sum of the peak areas of the various charge states of ziconotide, its TFA adducts and oxidized ziconotide. The sum of the response of the +3 (*m/z* 886) and +4 (*m/z* 665) ions of oxidized ziconotide obtained from extracted ion chromatograms was used in calculating its contribution to the total ion signal. The decrease in response of ziconotide was observed to be accompanied by slight increases in the response of the oxidized form. The percentage decrease in ziconotide over time, however, was not compensated for by the increase in oxidized product. Several possibilities could have contributed to the insignificant increase of the amount of oxidation product. These include the presence of L-methionine which reduces the oxidation of ziconotide, degradation of ziconotide through pathways other than oxidation, formation of degradation products that could not be separated or even detected by the method employed and loss of material due to adsorption.

The appearance of additional peaks in the chromatograms of the various samples was monitored for the formation of other possible degradation products of ziconotide. As shown in Figure 4-5, no additional peaks were observed even for the longest stored sample at 50 °C. The mass spectra of oxidized ziconotide for the various samples were also monitored to determine if methionine oxidation had proceeded to the formation of the sulfone derivative. With the ability

of mass spectrometry to differentiate compounds based on their masses, the addition of one or two oxygen molecules to the methionine residue of ziconotide should be easily distinguished. However, mass spectra of the peak corresponding to oxidized ziconotide for all test solution samples only confirmed the presence of methionine sulfoxide (1 oxygen added) and not methionine sulfone.

Conclusions

The HPLC-ESI-MS method optimized for the analysis of intact ziconotide was successfully validated and applied to the evaluation of ziconotide degradation. The intra- and inter-day accuracy and precision of quality control samples exhibited low percent relative errors and percent relative standard deviations that satisfy the method validation guidelines required by the FDA. All six calibration curves satisfied the guidelines for the minimum number of standards that needs to meet the accuracy and precision criteria for an analysis to be considered passing. Post-stability studies on ziconotide determined that solutions prepared in 1:99 ACN: H_2O with 0.1% HAc: 0.01% TFA remain stable at 12 °C for at least 24 hr. Application of this validated method to the analysis of test solution samples similar in composition to the commercial drug formulation, which were exposed to harsh oxidative conditions at various times, facilitated the determination of a rate constant for the degradation of ziconotide at 50 °C. This rate constant was determined to be $4.9 \pm 0.7 \times 10^{-3}$/hr. This result indicates that exposure of a 25 µg/mL ziconotide solution to 50 °C for 17 to 48 hr will reduce the concentration to 90% of the initial. The resulting plot of ln ziconotide concentration versus storage time at 50 °C and agreement between the half-life calculated using the derived rate constant and that determined from changes in percent initial concentration supported the assumption that the degradation of ziconotide could be a first- or pseudo first-order reaction. Additional experiments need to be

performed to establish the reproducibility of the results obtained for the degradation of ziconotide at 50 °C. Results pertaining to the rate of degradation of a drug substance, such as the ones presented here, provide useful information for proper handling and storage of ziconotide drug solution.

Compared to UV-vis spectrophotometry, mass spectrometry as a detection technique also offered greater specificity for the identification of compounds that elute from a column. Identification is based on mass-to-charge ratios of compounds and mass shifts which often correspond to structure modification as opposed to structure assignments based on UV-vis absorption maxima and retention times which may not be unique for a particular compound and requires the use of standards for identity confirmation.

Table 4-1. Intra- and inter-day accuracy and precision of quality control samples.

Calibration Curve	Intra-day Statistics (n=5)	Nominal Concentration (ng/µL) 0.060	0.60	6.0
1	Mean	0.060_1	0.57_2	5.7_7
	SD	0.001_7	0.04_2	0.2_1
	%RSD	2.8	7.3	3.6
	%RE	0.13	-4.6	-3.9
2	Mean	0.056_7	0.57_3	5.9_8
	SD	0.002_0	0.02_2	0.0_6
	%RSD	3.5	3.8	1.0
	%RE	-5.4	-4.6	-0.352
3	Mean	0.059_5	0.59_1	6.0_8
	SD	0.003_6	0.00_9	0.1_3
	%RSD	6.1	1.5	2.2
	%RE	-0.89	-1.5	1.3
4	Mean	0.052_8	0.58_3	6.0_5
	SD	0.001_6	0.02_8	0.1_6
	%RSD	3.0	4.8	2.6
	%RE	-12	-2.8	0.90
5	Mean	0.053_5	0.60_7	6.0_5
	SD	0.002_3	0.02_0	0.1_6
	%RSD	4.4	3.2	2.7
	%RE	-11	1.2	0.86
6	Mean	0.059_6	0.59_1	5.9_5
	SD	0.002_5	0.01_9	0.2_6
	%RSD	4.2	3.1	4.4
	%RE	-0.68	-1.5	-0.91
	Inter-day Statistics (n=30)			
	Mean	0.057_0	0.58_6	5.9_8
	SD	0.003_7	0.02_6	0.1_9
	%RSD	6.5	4.4	3.2
	%RE	-5.0	-2.3	-0.35

Intra-day statistics were obtained from 5 replicate samples for each concentration analyzed on a single run (n=5). Inter-day statistics were obtained by analyzing 6 batches of the QCs consisting of 5 replicate samples per batch (n=30). All replicates were prepared individually.

Table 4-2. Regression parameters for the time-delayed analysis of the six calibration curves of ziconotide.

Calibration Curve	m ± std. error	b ± std. error	R^2	Time Delay, hours
1	1.453 ± 0.028	-0.010 ± 0.004	0.9940	12
2	1.52 ± 0.03	-0.015 ± 0.004	0.9985	12
3	1.561 ± 0.018	-0.0132 ± 0.0023	0.9981	12
4	1.584 ± 0.025	-0.021 ± 0.003	0.9989	24
5	1.570 ± 0.023	-0.0191 ± 0.0030	0.9989	24
6	1.600 ± 0.025	-0.014 ± 0.003	0.9996	24

n = 11 except for CC4 with n=10, m = slope, b = y-intercept, R^2 = correlation coefficient

Table 4-3. Precision and accuracy of ziconotide calibration standards which were re-injected after 12 and 24 hr of initial analysis.

Nominal Concentration, ng/µL	n	Average Calculated Concentration, ng/µL	%RSD	%RE
0.050	6	0.051_8	4.6	3.6
0.080	6	0.076_4	5.7	-4.6
0.10	6	0.098_4	2.9	-1.6
0.30	6	0.29_6	2.7	-1.3
0.50	6	0.51_1	2.8	2.2
0.80	6	0.79_6	3.0	-0.51
1.0	6	0.99_7	2.8	-0.29
3.0	5	3.0_8	2.2	2.6
5.0	6	5.1_2	3.5	2.3
8.0	6	7.9_5	3.7	-0.63
10	6	9.8_9	3.3	-1.5

Calibration curves 1-3 were re-analyzed after 12 hr of initial run while 4-6 were analyzed after 24 hr.

Table 4-4. Intra- and inter-day accuracy and precision of time-delayed analysis of quality control samples.

Set	Intra-day	Nominal Concentration (ng/µL)		
	Statistics (n=5)	**0.060**	**0.60**	**6.0**
1	Mean	0.059_2	0.58_9	6.0_3
	SD	0.002_7	0.04_5	0.2_2
	%RSD	4.5	7.6	3.5
	%RE	-1.4	-1.9	0.48
2	Mean	0.058_5	0.58_5	5.9_4
	SD	0.004_1	0.021_7	0.2_6
	%RSD	7.0	3.7	4.3
	%RE	-2.5	-2.6	-1.0
3	Mean	0.056_3	0.60_2	5.8_8
	SD	0.002_8	0.02_2	0.2_6
	%RSD	4.9	3.6	4.5
	%RE	-6.2	0.3	-2.1
4	Mean	0.055_6	0.57_7	5.9_4
	SD	0.002_4	0.01_7	0.0_9
	%RSD	4.4	3.0	1.6
	%RE	-7.4	-3.9	-1.1
5	Mean	0.056_0	0.59_4	5.9_3
	SD	0.005_1	0.02_6	0.3_0
	%RSD	9.1	4.4	5.0
	%RE	-6.6	-0.98	-1.2
6	Mean	0.059_0	0.60_4	5.9_1
	SD	0.001_0	0.01_2	0.1_6
	%RSD	1.7	2.0	2.7
	%RE	-1.7	0.70	-1.6
	Inter-day Statistics (n=30)			
	Mean	0.057_4	0.59_2	5.9_4
	SD	0.003_3	0.025_6	0.2_1
	%RSD	5.8	4.3	3.5
	%RE	-4.3	-1.4	-1.1

The first 3 sets of QCs were analyzed after 12 hours of initial run while sets 4-6 were analyzed after 24 hr. Intra-day statistics were obtained from 5 replicate samples for each concentration analyzed on a single run (n=5). Inter-day statistics were obtained by analyzing 6 batches of the QCs consisting of 5 replicate samples per batch (n=30). All replicates were prepared individually.

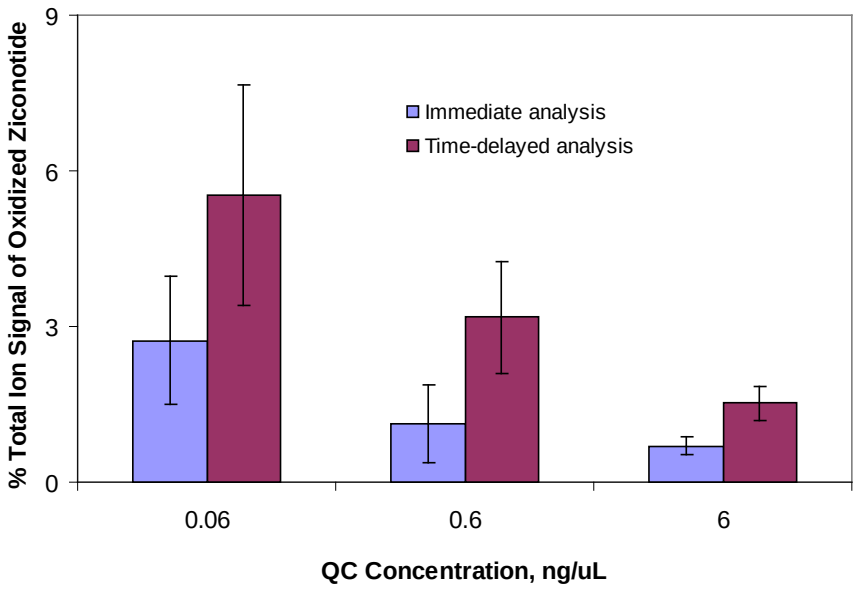

Figure 4-1. Response of oxidized ziconotide from QC samples analyzed immediately and with time delay. Samples analyzed with calibration curves 1-3 were re-analyzed after 12 hr while those with curves 4-6 were re-analyzed after 24 hr. The increase in oxidized ziconotide response of those analyzed with time delay contributed to the lower precision of QC samples in these batches.

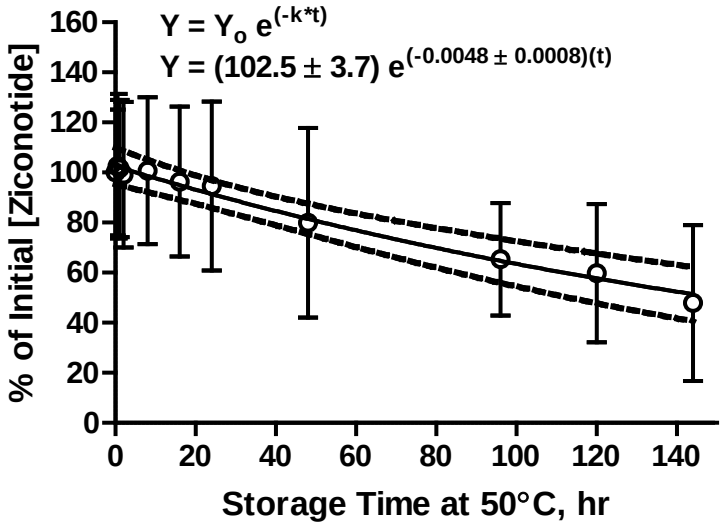

Figure 4-2. Changes in ziconotide concentration vs. time for test solutions stored at 50 °C and kept in-contact with air. The percentage of initial ziconotide concentration was plotted against storage time using an exponential function. The data are an average of 9-10 dilutions from 2 sample vials obtained from 2 separate experiments. Error bars represent the standard deviation of the replicates. The value for 90% stability was estimated to be 17 to 48 hr from the intersection of 90% ziconotide and the lower and upper 95% CL. The equation for the exponential decay and standard deviations of Y_o and k are also shown. Y_o: % of initial ziconotide concentration at time = 0 hr; k: rate constant

Table 4-5. Results of analysis of test solution samples stored at 50°C and kept in contact with air at various times.

Time, hr	n	Ave. Calc'd [Zic], ng/μL	Undiluted [Zic], ng/μL	% of $[Zic]_i$	% of $[Zic]_i$ SD	Undiluted [Zic], x 10^{-6} M
0	10	0.42_0	$21._0$	$100._0$	$25._2$	7.9_5
0.5	10	0.43_0	$21._5$	$102._6$	$28._9$	8.1_5
1	10	0.42_6	$21._3$	$101._6$	$27._4$	8.0_8
2	10	0.41_6	$20._8$	$99._1$	$29._0$	7.8_8
4	5	0.30_8	$15._4$	$73._5$	1.8_0	5.8_4
6	5	0.53_4	$26._7$	$127._3$	2.6_0	$10._1$
8	10	0.42_3	$21._1$	$100._7$	$29._4$	8.0_1
16	10	0.40_4	$20._2$	$96._4$	$30._0$	9.7_0
24	10	0.39_7	$19._8$	$94._6$	$33._7$	7.5_2
48	9	0.33_5	$16._8$	$79._9$	$37._9$	6.3_6
72	5	0.35_8	$17._9$	$85._3$	$7._0$	6.7_8
96	10	0.27_4	$13._7$	$65._3$	$22._5$	5.2_0
120	10	0.25_1	$12._6$	$59._8$	$27._5$	4.7_5
144	9	0.20_1	$10._1$	$47._9$	$31._1$	3.8_1
168	5	0.18_7	9.3_7	$44._6$	$1._7$	3.5_5
192	5	0.05_5	2.7_3	$13._0$	$1._0$	1.0_4

$[Zic]_{undiluted}$ = calculated [Zic] x 500 μL/10 μL

[Zic] in molarity = [Zic] in ng per μL/(FW of ziconotide x 1000)

FW of ziconotide = 2639.13 ng/nmol

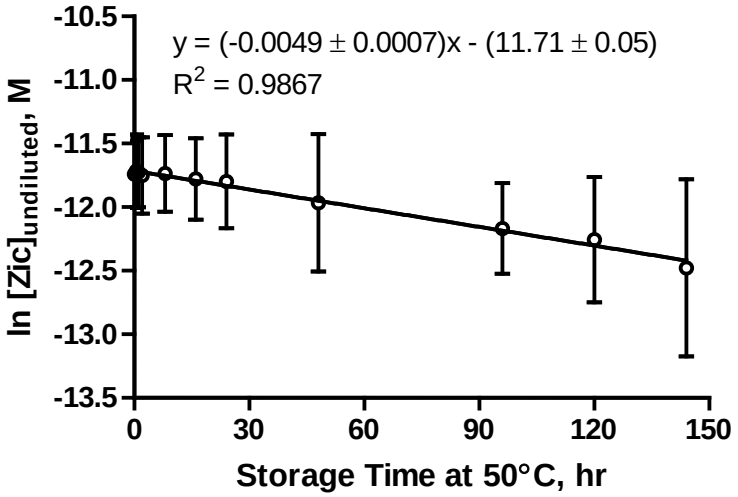

Figure 4-3. Plot of ln [Ziconotide]$_{undiluted}$ (in molarity) versus time. The rate constant for the degradation of ziconotide at 50 °C corresponds to the negative of the slope of the plot and was determined to be 4.9 ± 0.7 x 10^{-3}/hr. The data are an average of 9-10 dilutions from 2 sample vials obtained from 2 separate experiments. Error bars represent the standard deviation of the replicates. The line equation and standard deviations of the slope and y-intercept are also shown.

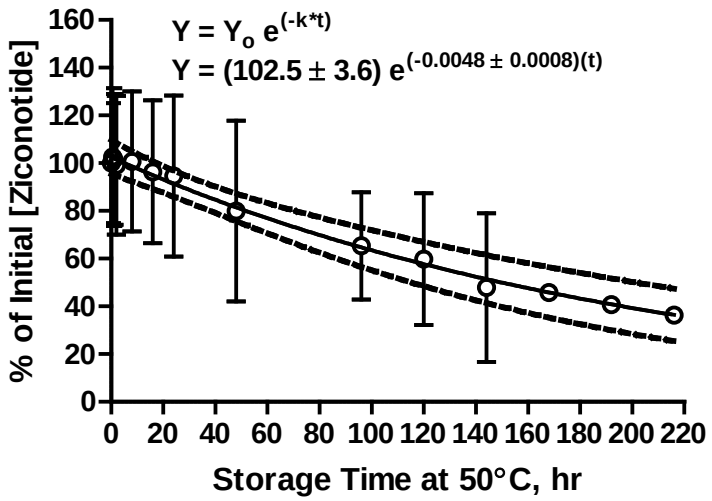

Figure 4-4. Changes in ziconotide concentration vs. time for 0 to 216 hr to extrapolate time to reach 50% ziconotide. Data for 168, 192 and 216 hr were calculated from the line equation of % initial [ziconotide] vs. time for 0 to 144 hr in order to extend the 95% CL band. The time it takes to reach 50% of the initial ziconotide concentration was extrapolated from the intersection of the lower and upper 95% CL and 50% ziconotide. This was determined to be 120 – 214 hr.

Table 4-6. Room temperature stability derived from $Q_{\Delta T}$ calculations and stability data at 37 °C.

E_a, kcal/mol	Q_{12}	Ziconotide Stability at 37 °C in Naïve Pumps, days	Calculated Stability at 25°C, days
10	1.83	13	24
15	2.48		32
20	3.35		44
25	4.54		59

The 90% stability of ziconotide at 37 °C was multiplied with the Q_{12} values for the various activation energies considered to obtain an estimate of the stability at room temperature. Stability was determined from the intersection of the lower 95% CL and 90% ziconotide.[77]

Table 4-7. Room temperature stability derived from $Q_{\Delta T}$ calculations and stability data at 50 °C.

E_a		Ziconotide Stability		Calculated Stability	
kcal/mol	Q_{25}	at 50°C, days		at 25°C, days	
		Lower 95% CL	Upper 95% CL	Lower 95% CL	Upper 95% CL
10	3.06	0.71	2.0	2	6
15	5.36			4	11
20	9.38			7	19
25	16.42			12	33

The 90% stability of ziconotide at 50 °C was multiplied with the Q_{25} values for the various activation energies considered to obtain an estimate of the stability at room temperature. Stability was determined from the intersection of the lower and upper 95% CL and 90% ziconotide.

Table 4-8. Comparison of experimental and calculated stability data at 50 °C.

E_a		Zic Stability	Calc'd Stability	Exp'tl Stability	
kcal/mol	Q_{13}	at 37°C, days	at 50°C, days	at 50°C, days	
				Lower 95% CL	Upper 95% CL
10	1.83	13	7	0.71	2.0
15	2.47		5		
20	3.34		4		
25	4.51		3		

The experimental value for 90% stability was obtained from the intersection of the lower 95% confidence limit and 90% ziconotide in Figure 4-2. Calculated stability data were obtained by dividing the published stability of ziconotide at 37 °C with the Q_{13} values for various activation energies.

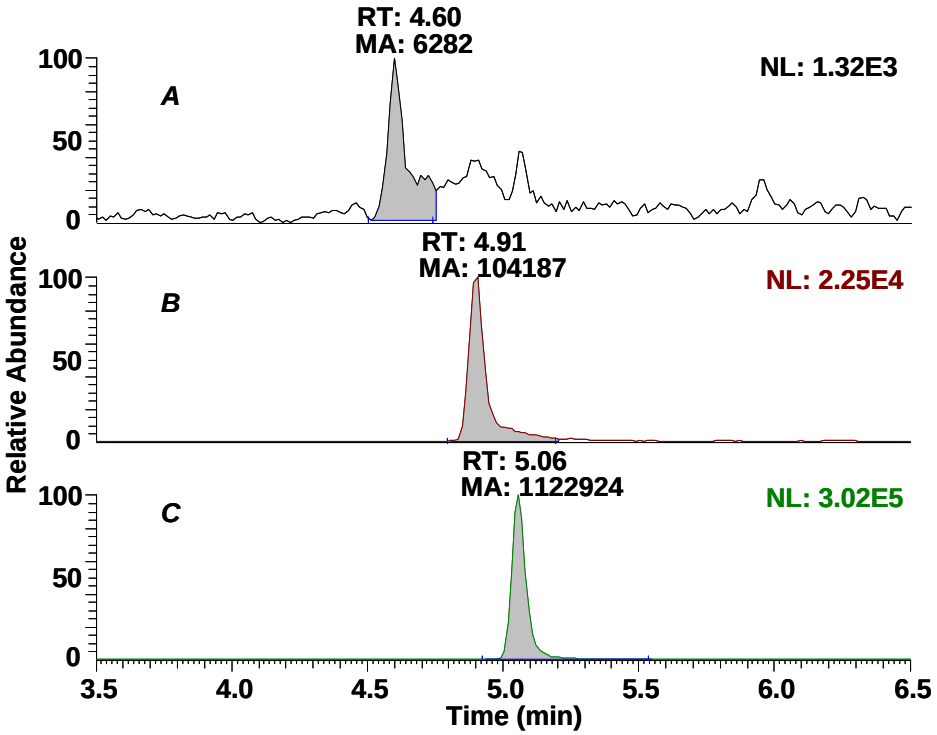

Figure 4-5. Extracted ion chromatograms of (*A*) oxidized ziconotide, (*B*) ziconotide and (*C*) ω-conotoxin GVIA from a test solution sample stored at 50 °C for 144 hr. RT: retention time in minutes, MA: manually integrated area

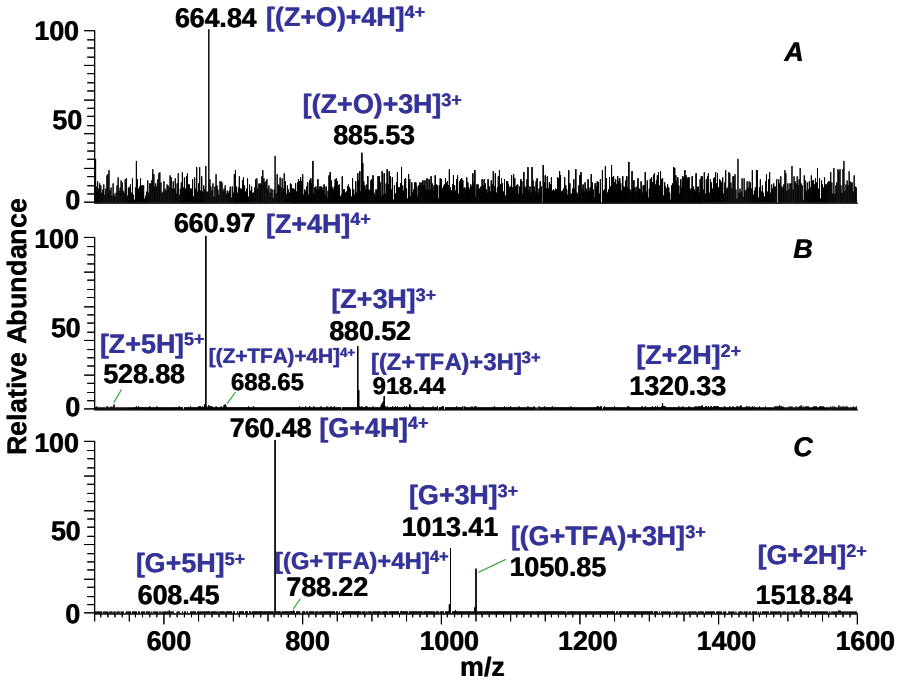

Figure 4-6. Full-scan mass spectra of (*A*) oxidized ziconotide, (*B*) ziconotide and (*C*) ω-conotoxin GVIA.

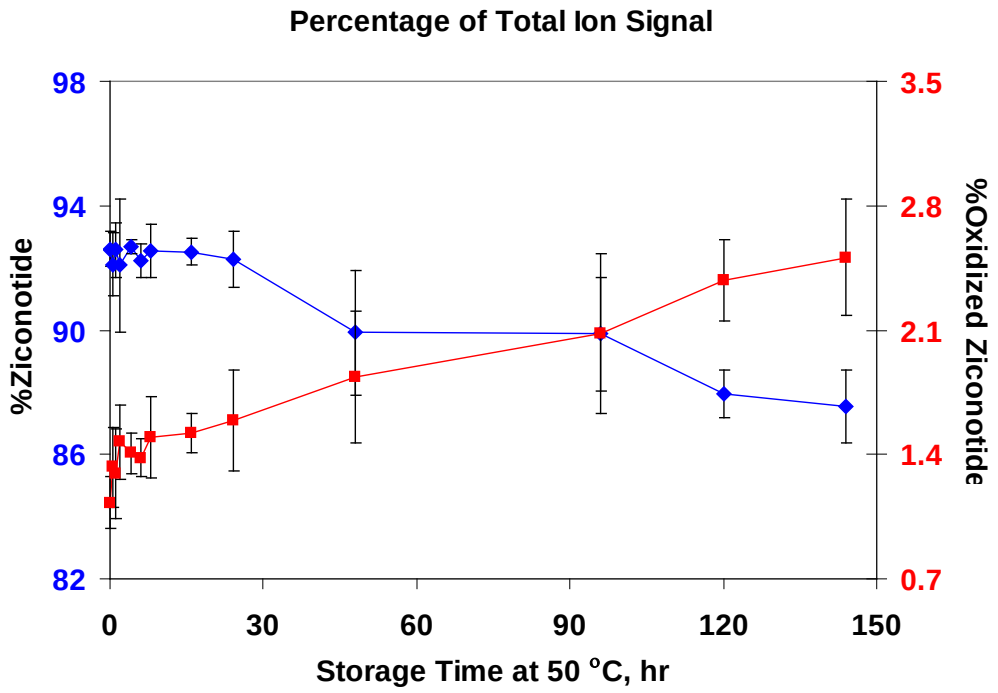

Figure 4-7. Summed response of the +3 and +4 charge states of ziconotide and oxidized ziconotide in test solutions stored at various times at 50 °C. The decrease in response of ziconotide was observed to be accompanied by slight increases in the response of the oxidized form. The total ion signal corresponds to the sum of the peak areas of the various charge states of ziconotide [*i.e.*, *m/z* 1320 (+2), *m/z* 881 (+3), *m/z* 661 (+4) and *m/z* 528 (+5)], its TFA adducts [*i.e.*, *m/z* 689 (+4), *m/z* 918 (+3) and *m/z* 955.5 (+3)] and its oxidized form [*i.e.*, *m/z* 665 (+4) and *m/z* 886 (+3)].

CHAPTER 5
CONCLUSIONS AND FUTURE DIRECTIONS

A robust and sensitive HPLC-ESI-MS method for the analysis of intact ziconotide was developed and validated. The limit of detection for this method was 0.02 ng of ziconotide on column. Tandem mass spectrometric analysis of intact ziconotide was also performed but the extensive cross-linking from its multiple disulfide bridges limits the structural information that can be derived from its MS/MS spectra. Reduction and alkylation of the disulfide bonds of ziconotide was carried out to eliminate the cross-linking and render the conopeptide more susceptible to collision-induced dissociation. Fragmentation of the reduced and alkylated ziconotide yielded more structurally relevant ions (*i.e.*, b and y ions from typical peptide bond cleavage) compared to that of the intact peptide. The limit of quantitation (0.50 ng on column) obtained for modified ziconotide, however, restricted the application of the method to complex sample matrices such as biological fluids. A stability-indicating assay for the quantitative determination of ziconotide in commercial-type formulations was successfully developed using the validated HPLC-ESI-MS method for intact ziconotide. The degradation of ziconotide in test solutions exposed to harsh oxidative conditions was evaluated. Results pertaining to the rate of degradation of ziconotide may provide useful information for proper handling and storage of the drug solution.

The detection and quantitation of ziconotide in complex sample matrices will definitely benefit from the enhancement in detection sensitivity offered by nanoflow electrospray ionization. Nanoelectrospray ionization (NSI) decreases detection limits up to two orders of magnitude compared to ESI.[83] The reduction of interference effects from salts and other species with the use of NSI has also provided improved sensitivity for peptides in samples contaminated by high levels of salts.[84, 85] The use of a nanobore or nanoscale liquid chromatography will

ensure accurate delivery of specified solvent compositions especially when using gradient elution, which in turn will provide accuracy and precision for experimental results. Care must be observed when modifying regular-bore or standard HPLC equipment for low flow rate experiments. This is because the contribution of extracolumn volumes in injectors and connecting tubing to bandspreading becomes more significant.[23]

The reduction and alkylation method developed should be optimized for ziconotide in plasma extracts if ziconotide will be detected from plasma samples, for instance. The presence of more abundant peptides other than ziconotide in plasma samples would require the use of other reagents like denaturing agents, buffers, chelating agents, etc. to eliminate possible interference from other matrix components and prevent aggregation and other unwanted interactions.[86, 87] Enzyme digestion of the reduced and alkylated ziconotide can also be explored for the generation of diagnostic fragment ions for the qualitative and quantitative determination of ziconotide.

Lastly, monitoring the degradation of ziconotide at 50 °C through several stages of half-life will improve the accuracy of the half-life determined. Performing the degradation study at another temperature will also provide relevant information about the rate of degradation of ziconotide which will help establish the accuracy of results obtained at 50 °C. Repeating the experiment conducted with a higher concentration of the oxygen scavenger, L-methionine, will help establish if the rate of degradation of ziconotide is affected by the amount of L-methionine present in solution.

APPENDIX
LIST OF FRAGMENT IONS

The following list of fragment ions was obtained from collision-induced dissociation (CID) of the +4 ions of the reduced and alkylated ω-conopeptides: ziconotide and ω-conotoxin GVIA. ProteinProspector's MS-Product software was used to generate the theoretical *m/z* of the fragment ions observed. The difference between the observed and theoretical *m/z* (Δm) was limited to ≤ 0.5 daltons (Da) for identification of the fragment ions (see Equation A-1). Fragment ions matching the theoretical fragment ions proposed for the peptide are labeled in red while those in black correspond to more than one fragment ion. The relative intensity of the 3 most abundant fragment ions are also in bold font.

$$\Delta m = /(\text{Observed } m/z - \text{Theoretical } m/z)/ \qquad \text{(A-1)}$$

Table A-1. Fragment ions of the +4 ion of modified ziconotide after CID at 35% collision energy.

Observed *m/z*	Relative Intensity	Theoretical *m/z*	Fragment ions (Δm)
474.31	3.67	473.96, 474.57, 474.61, 474.76	b_{20}-NH_3^{5+} (0.35), y_{19}-H_2O^{5+} (0.26), b_4 (0.3), y_{19}-NH_3^{5+} (0.45)
553.06	4.74	553.01	b_{14}^{3+} (0.05)
606.19	8.87	606.4	b_{15}^{3+} (0.21)
657.81	10.36	657.77, 658.27	y_{11}-H_2O^{2+} (0.04), y_{11}-NH_3^{2+} (0.46)
666.45	33.85	666.78	y_{11}^{2+} (0.33)
675.62	3.99	675.80, 675.87	y_{23}^{4+} (0.18), a_{12}^{2+} (0.25)
676.33	4.02	675.87	a_{12}^{2+} (0.46)
684.58	5.77	684.17	a_{17}^{3+} (0.41)
687.40	4.49	687.50, 687.83	b_{17}-H_2O^{3+} (0.10), b_{17}-NH_3^{3+} (0.43)
693.32	7.66	693.50	b_{17}^{3+} (0.18)
699.46	5.41	699.08, 699.33	b_{24}-H_2O^{4+} (0.38), b_{24}-NH_3^{4+} (0.13)

Table A-1 Continued

Observed *m/z*	Relative Intensity	Theoretical *m/z*	Fragment ions (Δm)
703.28	9.01	703.18, 703.34, 703.59	a_{18}^{3+} (0.10), y_{24}-H_2O^{4+} (0.06), b_{24}^{4+} or y_{24}-NH_3^{4+} (0.31)
707.72	20.62	707.84	y_{24}^{4+} (0.12)
712.17	33.92	712.52	b_{18}^{3+} (0.35)
716.30	**86.15**	715.81	y_{12}-NH_3^{2+} (0.49)
796.26	7.05	796.28	y_{19}^{3+} (0.02)
739.00	52.24	-	
819.78	17.15	819.97, 820.00	y_{20}^{3+} (0.19), b_{14}-H_2O^{2+} (0.22)
828.57	38.61	829.00	b_{14}^{2+} (0.43)
829.25	14.83	829.00	b_{14}^{2+} (0.25)
832.98	12.57	832.98	y_{21}-H_2O^{3+} (0.00)
838.59	40.68	838.99	y_{21}^{3+} (0.40)
839.35	20.53	838.99	y_{21}^{3+} (0.36)
846.91	8.73	847.01	b_{21}^{3+} (0.10)
869.99	5.91	870.03, 870.36	b_{22}-H_2O^{3+} (0.04), b_{22}-NH_3^{3+} (0.37)
881.43	12.18	881.71	y_{22}^{3+} (0.28)
888.99	8.76	889.05, 889.38	b_{23}-H_2O^{3+} (0.06), b_{23}-NH_3^{3+} (0.39)
889.88	4.70	889.38	b_{23}-NH_3^{3+} (0.50)
894.79	25.56	894.72, 895.05, 895.10	y_{23}-H_2O^{3+} (0.07), b_{23}^{3+} or y_{23}-NH_3^{3+} (0.26), a_{15}^{2+} (0.31)
*900.42	**100.00**	900.09, 900.59, 900.73	b_{15}-H_2O^{2+} (0.33), b_{15}-NH_3^{2+} (0.17), y_{23}^{3+} (0.31)
901.13	34.72	900.73	y_{23}^{3+} (0.40)
931.55	41.83	931.77	b_{24}-H_2O^{3+} (0.22)
932.23	26.19	932.10	b_{24}-NH_3^{3+} (0.13)
937.32	**87.82**	937.45	y_{24}-H_2O^{3+} (0.13)
937.96	83.03	937.78	b_{24}^{3+} or y_{24}-NH_3^{3+} (0.18)
1154.43	5.13	1154.34	y_{10}-H_2O (0.09)
1264.84	4.13	1261.50	b_{21}-NH_3^{2+} (0.34)

* MS^3 of *m/z* 900.4 confirmed the identity of the fragment ion as y_{23}^{3+}.

Table A-2. Product ions of the +4 ion of modified ω-conotoxin GVIA after CID at 35% collision energy.

Observed *m/z*	Relative Intensity	Theoretical *m/z*	Fragment ions (Δm)
625.73	1.98	625.78	y_4 (0.05)
726.49	1.17	726.88	y_5 (0.39)
753.55	0.84	753.59	y_{24}^{4+} (0.04)
775.41	2.53	775.35	y_{25}^{4+} (0.06)
801.22	0.89	801.24, 801.57	y_{18}-H_2O^{3+} (0.02), y_{18}-NH_3^{3+} (0.35)
807.03	15.64	806.90, 807.24, 807.40	b_{26}+H_2O^{4+} (0.13), y_{18}^{3+} (0.21), y_{26}^{4+} (0.37)
807.76	10.00	807.40	y_{26}^{4+} (0.36)
824.46	7.26	-	
834.05	5.43	-	
835.94	1.70	835.94	a_8-NH_3 (0.00)
889.56	1.06	889.67	y_{20}^{3+} (0.11)
918.54	2.26	918.70	y_{21}^{3+} (0.16)
947.58	2.33	947.72	y_{22}^{3+} (0.14)
967.08	4.57	966.74	y_{23}^{3+} (0.34)
977.64	2.61	978.12	y_{14}^{2+} (0.48)
998.15	7.31	998.11	a_{17}^{2+} (0.04)
998.78	6.34	998.44, 998.77	y_{24}-H_2O^{3+} (0.34), y_{24}-NH_3^{3+} (0.01)
1004.21	**100.00**	1044.44	y_{24}^{3+} (0.23)
1004.87	32.76	-	
1027.25	17.83	1027.47	y_{25}-H_2O^{3+} (0.22)
1028.16	5.85	-	
1033.22	**86.65**	1033.13	a_{18}-NH_3^{2+} (0.09)
1033.92	**27.05**	1033.47	y_{25}^{3+} (0.45)
1034.66	6.56	-	
1059.27	5.50	1059.71	y_{15}^{2+} (0.44)
1094.88	0.84	1094.74	y_{16}-NH_3^{2+} (0.14)
1154.22	1.61	1154.27	a_{11} (0.05)
1192.99	1.93	1192.80	b_{20}^{2+} (0.19)
1201.90	1.83	1201.85	y_{18}-NH_3^{2+} (0.05)
1209.68	10.01	-	
1210.39	12.60	1210.36	y_{18}^{2+} (0.03)

Table A-2 Continued

Observed *m/z*	Relative Intensity	Theoretical *m/z*	Fragment ions (Δm)
1210.97	6.29	-	
1253.23	6.4	-	
1254.27	5.83	1253.90	y_{19}^{2+} (0.37)
1334.07	1.21	1334.00	y_{20}^{2+} (0.07)
1377.47	0.63	1377.54	y_{21}^{2+} (0.07)
1420.93	0.54	1421.08	y_{22}^{2+} (0.15)
1449.23	0.31	1449.60	y_{23}^{2+} (0.37)

LIST OF REFERENCES

1. Craig, A. G., The Characterization of Conotoxins. *Journal of Toxicology-Toxin Reviews* **2000,** *19* (1), 53-93.

2. Olivera, B. M., Rivier, J., Scott, J.K., Hillyard, D.R., Cruz, L.J. , Conotoxins. *Journal of Biological Chemistry* **1991,** *266*, 22067-22070.

3. Myers, R. A.; Cruz, L. J.; Rivier, J. E.; Olivera, B. M., Conus Peptides as Chemical Probes for Receptors and Ion Channels. *Chemical Reviews* **1993,** *93* (5), 1923-1936.

4. Terlau, H.; Olivera, B. M., Conus Venoms: A Rich Source of Novel Ion Channel-Targeted Peptides. *Physiological Reviews* **2004,** *84* (1), 41-68.

5. Olivera, B. M.; Rivier, J.; Clark, C.; Ramilo, C. A.; Corpuz, G. P.; Abogadie, F. C.; Mena, E. E.; Woodward, S. R.; Hillyard, D. R.; Cruz, L. J., Diversity of Conus Neuropeptides. *Science* **1990,** *249* (4966), 257-263.

6. Livett, B. G.; Gayler, K. R.; Khalil, Z., Drugs from the Sea: Conopeptides as Potential Therapeutics. *Current Medicinal Chemistry* **2004,** *11* (13), 1715-1723.

7. Lewis, R. J.; Garcia, M. L., Therapeutic potential of venom peptides. *Nature Reviews Drug Discovery* **2003,** *2* (10), 790-802.

8. Adams, D. J.; Alewood, P. F.; Craik, D. J.; Drinkwater, R. D.; Lewis, R. J., Conotoxins and their Potential Pharmaceutical Applications. *Drug Development Research* **1999,** *46* (3-4), 219-234.

9. Newcomb, R.; Abbruscato, T. J.; Singh, T.; Nadasdi, L.; Davis, T. P.; Miljanich, G., Bioavailability of Ziconotide in Brain: Influx from Blood, Stability, and Diffusion. *Peptides* **2000,** *21* (4), 491-501.

10. Stix, G., A Toxin Against Pain. *Scientific American* **2005,** *292* (4), 88-93.

11. Wang, Y. X.; Bowersox, S. S., Analgesic Properties of Ziconotide, a Selective Blocker of N-type Neuronal Calcium Channels. *Cns Drug Reviews* **2000,** *6* (1), 1-20.

12. Olivera, B. M., Miljanich, G.P., Ramachandran, J., Adams, M.E. , Calcium Channel Diversity and Neurotransmitter Release: The ω-Conotoxins and ω-Agatoxins. *Annual Review of Biochemistry* **1994,** *63*, 823-867.

13. Bowersox, S.; Mandema, J.; TarczyHornoch, K.; Miljanich, G.; Luther, R. R., Pharmacokinetics of SNX-111, a Selective N-type Calcium Channel Blocker, in Rats and Cynomolgus Monkeys. *Drug Metabolism and Disposition* **1997,** *25* (3), 379-383.

14. Olivera, B. M.; Rivier, J.; Clark, C.; Ramilo, C. A.; Corpuz, G. P.; Abogadie, F. C.; Mena, E. E.; Woodward, S. R.; Hillyard, D. R.; Cruz, L. J., Diversity of Conus neuropeptides. *Science* **1990,** *249* (4966), 257-63.

15. Olivera, B. M.; Cruz, L. J.; Desantos, V.; Lecheminant, G. W.; Griffin, D.; Zeikus, R.; Mcintosh, J. M.; Galyean, R.; Varga, J.; Gray, W. R.; Rivier, J., Neuronal Calcium-Channel Antagonists - Discrimination between Calcium-Channel Subtypes Using Omega-Conotoxin from Conus-Magus Venom. *Biochemistry* **1987,** *26* (8), 2086-2090.

16. Krishnamurthy, T.; Prabhakaran, M.; Long, S. R., Mass Spectrometric Investigations on Conus Peptides. *Toxicon* **1996,** *34* (11-12), 1345-1359.

17. Belva, H.; Lange, C., Conformational Studies of Omega-Conotoxins Using Electrospray Mass Spectrometry. *Rapid Communications in Mass Spectrometry* **2000,** *14* (15), 1433-1439.

18. Jones, A.; Bingham, J. P.; Gehrmann, J.; Bond, T.; Loughnan, M.; Atkins, A.; Lewis, R. J.; Alewood, P. F., Isolation and Characterization of Conopeptides by High-Performance Liquid Chromatography Combined with Mass Spectrometry and Tandem Mass Spectrometry. *Rapid Communications in Mass Spectrometry* **1996,** *10* (1), 138-143.

19. Jakubowski, J. A.; Kelley, W. P.; Sweedler, J. V., Screening for Post-Translational Modifications in Conotoxins using Liquid Chromatography/Mass Spectrometry: An Important Component of Conotoxin Discovery. *Toxicon* **2006,** *47* (6), 688-699.

20. Chung, D.; Gaur, S.; Bell, J. R.; Ramachandran, J.; Nadasdi, L., Determination of Disulfide Bridge Pattern in Omega-Conopeptides. *International Journal of Peptide and Protein Research* **1995,** *46* (3-4), 320-325.

21. Moller, C.; Rahmankhah, S.; Lauer-Fields, J.; Bubis, J.; Fields, G. B.; Mari, F., A Novel Conotoxin Framework with a Helix-Loop-Helix (Cs Alpha/Alpha) Fold. *Biochemistry* **2005,** *44* (49), 15986-15996.

22. Berson, S. A.; Yalow, R. S., General Principles of Radioimmunoassay. *Clinica Chimica Acta* **2006,** *369*, 125-143.

23. Cunico, R. L.; Gooding, K. M.; Wehr, T., *Basic HPLC and CE of Biomolecules*. Bay Bioanalytical Laboratory, Inc. : Richmond, CA, 1998.

24. Davis, M. T.; Stahl, D. C.; Hefta, S. A.; Lee, T. D., A Microscale Electrospray Interface for Online, Capillary Liquid-Chromatography Tandem Mass-Spectrometry of Complex Peptide Mixtures. *Analytical Chemistry* **1995,** *67* (24), 4549-4556.

25. Stacey, C. C.; Kruppa, G. H.; Watson, C. H.; Wronka, J.; Laukien, F. H.; Banks, J. F.; Whitehouse, C. M., Reverse-Phase Liquid-Chromatography Electrospray-Ionization Fourier-Transform Mass-Spectrometry in the Analysis of Peptides. *Rapid Communications in Mass Spectrometry* **1994,** *8* (7), 513-516.

26. Emmett, M. R.; Caprioli, R. M., Micro-Electrospray Mass-Spectrometry - Ultra-High-Sensitivity Analysis of Peptides and Proteins. *Journal of the American Society for Mass Spectrometry* **1994,** *5* (7), 605-613.

27. Delahunty, C.; Yates, J. R., Protein Identification Using 2D-LC-MS/MS. *Methods* **2005,** *35* (3), 248-255.

28. Siuzdak, G., *The Expanding Role of Mass Spectrometry in Biotechnology*. MCC Press: San Diego, CA, 2003.

29. Cech, N. B.; Enke, C. G., Practical Implications of Some Recent Studies in Electrospray Ionization Fundamentals. *Mass Spectrom Rev* **2001,** *20* (6), 362-87.

30. Fenn, J. B.; Mann, M.; Meng, C. K.; Wong, S. F.; Whitehouse, C. M., Electrospray Ionization for Mass-Spectrometry of Large Biomolecules. *Science* **1989,** *246* (4926), 64-71.

31. Glish, G. L.; Vachet, R. W., The Basics of Mass Spectrometry in the Twenty-first Century. *Nature Reviews Drug Discovery* **2003,** *2* (2), 140-150.

32. Shen, Y. F.; Kim, J.; Strittmatter, E. F.; Jacobs, J. M.; Camp, D. G.; Fang, R. H.; Tolie, N.; Moore, R. J.; Smith, R. D., Characterization of the Human Blood Plasma Proteome. *Proteomics* **2005,** *5* (15), 4034-4045.

33. March, R. E., An Introduction to Quadrupole Ion Trap Mass Spectrometry. *Journal of Mass Spectrometry* **1997,** *32* (4), 351-369.

34. Schwartz, J. C.; Senko, M. W.; Syka, J. E. P., A Two-Dimensional Quadrupole Ion Trap Mass Spectrometer. *Journal of the American Society for Mass Spectrometry* **2002,** *13* (6), 659-669.

35. Radial Ejection and Dual Detection on the Finnigan LTQ Linear Ion Trap Mass Spectrometer. Product Support Bulletin 117, Thermo Electron Corporation.

36. Omega-conotoxin MVIIA (PDB ID: 1dw5); Protein Data Bank at the Research Collaboratory for Structural Informatics http://www.rcsb.org/pdb (accessed May 2007).

37. Barksdale, C. M.; Nordblom, G. D.; Miljanich, G. M.; Tarczy-Hornoch, K.; Kristipati, R.; Kugler, A. R., Development of a Radioimmunoassay for the Novel N-Type Calcium Channel Blocker. *J. Clin. Ligand Assay* **1996,** *19* (4), 229-233.

38. Lehninger, A. L.; Nelson, D. L.; Cox, M. M., *Principles of Biochemistry*. 2nd ed.; Worth Publishers: New York, 1993.

39. Parker, C. W., Radioimmunoassay. *Annual Review of Pharmacology and Toxicology* **1981,** *21*, 113-132.

40. Poppe, H., Column Liquid Chromatography. In *Chromatography*, 5th ed.; Heftmann, E., Ed. Elsevier: Amsterdam, 1992.

41. Finnigan LTQ Getting Started Manual (Revision B). Technical Publications, Thermo Electron Corporations: San Jose, CA, 2003.

42. Miller, J. N.; Miller, J. C., *Statistics and Chemometrics for Analytical Chemistry*. 5th ed.; Pearson Prentice Hall: Harlow, England ; New York, 2005.

43. Almeida, A. M.; Castel-Branco, M. M.; Falcao, A. C., Linear Regression for Calibration Lines Revisited: Weighting Schemes for Bioanalytical Methods. *Journal of Chromatography B* **2002,** *774* (2), 215-222.

44. Johnson, E. L., Reynolds, D.L., Wright, D.S., Pachla, L.A., Biological Sample Preparation and Data Reduction Concepts in Pharmaceutical Analysis. *Journal of Chromatographic Science* **1988,** *26*, 372-379.

45. Finnigan LTQ Hardware Manual (*Revision B*). Technical Publications, Thermo Electron Corporations: San Jose, CA, 2003.

46. Geng, X. D.; Regnier, F. E., Retention Model for Proteins in Reversed-Phase Liquid-Chromatography. *Journal of Chromatography* **1984,** *296* (Jul), 15-30.

47. Apffel, A.; Fischer, S.; Goldberg, G.; Goodley, P. C.; Kuhlmann, F. E., Enhanced Sensitivity for Peptide-Mapping with Electrospray Liquid-Chromatography Mass-Spectrometry in the Presence of Signal Suppression Due to Trifluoroacetic Acid-Containing Mobile Phases. *Journal of Chromatography A* **1995,** *712* (1), 177-190.

48. Jakubowski, J. A.; Sweedler, J. V., Sequencing and Mass Profiling Highly Modified Conotoxins Using Global Reduction/Alkylation Followed by Mass Spectrometry. *Analytical Chemistry* **2004,** *76* (22), 6541-6547.

49. Jakubowski, J. A.; Keays, D. A.; Kelley, W. P.; Sandall, D. W.; Bingham, J. P.; Livett, B. G.; Gayler, K. R.; Sweedler, J. V., Determining Sequences and Post-Translational Modifications of Novel Conotoxins in Conus victoriae using cDNA Sequencing and Mass Spectrometry. *Journal of Mass Spectrometry* **2004,** *39* (5), 548-557.

50. Synder, L. R.; Kirkland, J. J.; Glaich, J. L., *Practical HPLC Method Development*. John Wiley & Sons: NY, 1988.

51. Lagerwerf, F. M.; van Dongen, W. D.; Steenvoorden, R. J. J. M.; Honing, M.; Jonkman, J. H. G., Exploring the Boundaries of Bioanalytical Quantitative LC-MS-MS. *Trac-Trends in Analytical Chemistry* **2000,** *19* (7), 418-427.

52. Skoog, D. A.; Leary, J. J., *Principles of Instrumental Analysis*. 4th ed.; Saunders College Publishing: 1992.

53. Kaiser, H., Quantitation in Elemental Analysis 2. *Analytical Chemistry* **1970,** *42* (4), A26.

54. Long, G. L.; Winefordner, J. D., Limit of Detection. *Analytical Chemistry* **1983,** *55* (7), A712.

55. Food and Drug Administration Guidance for Industry Bioanalytical Method Validation, 2001, pp. 1-20. http://www.fda.gov/CDER/GUIDANCE/4252fnl.htm (accessed January 2007).

56. Shields, D.; Montenegro, R.; Ragusa, M., Chemical Stability of Admixtures Combining Ziconotide with Morphine or Hydromorphone during Simulated Intrathecal Administration. *Neuromodulation* **2005,** *8* (4), 257-263.

57. Reubsaet, J. L.; Beijnen, J. H.; Bult, A.; van Maanen, R. J.; Marchal, J. A.; Underberg, W. J., Analytical Techniques Used to Study the Degradation of Proteins and Peptides: Physical Instability. *J Pharm Biomed Anal* **1998,** *17* (6-7), 979-984.

58. Manning, M. C.; Patel, K.; Borchardt, R. T., Stability of Protein Pharmaceuticals. *Pharmaceutical Research* **1989,** *6* (11), 903-918.

59. Price-Carter, M.; Hull, M. S.; Goldenberg, D. P., Roles of Individual Disulfide Bonds in the Stability and Folding of an Omega-Conotoxin. *Biochemistry* **1998,** *37* (27), 9851-9861.

60. Yen, T. Y.; Yan, H.; Macher, B. A., Characterizing Closely Spaced, Complex Disulfide Bond Patterns in Peptides and Proteins by Liquid Chromatography/Electrospray Ionization Tandem Mass Spectrometry. *J Mass Spectrom* **2002,** *37* (1), 15-30.

61. Gray, W. R., Disulfide Structures of Highly Bridged Peptides: A New Strategy for Analysis. *Protein Sci* **1993,** *2* (10), 1732-48.

62. Neitz, S.; Jurgens, M.; Kellmann, M.; Schulz-Knappe, P.; Schrader, M., Screening for Disulfide-Rich Peptides in Biological Sources by Carboxyamidomethylation in Combination with Differential Matrix-Assisted Laser Desorption/Ionization Time-of-Flight Mass Spectrometry. *Rapid Communications in Mass Spectrometry* **2001,** *15* (17), 1586-1592.

63. Bean, M. F.; Carr, S. A., Characterization of Disulfide Bond Position in Proteins and Sequence-Analysis of Cystine-Bridged Peptides by Tandem Mass-Spectrometry. *Analytical Biochemistry* **1992,** *201* (2), 216-226.

64. Stults, J. T.; Bourell, J. H.; Canovadavis, E.; Ling, V. T.; Laramee, G. R.; Winslow, J. W.; Griffin, P. R.; Rinderknecht, E.; Vandlen, R. L., Structural Characterization by Mass-Spectrometry of Native and Recombinant Human Relaxin. *Biomedical and Environmental Mass Spectrometry* **1990,** *19* (11), 655-664.

65. Stephenson, J. L.; Cargile, B. J.; McLuckey, S. A., Ion Trap Collisional Activation of Disulfide Linkage Intact and Reduced Multiply Protonated Polypeptides. *Rapid Communications in Mass Spectrometry* **1999,** *13* (20), 2040-2048.

66. Fainzilber, M.; Nakamura, T.; Gaathon, A.; Lodder, J. C.; Kits, K. S.; Burlingame, A. L.; Zlotkin, E., A New Cysteine Framework in Sodium-Channel Blocking Conotoxins. *Biochemistry* **1995,** *34* (27), 8649-8656.

67. Lamoureux, G. V.; Whitesides, G. M., Synthesis of Dithiols as Reducing Agents for Disulfides in Neutral Aqueous-Solution and Comparison of Reduction Potentials. *Journal of Organic Chemistry* **1993,** *58* (3), 633-641.

68. Lundell, N.; Schreitmuller, T., Sample Preparation for Peptide Mapping - A Pharmaceutical Quality-Control Perspective. *Analytical Biochemistry* **1999,** *266* (1), 31-47.

69. Mendoza, J. A.; Zientek, K. D.; Eyler, J. R.; Prokai, L., Development of an LC/MS^n Method for the Detection of Ziconotide in Horse Plasma. In *Proceedings of the 55th ASMS Conference and Allied Topics*, Indianapolis, IN, 2007.

70. MS-Product Software from ProteinProspector (v. 4.27.2 Basic) at the Mass Spectrometry Facility of the University of California, San Francisco. http://prospector.ucsf.edu/cgi-bin/msform.cgi?form=msproduct (accessed April 2008).

71. Ingle, J. D.; Crouch, S. R., *Spectrochemical Analysis*. Prentice Hall: Upper Saddle River, N.J., 1988; p 171-176.

72. Abbatiello, S. E. L. Mass Spectrometric Studies of Asparagine Synthetase and its Role in the Drug-Resistant Form of Acute Lymphoblastic Leukemia. University of Florida, Gainesville, FL, 2006.

73. Causon, R., Validation of Chromatographic Methods in Biomedical Analysis - Viewpoint and Discussion. *Journal of Chromatography B* **1997,** *689* (1), 175-180.

74. Environmental Protection Agency, 1990, 40 Code of Federal Regulations Part 136, Appendix B. Definition and Procedure for the Determination of the Method Detection Limit - Revision 1.11. http://www.setonresourcecenter.com/CFR/40CFR/P136_008.HTM (accessed April 2009).

75. Stability Considerations in Dispensing Practice. In *United States Pharmacopeia*, 30th ed.; United States Pharmacopeial Convention, Inc.: Rockville, MD, 2007.

76. O'Donnell, P. B.; Bokser, A. D., Stability of Pharmaceutical Products. In *Remington, the Science and Practice of Pharmacy* 21st ed.; Lippincott Williams and Wilkins: Baltimore, MD, 2006; pp 1025-1036.

77. Shields, D. E.; Liu, W.; Gunning, K.; Montenegro, R., Statistical Evaluation of the Chemical Stability of Ziconotide Solutions during Simulated Intrathecal Administration. *J Pain Symptom Manage* **2008,** *36* (1), e4-6.

78. PRIALT package insert. San Diego, CA: Elan Pharmaceuticals, Inc.: 2007.

79. Atkins, P. W., *Physical Chemistry*. 6th ed.; W.H. Freeman and Company: NY, 1998.

80. Kennon, L., Use of Models in Determining Chemical Pharmaceutical Stability. *Journal of Pharmaceutical Sciences* **1964,** *53* (7), 815-818.

81. Pharmaceutical Stability. In *United States Pharmacopeia*, 30th ed.; United States Pharmacopeial Convention, Inc.: Rockville, MD, 2007.

82. Biotechnology-derived Articles. In *United States Pharmacopeia*, 23rd ed.; United States Pharmacopeial Convention, Inc.: Rockville, MD, 2005.

83. Wan, H.; Umstot, E. S.; Szeto, H. H.; Schiller, P. W.; Desiderio, D. M., Quantitative Analysis of [Dmt(1)]DALDA in Ovine Plasma by Capillary Liquid Chromatography-Nanospray Ion-Trap Mass Spectrometry. *J Chromatogr B Analyt Technol Biomed Life Sci* **2004,** *803* (1), 83-90.

84. Karas, M.; Bahr, U.; Dulcks, T., Nano-electrospray Ionization Mass Spectrometry: Addressing Analytical Problems Beyond Routine. *Fresenius Journal of Analytical Chemistry* **2000,** *366* (6-7), 669-676.

85. Schmidt, A.; Karas, M.; Dulcks, T., Effect of Different Solution Flow Rates on Analyte Ion Signals in Nano-ESI MS, or: When Does ESI Turn Into Nano-ESI? *Journal of the American Society for Mass Spectrometry* **2003,** *14* (5), 492-500.

86. Westermeier, R.; Naven, T., *Proteomics in Practice*. Wiley-VCH: Weinheim, 2002.

87. Walker, J. M., *The Protein Protocols Handbook*. Humana Press: Totowa, NJ, 2002.

BIOGRAPHICAL SKETCH

Jhoana Avendaño Mendoza was born in Bataan, Philippines in 1977. Her acceptance as a scholar at the Philippine Science High School greatly nurtured her interest in the sciences. In April 1998, she completed her Bachelor of Science degree in Chemistry at the University of the Philippines in Diliman, Quezon City, where she worked on the development and validation of a potentiometric method for the determination of organophosphates in natural waters under the direction of Dr. Cynthia Grace Gregorio. She worked as a research assistant at the Seaweed Chemistry section of the Marine Science Institute, University of the Philippines where she tested the feasibility of a carrageenophyte as a test organism for toxicity testing before joining the Institute of Chemistry as a junior faculty. From 1999 to 2003, she taught and supervised laboratory classes in general, analytical and organic chemistry in the same institute where she earned her undergraduate degree. In August 2003, she started graduate studies at the Chemistry Department of the University of Florida where she joined the research group of Dr. John R. Eyler. Collaborative efforts between the Chemistry Department and the College of Veterinary Medicine Racing Laboratory paved the way for her to work on developing liquid chromatography and mass spectrometric methods to analyze small molecules and peptides. She plans to explore the vast field of research opportunities where she can use and further improve her knowledge and skills in liquid chromatography – mass spectrometric method development to study and analyze complex samples.